Post-CHOPS EOR using Gas Solvents and Air

by

Ye-Ji Soh

A thesis submitted in partial fulfillment of the requirements for the degree of

Master of Science

In

Petroleum Engineering

Department of Civil and Environmental Engineering
University of Alberta

Abstract

As a follow-up method after CHOPS (Cold Heavy Oil Production with Sands), CSI (Cyclic Solvent Injection) was widely accepted in the oil industry. After injected gas solvents with high pressure are dissolved in a heavy-oil reservoir, produced oil shows dispersed gas-phase in the oil, which is known as "foamy oil".

This thesis reports an experimental study of foamy oil created by various gas solvents, such as CH_4, CO_2, mixture-form of CH_4 and C_3H_8, or a combination of gas solvents with air. The particular focus was on air used as an EOR (enhanced oil recovery) agent due to its low cost. Experimental data shows that methane live oil -primary- production by depletion gave about 14% oil recovery. But, with additional CO_2 huff 'n' puff, recovery increased by around 15%, totaling 29% recovery. Methane-propane mixture only recovered about 5% due to decreased foamy effect by good mixing property of propane. Next, different pressure depletion rates, namely -0.23, -0.51, and -1.53 psi/minute, were applied and more oil was produced with increasing depletion rates.

Two schemes using air (alternate injection and co-injection) were carried out with CH_4 and CO_2 and three huff-n-puff cycles were tested. As a result, air huff-n-puff (HnP) followed by 2-cycles of CH_4 HnP showed 36.21% recovery, while air HnP followed by 2-cycles of CO_2 HnP yielded 30.36% oil recovery. When gas solvents and air were injected together, air 50%-CO_2 50% and air 50%-CH_4 50% recovered 29.85% and 23.74% of total oil-in-place, respectively.

A numerical study was also conducted in core-to-field-scale, predominantly on methane foamy oil production in various scenarios; e.g. by assigning different well patterns and injection/soaking periods. The solution GOR (gas oil ratio) versus saturation pressure data from methane depletion

experiments was matched using the Peng-Robinson equation of state method and the K-values were generated by the Crookston equation. The K-values, which model equilibrium condition of the fluid, were used with reaction coefficients, which helped in representing non-equilibrium status of foamy oil. Core-scale simulation showed mostly less than 5% error, which can be accepted as a valid match. These matched data were used in a field-scale model to analyze the performance of cyclic methane injection.

In field scale modeling, 15-well data from a CHOPS field in Alberta, Canada were history matched and 6-cycle CSI performances were followed as post-CHOPS with different well patterns (central, peripheral, all-wells). In field scale modeling, all-well huff 'n' puff-type pattern brought about slightly higher oil recovery than central and peripheral well patterns. Sensitivity analyses were carried out with a variety of scenarios by changing injection/soaking period and pressure decline rates. The ratio of injection to soaking period was observed to be more important than the injection period itself in terms of production efficiency.

Acknowledgements

First of all, I would like to express my deepest gratitude to my parents and brother for believing in me and encouraging me not only during my 2-year master's study, but also throughout my life. Their advice – "Trust in God, do your best in what you like, be happy, and never lose humor" – meant a lot to me, especially whenever passing through hard times here, and finally I am able to stand successfully at the final stage of my study. In addition to my parents, I'd like to deliver my heartfelt thanks and love to my grandma whom I respect most of all for showing me how to live my life decently.

I truly appreciate having had a good supervision in Dr. Tayfun Babadagli, whom always gave me useful advice, guidance, and continuous support. This research was conducted under Dr. Babadagli's NSERC Industrial Research Chair in Unconventional Oil Recovery (industrial partners are Petroleum Development Oman, Total E&P Recherche Development, SIGNa Oilfield Canada, Saudi Aramco, Devon) and an NSERC Discovery Grant (No: RES0033730). I gratefully acknowledge these supports.

Sincere thanks should be given to our laboratory technicians, Lixing Lin, Mihaela Istratescu, and Todd Kinnee, who helped me a lot whenever I was faced with troubles conducting experiments. I also want to convey thanks to Pamela Keegan who carefully edited my papers and to the other EOGRRC group members for being together in this journey.

Special thanks to Juan Jose Martinez, who has been by my side and caring for me literally throughout my entire 2-year study. Also, I feel very appreciative of meeting all the friends from Joshua Generation of Antioch church, as well as the comforting sermon every Sunday from Rev. Henry Han. All the warm memories of mine would not have been made possible without them.

I am also very grateful to Dr. Hyun-don Shin and Dr. Farouq Ali, who led me to have interest in unconventional resources and always truly cared for me and for giving genuine and sound advice whenever I needed. I feel very blessed to have them as my mentors in my life. Finally, to all of my professors from the Department of Energy Resource Engineering in Inha University who provided decent education during my undergraduate year, I'd like to express my earnest thanks.

Contents

Chapter 1 Introduction..... 1

1.1 Overview..... 2

1.2 Backgrounds and Statement of Problem..... 2

1.3 Research Objectives..... 3

1.4 Structure of the Thesis..... 3

1.5 References..... 4

Chapter 2 Cost Effective Heavy-Oil Recovery after Primary Production: Optimization of Methane Use in Cyclic Solvent Injection through Experimental and Numerical Studies..... 5

2.1 Preface..... 6

2.2 Introduction..... 7

2.3 Experimental Study..... 8

2.4 Results and Analyses..... 9

2.4.1 Methane (followed by CO_2 huff-n-puff) case..... 9

2.4.2 Methane-propane mixture case..... 11

2.4.3 Comparative analysis of gas-bubble sizes..... 12

2.5 Numerical Study..... 14

2.5.1 Core-scale simulation..... 15

2.5.2 Field-scale simulation..... 16

2.6 Conclusions..... 19

2.7 References..... 20

Chapter 3 Cost-Effective Heavy Oil Recovery by Gas Injection: Improvement of the Efficiency of Foamy Flow and Pressurization..... 44

3.1 Preface..... 45

3.2 Introduction..... 46

3.3 Experimental Work 47
3.4 Results and Analysis 48
3.4.1 Pressure differential 48
3.4.2 Comparison of methane (CH_4) live oil production in different scenarios 50
3.4.3 The importance of the amount of air injected 51
3.4.4 Production mechanisms of air huff-n-puff and the effect of air phase on the subsequent cycles 51
3.4.5 Gas chromatography and SARA analyses 53
3.4.6 Producing gas-to-oil ratio (GOR) 53
3.4.7 Different foamy oil behaviour 54
3.5 Economic Analysis 56
3.6 Conclusions 57
3.7 References 58
Chapter 4 Conclusions and Contributions 83
4.1 Conclusions and Contributions 84
References 86

List of Tables

Table 2.1—SARA Analysis of original oil and the oil obtained after CH_4 live oil production. .. 22
Table 2.2—Sand-pack properties of RUN 1 and RUN 2. 23
Table 2.3—Results of RUN 1 and RUN 2. 23
Table 2.4—Times when 1st/2nd end/peak appeared (hour). 25
Table 2.5—Sand-pack properties for methane-propane mixture case. 26
Table 2.6—Results of CH_4-C_3H_8 mixture cases. 26
Table 2.7—Time when 1st/2nd end/peak appeared (hour). 28
Table 2.8—Summary of experimental results - CO_2 results from Rangriz-Shokri and Babadagli (2016). 29
Table 2.9—Results of CH_4 live oil core flooding with different depletion rates. 31
Table 2.10—SARA results from initial oil and after the -0.23 psi/min experiment. 31
Table 2.11—Fluid characteristics in modeling 'Methane' case. 33
Table 2.12—Fluid characteristics in modeling 'Different depletion rates' case. 33
Table 2.13—Comparison of experimental and numerical values – Sand-pack properties. 34
Table 2.14—Comparison of experimental and numerical results (1). 34
Table 2.15—Comparison of experimental and numerical results (2). 35
Table 2.16—Total oil recovery factor [%] after each cycle. 35
Table 2.17—Comparison of CH_4 and CO_2 field-scale simulation results - 3-cycle Injection. 37
Table 2.18—Description of constraints/conditions. 37
Table 3.1—Sand-pack properties. 60
Table 3.2−Experimental results. 61
Table 3.3—GC results of the produced gas. 65
Table 3.4−Comparison of CH4 live oil production in different scenarios: Cases 1, 2 from Soh et al. (2017). 67
Table 3.5—SARA results of the produced oil. 71
Table 3.6— Viscosity of produced oil. 71

List of Figures

Figure 2.1—Experimental set-up (Rangriz-Shokri and Babadagli 2016). 22
Figure 2.2—Numbered pressure ports. 22
Figure 2.3—Pressure Profile of Methane Case - (a) Run 1 (b) Run 2: 1st (c) Run 2: 2nd. 24
Figure 2.4—Pressure profile of CO_2 huff 'n' puff - (a) RUN 1 (b) RUN 2. 25
Figure 2.5—Pressure differential between P2 and P7 for RUN 1 (left) and RUN 2 (right). 25
Figure 2.6—Drawing of foamy oil behaviour of (a) CH_4 and (b) CO_2. 26
Figure 2.7—Pressure Profile of CH_4-C_3H_8 mixture Cases for (a) CH_4 62%-C_3H_8 38% and (b) CH_4 50%-C_3H_8 50%. 27
Figure 2.8—Comparison of ΔP between CH_4 62%-C_3H_8 38% and CH_4 50%-C_3H_8 50%. 28
Figure 2.9—Similar shape of graphs - pressure differential and incremental oil production in 'CH_4 62%-C_3H_8 38%'(left) and CH_4 50%-C_3H_8 50% cases (right). 28
Figure 2.10—Cumulative oil and gas production of CH_4 62%-C_3H_8 38% (left) and CH_4 50%-C_3H_8 50% (right). 29
Figure 2.11—Pressure chart for -0.23 psi/min. 30
Figure 2.12—Pressure chart for -0.51 psi/min. 30
Figure 2.13—Pressure chart for -1.53 psi/min. 30
Figure 2.14—Oil recovery factor vs. pressure. 31
Figure 2.15—Simulated sand-pack model. 32
Figure 2.16—PVT experiment result: Solution GOR vs. pressure. 32
Figure 2.17—Schematic of reaction 1 and 2. 32
Figure 2.18—Well Patterns. Red: Injectors, white: producers in cases of (a) Central (b) Peripheral and (c) All-Wells. 35
Figure 2.19—Total Oil Recovery Factor % in case of (a) 1-month Injection and (b) 4-month Injection. 36
Figure 2.20—1-month injection/half-month soaking. 38
Figure 2.21—3-month injection/1.5-month soaking. 39
Figure 2.22—3-month injection/half-month soaking. 40
Figure 2.23—Cumulative oil production vs. Time for 'DP X' case (left) and 'DP O' case (right). 41
Figure 2.24—Scenario 1: 1-month Injection/half-month Soaking – left: Daily oil production rate, right: Cumulative oil production. 41

Figure 2.25—Scenario 2: 3-month injection/1.5-month soaking – left: Daily oil production rate, right: Cumulative oil production. 42
Figure 2.26—Scenario 3: 3-month injection/half-month soaking – left: Daily oil production rate, right: Cumulative oil production. 42
Figure 2.27—Results of three injection/soaking scenarios for each depletion-rate case..... 43
Figure 3.1—Experimental set-up (Rangriz-Shokri and Babadabli 2016). 60
Figure 3.2—Schematic of pressure ports. 60
Figure 3.3—Pressure/ΔP profile for air huff-n-puff from Exp. 1. 61
Figure 3.4—Pressure/ΔP profile for air huff-n-puff from Exp. 2. 62
Figure 3.5—Pressure/ΔP profile for CH_4 huff-n-puff - Cycle 1 (Exp. 1)..... 62
Figure 3.6—Pressure/ΔP profile for CH_4 huff-n-puff - Cycle 2 (Exp. 1)..... 62
Figure 3.7—Pressure/ΔP profile for CO_2 huff-n-puff - Cycle 1 (Exp. 2)..... 63
Figure 3.8—Pressure/ΔP profile for CO_2 huff-n-puff - Cycle 2 (Exp. 2)..... 63
Figure 3.9—Pressure/ΔP profile for Air 50%-CO_2 50% - Cycle 1..... 64
Figure 3.10—Pressure/ΔP profile for Air 50%-CO_2 50% - Cycle 2..... 64
Figure 3.11—Pressure/ΔP profile for Air 50%-CO_2 50% - Cycle 3. 64
Figure 3.12−—Pressure/ΔP profile for Air 50%-CH_4 50% - Cycle 1. 65
Figure 3.13—Pressure/ΔP profile for Air 50%-CH4 50% - Cycle 2. 66
Figure 3.14—Pressure/ΔP profile for Air 50%-CH4 50% - Cycle 3. 66
Figure 3.15—Pressure/ΔP profile for '-0.23 psi/min' in Case I (Soh et al. 2017). 67
Figure 3.16—Pressure/ΔP profile for '-0.51 psi/min' in Case I (Soh et al. 2017). 68
Figure 3.17—Pressure/ΔP profile for '-1.53 psi/min' in Case I (Soh et al. 2017). 68
Figure 3.18—Oil recovery factor vs. Pressure – Exp. 1. 69
Figure 3.19—Oil recovery factor vs. Pressure - Exp. 2..... 69
Figure 3.20—Oil recovery factor vs. Pressure - Exp. 3..... 70
Figure 3.21—Oil recovery factor vs. Pressure - Exp. 4..... 70
Figure 3.22—Oil GC Result (x-axis - Carbon no.): Blue - Total mass % change from initial oil to air HnP, Red - from air HnP to Exp. 1 - Cycle 1, Green - from Exp. 1 – Cycle 1 to 2..... 72
Figure 3.23—Oil GC Result (x-axis - Carbon no.): Blue - Total mass % change from initial oil to air HnP, Red - from air HnP to Exp. 2 - Cycle 1, Green - from Exp. 2 – Cycle 1 to 2..... 72

Figure 3.24—Oil GC Result (x-axis - Carbon no.): Blue - Total mass % change from initial oil to air 50%-CO2 50% Cycle 1, Red - from air 50%-CO2 50% Cycle 1 to Cycle 2, Green - from Cycle 2 to Cycle 3. 73
Figure 3.25—Oil GC Result (x-axis - Carbon no.): Blue - Total mass % change from initial oil to air 50%-CH4 50% Cycle 1, Red - from air 50%-CH4 50% Cycle 1 to Cycle 2, Green from Cycle 2 to Cycle 3. 73
Figure 3.26—GOR and Oil Recovery Factor for air huff-n-puff from Exp. 1. 74
Figure 3.27—GOR and Oil Recovery Factor for air huff-n-puff from Exp. 2. 74
Figure 3.28—GOR and oil recovery factor for CH4 huff-n-puff - Cycle 1 (Exp. 1). 75
Figure 3.29—GOR and oil recovery factor for CH4 huff-n-puff - Cycle 2 (Exp. 1). 75
Figure 3.30—GOR and oil recovery factor for CO2 huff-n-puff - Cycle 1 (Exp. 2). 76
Figure 3.31—GOR and oil recovery factor for CO2 huff-n-puff - Cycle 2 (Exp. 2). 76
Figure 3.32—GOR and oil recovery factor for air 50%-CO2 50% - Cycle 1 (Exp. 3). 77
Figure 3.33—GOR and oil recovery factor for air 50%-CO2 50% - Cycle 3 (Exp. 3). 77
Figure 3.34—GOR and oil recovery factor for air 50%-CH4 50% - Cycle 1 (Exp. 4). 78
Figure 3.35—GOR and oil recovery factor for air 50%-CH4 50% - Cycle 2 (Exp. 4). 78
Figure 3.36—GOR and oil recovery factor for air 50%-CH4 50% - Cycle 3 (Exp. 4). 79
Figure 3.37—Oil production in 'Air Huff-n-Puff' (t = hour): Yellow circles on where bubbles appeared. 79
Figure 3.38—Oil production in Exp. 1 – Cycle 2 (t = hour): Yellow circles on where bubbles appeared. 80
Figure 3.39—Oil production in Exp. 2 – Cycle 1 (t = hour): Yellow circles on where bubbles appeared. 80
Figure 3.40—CH_4 gas bubble size (0.5-1 cm, the height of yellow arrow) during Exp. 1 – Cycle 2. 81
Figure 3.41—Air 50%+CO2 50% gas bubble size (1.25-2.5 cm, the height of yellow arrow) during Exp. 3 – Cycle 2. 81
Figure 3.42—Oil production in Exp. 4 – Cycle 2 (t = hour): Yellow arrows pointed where bubbles appeared. 82
Figure 3.43−Oil recovery summary for each experiment. 82

Chapter 1 Introduction

1.1 Overview

As it becomes more difficult to find new conventional oil reservoirs, attention from world energy industry is leaning to unconventional resources. Especially, for Canada and Venezuela, which have about 35-40% of the world's resources of <20° API heavy oil (Dusseault 2002), it is more crucial to develop oil recovery technologies. In spite of a big progress in developing them, e.g. SAGD, CSS, VAPEX, there is still a huge portion of unexploited oil reservoirs left. Around 80% of heavy oil reservoirs in Western Canada remains as a significant challenge, in that these reservoirs are too thin to apply thermal recovery methods, due to enormous heat loss or the disturbance from the bottom water to steam injected.

CHOPS (Cold Heavy Oil Production with Sands) emerged as a promising technology to recover oil from these thin reservoirs. However, because of its low oil recovery factor of ~5-15%, a further step was necessary in order for CHOPS to be more feasible; accordingly, post-CHOPS was suggested. As one of the favourable post-CHOPS technologies, CSI (Cyclic Solvent Injection) has been proposed because the solvents can fill the wormholes (high permeability paths created by the sand production) and efficiently contact oil left in the matrix of the reservoir. Despite this, because of the high costs of injected gases, particularly with the current low oil price, efforts are needed to optimize the process by selection of proper gas type (or gas combinations) and suitable injection scheme. Furthermore, when each solvent or solvent-combination is dissolved into or ex-solved out of heavy oil, the solvent shows different chemical and physical behaviours, which in turn establish a high need for investigation to better understand the operation conditions.

1.2 Backgrounds and Statement of Problem

Huge portions of unexploited thin reservoirs have turned researchers to focus on developing non-thermal recovery technologies. CHOPS (Cold Heavy Oil Production with Sands) is the one which has been under the spotlight; however, due to its low oil recovery (~5-15%), follow-up processes, i.e. *post-CHOPS*, has been in high demand to be studied. CSI (Cyclic Solvent Injection) is one of the favourable post-CHOPS technologies in that solvents can function as pressurizing materials for depleted reservoirs and can flow and contact heavy oil efficiently in wormholes made by sand influx. When solvents are injected to reservoir with high pressure, they

are dissolved into heavy oil. Later, when the oil production starts with pressure depletion, dissolved gas tries to come out but is suppressed by high oil viscosity and, in turn, stays in dispersed-phase in the oil. This phase is known as "Foamy oil".

Most of the earlier studies focused on the performance of foamy oil or the factors that affect foam quality. Yet, studies on specific solvents individually and their chemical and physical behaviours with heavy oil are limited. Also, due to the high cost of gas solvents used in the gas injection schemes of EOR, it is highly necessary to seek more economical types of solvents.

1.3 Research Objectives

The main objectives of the study were the following:

- ✓ Understand chemical and physical behaviours of foamy oil made with various economical gas-solvents; e.g. methane (CH_4), carbon-dioxide (CO_2), mixed form of methane and propane (C_3H_8), and mixed form of air and CH_4/CO_2.
- ✓ Determine the economical types of gas-solvents that can be used in Cyclic Solvent Injection (CSI) and each of their appropriate operating conditions; e.g. controlling pressure depletion rate and injection/soaking schemes.

1.4 Structure of the Thesis

This is a paper-based thesis including four chapters.

Chapter 1 includes an overview, a statement of problem, and research objectives.

Chapter 2 contains both experimental and numerical studies focusing on methane use as a solvent in Cyclic Solvent Injection (CSI). In the experimental study, to make the most use of methane foamy oil production, CO_2 huff-n-puff was followed after and also the mixture-form with propane in different mix-ratio was tested as a gas-solvent. Pressure depletion rate was given as a controlling factor to methane foamy oil production. In the numerical study, core-scale simulation was done to match with experimental results and these matched chemical/physical values were used to proceed into field-scale simulation. Different well patterns and injection/soaking schemes were simulated to optimize operating conditions.

In Chapter 3, air was used as a new pressurizing material with solvents (CH_4 and CO_2) having high foaming capability in cyclic solvent injection (CSI) experiments. Specific analyses were done, focusing on pressure differentials, the amount of air injected, production mechanisms, GC (gas chromatography)/SARA results, producing gas oil ratio (GOR) and different foaminess of each live oil.

Chapter 4 presents the overall conclusions of the studies shown in Chapters 2 and 3, as well as the contributions achieved by this study.

1.5 References

Alshmakhy, A. and Maini, B. B. 2012. Effects of Gravity, Foaminess, and Pressure Drawdown on Primary-Depletion Recovery Factor in Heavy-Oil Systems. *JCPT* 51 (06). doi:10.2118/163067-PA.

Dusseault, M.B. (2002). Chapter 2. Alberta Government. "*World Conventional and Heavy Oil, CHOPS: Cold heavy oil production with sand in the Canadian heavy oil industry"*. p. 46-47. Retrieved from https://open.alberta.ca/publications/2815953. Accessed on July 20th 2017

Chapter 2 Cost Effective Heavy-Oil Recovery after Primary Production: Optimization of Methane Use in Cyclic Solvent Injection through Experimental and Numerical Studies

** Submitted to *Fuel* journal.
** Presented at the *SPE Annual Technical Conference and Exhibition, Dubai, U.A.E*. in September 2016.
(A New Modeling Approach to Optimize Methane-Propane Injection in a Field After CHOPS, SPE-181322-MS)

2.1 Preface

Although cold heavy oil production with sands (CHOPS) is an economically attractive method, ultimate recovery does not exceed 15%. Cyclic solvent injection (CSI) has been under consideration as a follow-up EOR application in the industry. This method targets extracting large amounts of remaining oil in the matrix by solvent diffusion, taking advantage of its high contact area with wormholes. Methane and propane are two potential solvents to be used in this practice. Methane is preferred due to its availability and stronger foaming characteristics, while propane has lower foaming but better mixing capability.

A far-reaching core- to field scale- study was conducted in this paper to test out the potential of pure methane and its mixture with propane as well as CO_2 as prospective CSI solvents. After geological properties of the sand-pack (1.5m-length and 5cm-diameter) were measured, live oil (saturated with methane and methane-propane mixture at different ratios) production was carried out with certain pressure decline rates: -0.51 psi/min from 500 to 190 psi and -0.23 psi/min from 190 to 70 psi. Pressure data with time was monitored through eight equally spaced transducers. The solution GOR from the live oil saturated with methane vs. pressure was matched using the Peng-Robinson (1976) EOS method. The data points starting injection period (representing equilibrium condition) were fitted to develop K values using the Crookston equation. These matched data were carried to a field scale model to analyze the CSI performance for methane. In field scale modeling, 15-well data from a CHOPS field in Alberta, Canada were history matched and 6-cycle CSI performances were followed as post-CHOPS with different well patterns (central, peripheral, all-wells).

As a result of these experiments, methane showed about 14% oil recovery but with additional CO_2 huff 'n' puff, around 15% recovery was added, which gave 29% recovery in total. Methane-propane mixture resulted in a lower oil recovery of about 5% due to decreased foamy effect. Valid core-scale simulation was completed by tuning K-values and considering non-equilibrium or equilibrium impact depending on solvent type, showing mostly less than 5% error. In a field-scale modeling, central and peripheral well patterns yielded oil recoveries consistent with the experiments while all-well huff 'n' puff- type pattern showed a slightly higher value.

Based on the outcome of the methane and methane-propane mixture experiments, it was of more importance to further study the way to enhance the foaminess in methane-live oil recovery.

Different pressure depletion rates, namely -0.23, -0.51, and -1.53 psi/min, were applied and more oil was produced with increasing depletion rates. These experimental results were simulated at the core scale and the change of reaction coefficients was considered with varying decline rates. In field-scale modeling, sensitivity analyses were done with a variety of scenarios by changing injection/soaking period and pressure decline rates. The ratio of injection to soaking period was observed to be more critical than the injection period itself in terms of production efficiency. Also, the influence of pressure depletion rate as a new constraint in the simulation work was studied.

Key words: Cyclic solvent injection, post-CHOPS EOR, propane and methane mixture, actual field case, foamy oil core-flooding, pressure depletion tests.

2.2 Introduction

Cyclic solvent injection (CSI) has been proposed as a feasible method for post-CHOPS EOR in thin reservoirs. The solvents fill the wormholes and contact the oils left in the matrix of the reservoir. Considerable efforts have been made related to CSI testing the applicability of different solvents experimentally and numerically (Dong et al. 2012; Chang and Ivory 2013; Du et al. 2014; Chang et al 2015; Rangriz-Shokri and Babadagli 2016). In a recent attempt, Ivory et al. (2010) numerically showed that 28% C_3H_8-72% CO_2 mixture as a CSI material result in 50% recovery in 6 cycles. They observed that because of higher solubility of C_3H_8, a large portion of C_3H_8 gas came out much before CO_2 did.

Bjorndalen et al. (2012) also studied the foaminess of heavy oil saturated with different solvents (CH_4, C_3H_8, CO_2) and concluded that the more nucleation sites of gas formed, the higher the oil recovered. Dong et al. (2012) reported that using propane as solvent and methane to chase gas increased the total oil recovery to 34.3% after 6 cycles, whereas six cycles of methane resulted in only 4.27% recovery. Focusing on non-equilibrium behaviour of solvents, Wang et al. (2015) carried out PVT experiments with methane and propane. They observed in the methane case that when the higher pressure decline rate was applied, the longer the foaminess maintained, leading to higher oil recovery, where the experiment with propane showed the opposite. In addition, Rangriz-Shokri and Babadagli (2016) presented several sets of CO_2 foamy flow-depletion

experiments with numerical simulation using non-equilibrium behaviour of pure CO_2 in CSI after CHOPS. Bera and Babadagli (2016) implemented relative permeability studies by making three different types of foamy oils saturated with CO_2, methane, and propane. Their experiments showed oil relative permeability with CO_2 was the highest oil recovery, followed by methane and propane. From their results, starting from 400psi, CO_2 accomplished about 55% recovery of original oil in place (OOIP), while methane and propane showed 15% and 17% recoveries, respectively.

CSI after CHOPS needs to be further investigated to understand the foamy oil recovery under depletion, solubility of different solvents in oil, and the ultimate effect of these on the recovery. Upscaling to the field scale is also a critical issue and the lack of experimental data is one of the drawbacks in performing reliable field-scale modeling. This paper presents a comprehensive core- to field-scale study that tests the suitability of using methane and methane-propane mixture as potential CSI solvents for post-CHOPS EOR applications.

2.3 Experimental Study

A horizontally positioned sand-pack with 1.5 m-length and 5 cm-diameter was filled up with 250-500µm size of sands. The sand-pack was initially positioned in a vertical direction by pouring/hammering sands into the core holder to pack it compactly. CO_2 was flushed through the sand-pack to remove any air trapped in the pores. Whilst saturating the sand-pack with brine, its porosity was estimated by knowing the volume of injected water. Permeability was measured by injecting the brine at different rates and was calculated by applying Darcy's law. Next, 1.2 PV of dead oil was injected to reach the irreducible water saturation and to maintain initial oil saturation. The dead oil (specific gravity of 0.995 and viscosity of 17,500 cp) was obtained from a CHOPS reservoir in Eastern Alberta.

To remove any occurrence of initial free-gas saturation, brine was injected at a very slow injection rate and the ports of six pressure transducers were opened one-by-one to release any gas. Meanwhile, live oil was prepared separately in two transfer vessels. About 700 ml of dead oil was injected to each of two transfer vessels and then were connected to corresponding gas tank, which was set at 500 psi. Note that in the methane-propane mixture case, to control the volume percentage of each gas, certain volumes of methane and propane were moved to ISCO

pump first and then this mixture-form gas was injected to transfer vessel. Live oil, after about 2 days of saturation, was transferred into the sand-pack replacing the dead oil, which had been injected previously to obtain initial water saturation. The reason why live oil was made separately and transferred to the sand-pack rather than following huff-n-puff manner is to assume even foaminess quality across the sand-pack. Live oil production was implemented with two sets of pressure-decline rates: 500 to 190 psi with -0.51 psi/min and 190 to 70 psi with -0.23 psi/min, which was achieved using a back-pressure regulator (BPR) at the outlet. Eight pressure transducers (six on the core holder and two at the inlet and outlet ports) recorded the pressure change with time. Experimental set-up is shown in **Figure 2.1** and the pressure ports are numbered from P1 to P8, illustrated in **Figure 2.2**.

CO_2 huff 'n' puff experiments were carried out to test the potential of additional recovery by CO_2 injection as a secondary recovery method. SARA results of initial dead oil ('Before' row) and the oil after methane live oil production ('After' row) are illustrated in **Table 2.1**.

2.4 Results and Analyses

2.4.1 Methane (followed by CO_2 huff-n-puff) case

Two sets of experiments with different sand-pack properties were done followed by CO_2 huff 'n' puff injection. The specific characteristics of each set are summarized in **Table 2.2**. The results of experiments are shown in **Table 2.3**. The initial methane phase was repeated twice in Run 2 for repeatability.

The pressure values recorded during methane and succeeding CO_2 experiments are provided in the charts given in **Figures 2.3 and 2.4**, respectively. The parts circled in red are the regions where the pressure difference started to be obvious. This region was observed to start earlier for the CO_2 injection case than for the methane case. Note that since the back pressure regulator (BPR) is located at the outlet, once P8 reached 70 psi, pressure depletion was over and was waited until all the pressure ports showed around 70 psi. The first methane experiment was stopped before all the ports reached ~70 psi where even 40 psi difference between P2 and P7 was observed. On the other hand, the 2nd methane case of RUN 2 was continued until every pressure

transducer reached 70 psi, which took 18 hours longer than the previous run. This led to a higher oil recovery factor.

More details about the pressure differential (ΔP = P2-P7) are shown in **Figure 2.5**. For both methane and CO_2 huff 'n' puff cases, a twisted M-shape of similar pattern can be observed in Figure 2.5 (two peak points). The second peak was observed to be higher, except the CO_2 huff 'n' puff from RUN 1. When comparing the time when $1^{st}/2^{nd}$ depletion stage was ended (referred to '$1^{st}/2^{nd}$ end' in **Table 2.4** and $1^{st}/2^{nd}$ peak showed up, it can be concluded that the 2^{nd} peak emerged around the same time when the 2^{nd} depletion stage has finished. However, the 1^{st} end time did not seem much correlated to the 1^{st} peak time, which showed from minimum about a 10-minute difference to maximum of about a 6-hour difference. From the 2^{nd} peak, around which the last pressure transducer reached 70 psi, the pressure differential decreased to an equilibrium state. Until that point, the oil/gas production went on. Therefore, if RUN 1 was finished like RUN 2, the expected ΔP trend line would have been the red-colored line drawn in the left one of Figure 2.5, and a greater amount of oil/gas would have been produced. Also, since the 2^{nd} peak of the methane case (RUN 1) was about twice as high as the methane case of RUN 2, it would have taken longer to reach pressure-equilibrium.

This can be attributed to the degree of how well solvent is saturated or to the difference in permeability. More research and detailed analysis are needed to clarify this. When comparing the results of oil recoveries among only the same solvent cases, mostly higher pressure differential brought about more oil recovery. However, higher pressure differential does not always mean a higher oil recovery, when compared with using one solvent (e.g. CH_4) to another (e.g. CO_2), due to different foamy oil behaviour (compare the pressure differences in Fig. 2.5). From a previous study by Bjorndalen et al. (2012) that mentioned CO_2 foamy oil contains more gas nucleation sites than the CH_4 one does, it could be surmised that CO_2 gas bubbles are more evenly spread than the CH_4 ones are (Figure 2.6). This also means that for CO_2 foamy oil case, the difference between the number of nucleation sites placed at P1 to P2 and P7 to P8 is smaller, compared with the one in CH_4 foamy oil case, which could be one of the reasons for having a small pressure differential. Hence, it can be stated that CO_2 foamy oil has more sites that have driving force for oil production, compared with CH_4 foamy oil, which causes higher oil recovery.

After methane experiments were finished, CO_2 was injected for 15 and 30 minutes for RUN 1 and RUN 2, respectively, of which the pressure was controlled at 500 psi. The soaking time for both cases was about 4 days. The difference in the injection time did not have a large impact on ultimate oil recovery at the end. Obviously, the gas produced was greater in the latter case. As a result, CO_2 played an important role in giving additional recovery after methane foamy oil production, which made the total oil recovery about 30%.

2.4.2 Methane-propane mixture case

Two methane-propane mixture experiments - CH_4 62%-C_3H_8 38% and CH_4 50%-C_3H_8 50% - were operated following the same procedure as the methane case; note that the percentage here corresponds to a volume percentage. The details of the sand-pack are shown in **Table 2.5** and the results of experiments are presented in **Table 2.6.** The pressure changes with time recorded are in the charts provided in **Figure 2.7**.

Unlike the methane with CO_2 huff 'n' puff cases, no distinctive pressure differential between P2 and P7 was observed in the pressure profiles. In case of methane-propane mixtures, ΔP charts showed M-shape profiles, which are caused by an *abrupt* increase of ΔP (**Figure 2.8**) in the beginning as opposed to the methane and CO_2 cases, which showed a *gradual* increase (Fig. 2.5). Also, in contrast to the methane and CO_2 cases (the 2nd peak was higher) the 1st peak was shown to be higher. As seen in **Table 2.7**, the time when the 1st peak appeared was not related at all to the time when the 1st depletion stage ended. The 2nd peak emerged around a similar time to when the 2nd depletion stage ended, as similar to the methane and CO_2 cases. To observe more details about the effect of pressure differential, the pressure differential per minute and the incremental oil production (ΔOP) per minute are given in **Figure 2.9**. One may observe from these plots that incremental oil production volume per minute followed a consistent ΔP trend. Eventually, more oil (and gas) was produced in the cases of lower propane concentration (Table 2.6, **Figure 2.10**). More discussion is provided in the next section by comparing the bubble sizes of the methane, CO_2 huff 'n' puff, and methane-propane mixture cases.

In summary, the biggest oil recovery was achieved by CO_2 huff 'n' puff done after the methane case, followed by methane and methane-propane mixture cases. The final comparison results,

including pure CO_2 case data obtained from Rangriz-Shokri and Babadagli (2016) are shown in **Table 2.8**. When methane live oil was produced with additional CO_2 huff 'n' puff, it showed great potential for foamy oil recovery compared with the pure CO_2 experimental results. In other words, economically speaking, it can be expected that the combination of methane and CO_2 live oil recovery costs less and recovers more oil than pure CO_2 live oil recovery does.

2.4.3 Comparative analysis of gas-bubble sizes

Looking at all of the results from the different experiments, CO_2 yielded the highest oil recovery succeeded by methane and methane-propane mixture. Methane and CO_2 gas bubbles inside the oil were coalesced together and eventually formed a continuous gas phase. Since the size of bubble itself for CO_2 is larger than methane, as observed during experiments, the size of continuous-phase gas is also larger for CO_2 than the one for methane, which led to higher oil recovery.

The main purpose of mixing methane and propane was to clarify the effect of a "strong" solvent on the recovery (higher mixing rate with oil) and improvement of the foamy nature (Diedro at al. 2015). The results were not promising, because when they mixed, their two different bright sides – methane having good foaminess, propane having good mixing ability with oil – became darkened. The foamy behaviour was reduced by adding propane. The fluids condition became closer to equilibrium from non-equilibrium, which did not allow enough time for gas bubbles to be released out of the saturated oil to develop a larger bubble size. It was visually observed that the methane-propane gas bubbles were burst more often than the methane and CO_2 cases. Hence, the heavy oil saturated with methane-propane mixture did not have enough driving force to push oil to be produced, which resulted in a lower oil recovery than the pure methane case. Similar tests were performed for propane-CO_2 mixture foamy oil in another study (Bjorndalen et al. 2012), which showed much fewer number of gas clusters than CO_2 foamy oil did, and had a good match with CO_2 equilibrium curve. Based on our observations and this analysis, one may conclude that the solvent showing good mixing property, which in this case is propane, is best not to be used with the one having good foaming property, which can be CH_4 or CO_2.

2.4.4 Methane-live oil core flooding with different depletion rates

According to the study from Sheng et al. (1999), the impact of pressure depletion rate on foamy-oil solution gas drive results from supersaturation, which affects the number of active nucleation sites. The degree of supersaturation controls the spacing of gas nuclei that influences gas saturation established before the phase of gas becomes continuous. It is crucial to understand the time when this gas saturation is made, because from this point, the oil recovery efficiency is decreased. Also, it was observed by multiple researchers (Handy 1958; Maini et al. 1996) that if the pressure depletion rate is higher, gas tends to stay dispersed, which leads higher oil recovery.

Based on the former studies and the results from methane-propane mixture cases in this paper that showed methane played a good role in contributing foaminess, which is advantageous to live oil production. Then, more specific studies were done with different depletion rates to methane-live oil core flooding. Unlike previous cases, which gave change to depletion rate in the middle of experiment, only one depletion rate was employed to the end for each experiment: -0.23 psi/min, -0.51 psi/min, and -1.53 psi/min. Average pressure and pressure differential, ΔP, which is the pressure difference between P2 and P7, are shown in **Figures 2.11 to 2.13** in the order of -0.23, -0.51, and -1.53 psi/min cases.

ΔP graphs seem to have two humps with which the graphs were divided into section 1 and 2. With increasing depletion rates, the size of the first hump (section 1) shrinks and this makes the second hump (section 2) starts earlier. From a previous study by Maini (2001), it is well-known that solution-gas drive in heavy oils accompanies thermodynamic non-equilibrium. This makes releasing process of dissolved gas bubbles in heavy oil much slower than the one shown in conventional solution-gas drive. When the first bubble is perfectly separated from oil after long duration of entrapment in foamy oil, the pressure at this moment is called “pseudo” bubble-point pressure (P_b).

Before “pseudo” P_b is reached, only tiny bubbles separately exist in the core system and oil production results from expanded oil volume (Tang and Firoozabadi 2001); therefore, oil is not greatly produced in this period (**Figure 2.14**). This can also be confirmed with small amplitude of ΔP, which was observed to be related to oil production in the methane-propane mixture case.

Hence, about 450 to 500 psi can be concluded to be pseudo bubble-point pressure in these experiments, where ΔP amplitude is small (section 1).

Later, ΔP increases dramatically, as separated gas bubbles start nucleating to make gas stream, and from this point, oil is produced by actual foamy oil behaviour (Firoozabadi and Aronson, 1999). The pressures when the oil recoveries start to rise abruptly are shown in the yellow circled areas in Figures 2.11 to 2.13, near the middle points of the slopes. This indicates that it takes a bit of time for ΔP increase to effectively affect oil recovery. This delay of ΔP impact on the actual oil production is supposedly due to the length of tubing located between the outlet and the oil collector. ΔP increment in section 2 is ceased at pressure of around 70 psi, which is the one set to be the final pressure. Needless to say, further pressure drop does not give more energy for new gas bubbles to be nucleated, and ΔP starts to decrease.

As mentioned earlier, high pressure depletion rate is a critical key factor inducing higher oil recovery. However, it was observed in this study that foam quality was of huge importance to lead to increased oil recovery as well as high depletion rate. Looking at the results in **Table 2.9**, the case of -0.51 psi/min gave 0.37% higher oil recovery than the -1.53 psi/min. The -0.51 psi/min experiment started right after all the pressure ports showed 550 psi, while the -1.53 psi/min case began a few hours later. This means that the former case (when bubbles are more uniformly distributed) results in better oil recovery than the latter case (waiting a few hours for the bubbles to collide each other and gather to the end). Therefore, it can be said that after achieving a certain high value of depletion rate, the foam quality (the degree of well distribution of gas-bubble) gives the highest importance to bring great oil recovery. No specific patterns can be found in oil composition change when looking at SARA results (refer to Table 2.1 and **Table 2.10**). There was increase in saturates, asphaltenes, and aromatics and decrease in resins in as shown in Table 2.1. However, in Table 2.10, increase in resins and aromatics decrease in saturates and asphaltenes were observed.

2.5 Numerical Study

The solution GOR from the live oil saturated with methane vs. pressure was matched using Peng-Robinson EOS (Peng and Robinson 1976) method. For the characterization of heavy oil and solvent, methane, EOS modeling was carried out using the PVTi module of ECLIPSE

software. The experimental PVT data of solution GOR is shown in **Figure 2.16**. The data points of injection period (representing equilibrium condition) were fitted to develop K values using Crookston equation:

$$K(P,T) = \left(A + \frac{B}{P} + C * P\right) * \exp(-\frac{D}{T-E}) \quad (1)$$

The main energy for improved oil recovery is caused by delaying the coalescence of gas bubbles. This physics was represented by using two reaction coefficients: Reaction 1 and Reaction 2 (**Figure 2.17**). Reaction 1 illustrates the moment that the dissolved gas bubbles are clustered to have enough size to be trapped in the pores. Reaction 2 explains the moment that this trapped gas is gathered to form free-gas phase. The reaction rates are defined by the Arrhenius equation:

$$\text{Reaction Rate} = Ae^{\frac{-E_a}{RT}} \Pi C^N \quad (2)$$

where A is pre-exponential factor, which corresponds to reaction constant, E_a is activation energy, R is the universal gas constant, T is temperature, Π is the product operator, C is each component concentration, and N is the order of C, which relies on each component.

In this paper, the terms of activation energy (E_a) and the order of concentration (N) are neglected. Consequently, the reaction rate is only comprised of a reaction constant, A. The fluid characteristics used in modeling are shown in **Tables 2.11 and 2.12**; component volatility and liquid-compressibility types were obtained from the technical descriptions given in the software manual (ECLIPSE Technical Description 2014).

2.5.1 Core-scale simulation

The sand-pack was simulated (**Figure 2.15**) to the similar size as in experimental sand-pack, with 50, 1, and 1 grid(s) in the x, y, z directions, respectively. The dimension of each grid is 0.025, 0.045, and 0.045 m in the x, y, z directions. The properties of simulated core holder were assumed to be isotropic and homogeneous.

Sand-pack properties and experimental results of the methane case (Run 1, Run 2) and methane-live oil with different depletion rates case (different depletion rates) are compared with the simulation outcome in **Tables 2.13-15**.

2.5.2 Field-scale simulation

Real data of a CHOPS field with 15 wells from Alberta were used for field-scale reservoir simulation. The details of the original model can be found in Rangriz-Shokri and Babadagli (2012, 2016). The total volume is comprised of 41, 41, and 5 grids in the x, y, and z directions, respectively, and each grid is 60 m, 60 m, and 1 m, having a 22.24-acre drainage area for a single well. Wormholes were generated in the middle of production zone following a fractal model based on matching the sand production history (Rangriz-Shokri and Babadagli 2012). Field reservoir properties and fluid flow models used in simulation were obtained from Rangriz-Shokri and Babadagli (2016).

2.5.2.1 Cyclic Methane injection with different well patterns.

Cyclic methane injection as a post-CHOPS method was simulated using three different (central, peripheral, all wells) models (**Figure 2.18**). 'Central' and 'peripheral' are literally the cases that the injectors are located in the central and peripheral parts of the well-pad. 'All wells' refers to all wells used as injectors and turning into producers.

Six cycles in total were repeated with the CH_4 injection rate of 2,000m^3/day. Different injection time of 1 month and 4 months were conducted to see the impact of the injecting period on the ultimate oil recovery. After 6 cycles, as a result, central and peripheral patterns brought a similar value of 24.3% of oil recovery, in both cases of 1-month and 4-months injection, and All-Wells pattern showed about 0.5% more for 1-month and 1% more for 4-month injection. Total oil recovery factors are shown in **Table 2.16 and Figure 2.19**.

Rangriz-Shokri and Babadagli (2016) performed this field-scale simulation with pure CO_2 using 3 cycles. The results from the 3-cycle injection of methane and CO_2 are compared in **Table 2.17**, which shows that for CO_2, the injection time affected greatly on ultimate oil recovery, while methane was not impacted largely by this. All conditions or constraints in this model are described in **Table 2.18**.

2.5.2.2 Cyclic Methane Injection with and without depletion rate in different injection/soaking scenarios.

To consider the influence of depletion rate on oil recovery in field-scale, a small modification was added to the previous constraints (Table 2.18). Pressure depletion rate was calculated as follows, not giving any difference to producing duration:

$$\frac{500\ psi}{x\ psi/min} \div 60 \div 24 = 360\ days$$
$$\therefore x \approx 0.0009645\ psi/\min \approx 0.096\ bar/day \quad (3)$$

Three various injection/soaking scenarios were simulated: Scenario 1: 1-month (30-day) injection/half-month (15-day) soaking; Scenario 2: 3-month injection/1.5-month soaking; Scenario 3: 3-month injection/half-month (15-day) soaking. The results of injection/soaking scenarios and the status of depletion rate are shown in **Figures 2.20 to 2.22**. 'DP X' signifies when production was simulated with the constraints shown in Table 2.18 (no pressure depletion rate), while 'DP O' means when pressure depletion rate was added to the ones in Table 2.18. Well pattern chosen here was All-well, and 6-cycle was repeated.

Having the pressure depletion rate, less oil was produced for injection/soaking scenarios. Sudden pressure drop ('DP X' case when depletion rate was not given as a constraint) led to higher oil recovery while gradual drop ('DP O' case when depletion rate was given as constraint) did not. However, using depletion rate is more similar to realistic cases than just setting BHP (Bottom-Hole-Pressure) and oil production rate as constraints, which is the condition of 'DP X'.

In early time (**Figure 2.23**), the amount of oil produced per time, which is the slope of the graph, does not show a big difference among various scenarios 1, 2, and 3. In other words, spending more time and more solvents during injecting or soaking for scenario 2 and 3 than for scenario 1 did not turn out to be beneficial in terms of giving more oil production. As time goes on, on the other hand, these slopes change and the difference between using different scenarios becomes clearer, in which the 'DP O' case shows more obvious change than 'DP X' case does. In later stage, it can be expected from the slope changes that scenario 3 would produce the greatest amount of oil, followed by scenario 2, then and 1. Hence, it can be said that setting proper time period of injection and soaking is crucial to deliver more oil efficiently.

To see the effect of depletion rate on oil recovery in field-scale, three different pressure depletion rates were chosen: -0.43 bar/10day, -0.96 bar/10day, and -2.88 bar/10day. The reason for choosing these declining rates was to realize the core-scale setting with -0.23 (about 2.22 times smaller than 0.51), -0.51, and -1.53 (3 times faster than 0.51) psi/min. -0.43 bar/10 day corresponds to -0.23 psi/min, -0.96 bar/10 day does to -0.51 psi/min, and -2.88 bar/day does to -1.53 psi/min. The outcomes of scenarios 1, 2 and 3 are illustrated in **Figures 2.24 to 2.26**. Each scenario shows a different reaction of oil production to different depletion rate. In scenario 1, the slope, from the beginning to later, of cumulative oil production vs. time is increasing with depletion rate (Figure 2.24); the faster the depletion rate, the higher the oil rate is produced with time. In spite, in scenario 2 (Figure 2.25), due to longer periods of injection and soaking, the plateaus in the graphs of Figure 2.25 is longer than the ones in Figure 2.24. Because of this, until about 5,800 days have past, lower depletion rate cases, such as the -0.43 bar/10-day case and the -0.96 bar/10-day case produce more oil than the higher rate (-2.88 bar/10day) does. However, since the slope of cumulative oil production to time is higher at greater depletion rate, the oil production of the -2.88 bar/10 day case catches up the ones of the -0.43 bar/10 day and -0.96 bar/10-day cases after about 5,800 days. If comparing case -0.43 bar/10-day with -0.96 bar/10-day, cumulative oil productions of both are higher than each other back and forth. Hence, when deciding depletion rate between these cases, one of them should be chosen depending on preferred producing time and economic feasibility of solvent used with this production time. The same phenomena can be observed in scenario 3 (Figure 2.26), as well.

When analyzing the results (**Figure 2.27**) from three different injection/soaking scenarios for each depletion rate, it can be seen that the lower the depletion rate is, the lower sensitivities of cumulative oil production to different injection/soaking scenarios are. If planning to produce oil in a short-period of time, there would be no need, economically speaking, to apply long injection and soaking times. Also, making depletion rate higher from -0.43 bar/10-day to -0.96 bar/10-day did not give a significant difference in generating greater amount of oil. To take advantage of the impact of depletion rate, more extreme change to the rate were needed (compare the result of **Figure 2.27a-b** with **2.27c** at certain points of time).

2.6 Conclusions

1. The pressure differential between the inlet (injector) and outlet (producer) of the core-holder (reservoir) in lab (field)-scale can be a good marker of foamy oil behaviour associated with oil and gas production.
2. Depending on the solvent type, the pressure differential vs. time behaviour is different. Comparing the cases using the same solvent, the one showing higher pressure differential led to higher oil/gas recovery. However, when different solvents are compared, this might not be valid because of the different foamy oil behaviour. In the case of CO_2, better foaminess and accordingly more nucleation of gas bubbles were observed, even with lower pressure differentials.
3. Methane-propane mixture is not a promising foamy agent due to reduced foaminess of methane by the good mixing property of propane. Hence, the solvents that yielded good foaminess with heavy oil (CO_2 and CH_4) and the solvents with good mixing capability (C_3H_8) should not be injected in the mixed form.
4. Since methane-propane mixture reduces the foaminess of methane and non-equilibrium status turns into equilibrium condition, equilibrium methane-behaviour is suitable to be applied to numerical simulation of methane-propane mixture live oil production.
5. From below pseudo bubble-point pressure, ΔP increases dramatically, as separated gas-bubble chunks starts congregating or nucleating to make gas stream, from which oil is produced by actual foamy behaviour.
6. Generally, the higher the depletion rate is applied, the greater amount of oil is produced. However, after achieving a certain high value of depletion rate, the foam quality gives the greatest significance in achieving great oil recovery, which is the degree to which gas bubbles in foamy oil are well-distributed in the system.
7. Tuning K-values and having proper reaction coefficients are useful approaches to include the foamy oil behaviour in core- and field-scale simulations.
8. As a result of field-scale simulation, central and peripheral well patterns showed similar oil recoveries, whilst all-wells pattern showed a slightly higher recovery. Also, setting the proper period of injection and soaking time is crucial to deliver more oil efficiently.

2.7 References

Bera, A. and Babadagli, T. 2016. Relative Permeability of Foamy Oil for Different Types of Dissolved Gases. *SPE Res Eval & Eng*. 19 (4). SPE-180913-PA. http://dx.doi.org/10.2118/180913-PA.

Bjorndalen, N., Jossy, E., and Alvarez, J. 2012. Foamy Oil Behaviour in Solvent Based Production Processes. SPE Heavy Oil Conference Canada, Calgary, Alberta, 12-14 June. SPE-157905-MS. http://dx.doi.org/10.2118/157905-MS.

Chang, J. and Ivory, J. 2013. Field-Scale Simulation of Cyclic Solvent Injection (CSI). *J Can Pet Technol*. 52 (4). SPE-157804-PA. http://dx.doi.org/10.2118/157804-PA.

Chang, J., Ivory, J., and London, M. 2015. History Matches and Interpretation of CHOPS Performance for CSI Field Pilot. SPE Canada Heavy Oil Technical Conference, Calgary, Alberta, 9-11 June. SPE-17466-MS. http://dx.doi.org/10.2118/174466-MS.

Diedro, F., Bryan, J., Kryuchkov, S. et al. 2015. Evaluation of Diffusion of Light Hydrocarbon Solvents in Bitumen. SPE Canada Heavy Oil Technical Conference, Calgary, Alberta, 9-11 June. SPE-174424-MS. http://dx.doi.org/10.2118/174424-MS.

Du, Z., Zeng, F., and Chan, C. 2014. Effects of Pressure Decline Rate on the Post-CHOPS Cyclic Solvent Injection Process. SPE Heavy Oil Conference Canada, 10-12 June. SPE-170176-MS. http://dx.doi.org/10.2118/170176-MS.

ECLIPSE Technical Description. 2014, Schlumberger.

Firoozabadi, A. and Aronson, A. 1999. Visualization and Measurement of Gas Evolution and Flow of Heavy and Light Oil in Porous Media. *SPE Reservoir Evaluation & Engineering* 2 (6). doi:10.2118/59255-PA.

Handy, L. L. 1958. A laboratory study of Oil Recovery by Solution Gas Drive. *Trans. AIME* 213: 310-315.

Ivory, J., Chang, J., Coates, R. et al. 2010. Investigation of Cyclic Solvent Injection Process for Heavy Oil Recovery. *J Can Pet Technol*. 49 (09). http://dx.doi.org/10.2118/140662-PA.

Maini, B. B., Sheng, J. J. and Bora, R. 1996. Role of foamy oil flow in heavy oil production. International Energy Agency (IEA) Workshop/Symp. on EOR, Sydney, Australia, Sept. 29-2 Oct.

Maini, B. B. 2001. Foamy-Oil Flow. *JPT* 53 (10). doi:10.2118/68885-JPT.

Peng, D. Y. and Robinson, D.B. 1976. A New Two-Constant Equation of State. *Industrial and Engineering Chemistry: Fundamentals* 15: 59–64. doi:10.1021/i160057a011.

Rangriz-Shokri, A. and Babadagli, T. 2012. An Approach to Model CHOPS (Cold Heavy Oil Production with Sand) and Post-CHOPS Applications. SPE Annual Technical Conference and Exhibition, San Antonio, Texas, 8-10 October. SPE-159437-MS. http://dx.doi.org/10.2118/159437-MS.

Rangriz-Shokri, A. and Babadagli, T. 2016. Experimental and Numerical Core-to-Field Scale Modeling of Non-Equilibrium CO_2 Behaviour in Post-CHOPS Applications. Submitted to *SPE Reservoir Evaluation and Engineering* 2016 (under review).

Sheng, J.J., Maini, B.B., Hayes, R.E. et al. 1999. Critical Review of Foamy Oil Flow. *Transport in Porous Media* 35 (2):157-187. doi:10.1023/A:1006575510872.

Tang, G. and Firoozabadi, A. 2001. Effect of GOR, Temperature, and Initial Water Saturation on Solution-Gas Drive in Heavy-Oil Reservoirs. SPE Annual Technical Conference and Exhibition, New Orleans, Louisiana, 30 September-3 October. :10.2118/71499-MS.

Wang, H., Zeng, F., and Zhou, X. 2015. Study of the Non-Equilibrium PVT Properties of Methane- and Propane-Heavy Oil Systems. SPE Canada Heavy Oil Technical Conference, Calgary, Alberta, 9-11 June. SPE-1794498-MS. http://dx.doi.org/10.2118/174498-MS.

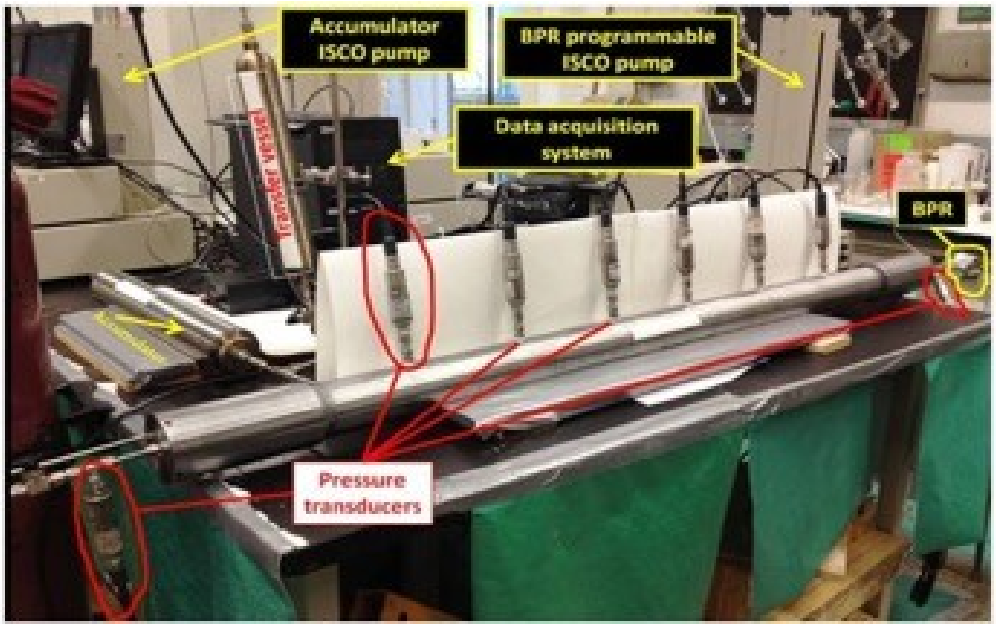

Figure 2.1—Experimental set-up (Rangriz-Shokri and Babadagli 2016).

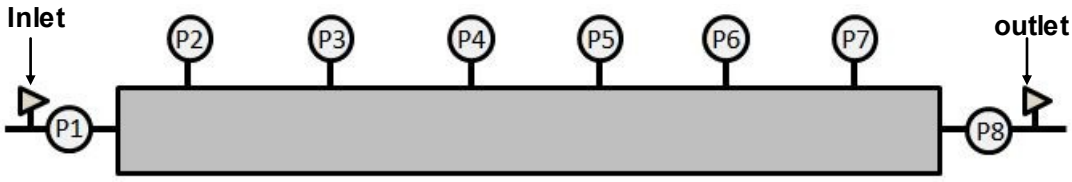

Figure 2.2—Numbered pressure ports.

	Saturates	Asphaltenes	Resins	Aromatics
Before	34.75	13.83	26.53	24.13
After	35.57	14.75	24.55	24.42

Table 2.1—SARA Analysis of original oil and the oil obtained after CH_4 live oil production.

Data	RUN 1	RUN 2
Avg. porosity (%)	39.58	37.93
Avg. permeability (mD)	12,657	989.13
Initial water saturation (%)	9.51	1.14

Initial oil saturation (%)	90.49	98.86
Free gas saturation (%)	0	0

Table 2.2—Sand-pack properties of RUN 1 and RUN 2.

Data	RUN 1		RUN 2		
	CH_4 live oil	Followed by CO_2	CH_4 live oil (1^{st})	CH_4 live oil (2^{nd})	Followed by CO_2
Produced Oil [ml]	120	114	98	131	114
Produced Gas [ml]	3,447	4,300	2,378	2,755	22,376
Cum. Producing GOR [vol/vol]	28.725	37.72	24.265	21.03	196.28
Oil Recovery Factor (%)	13.22	14.476	11.06	14.786	15.1
Total Oil Recovery Factor %	27.7		29.886		

Table 2.3—Results of RUN 1 and RUN 2.

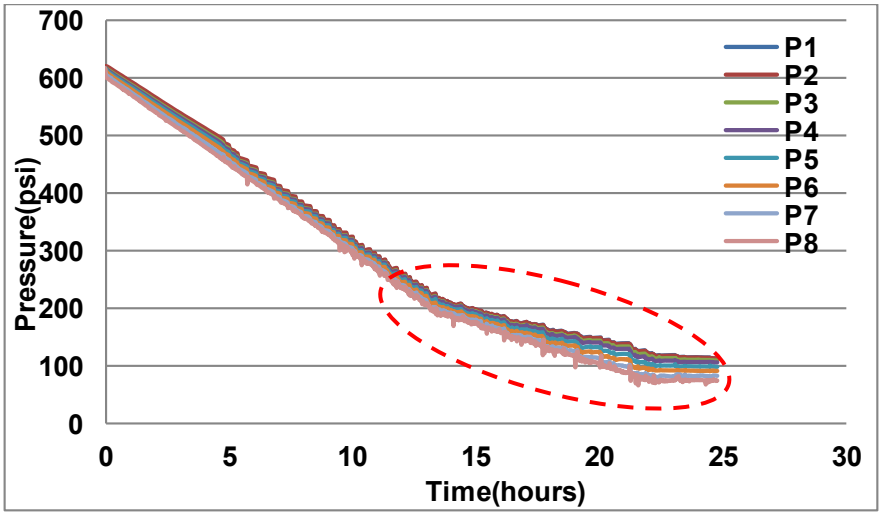

(a)

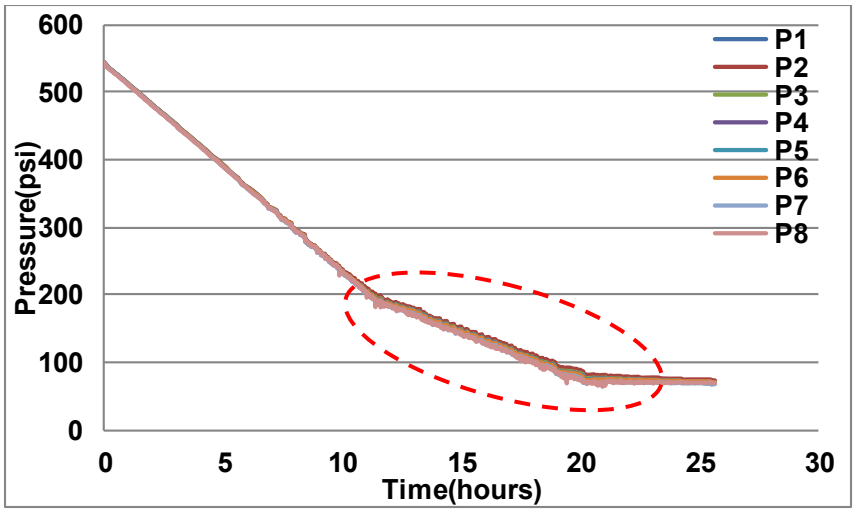

(b)

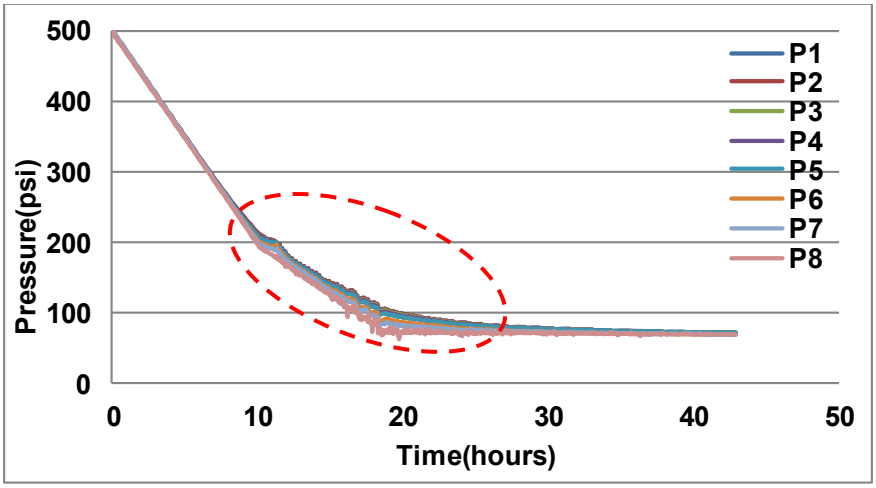

(c)

Figure 2.3—Pressure Profile of Methane Case - (a) Run 1 (b) Run 2: 1st (c) Run 2: 2nd.

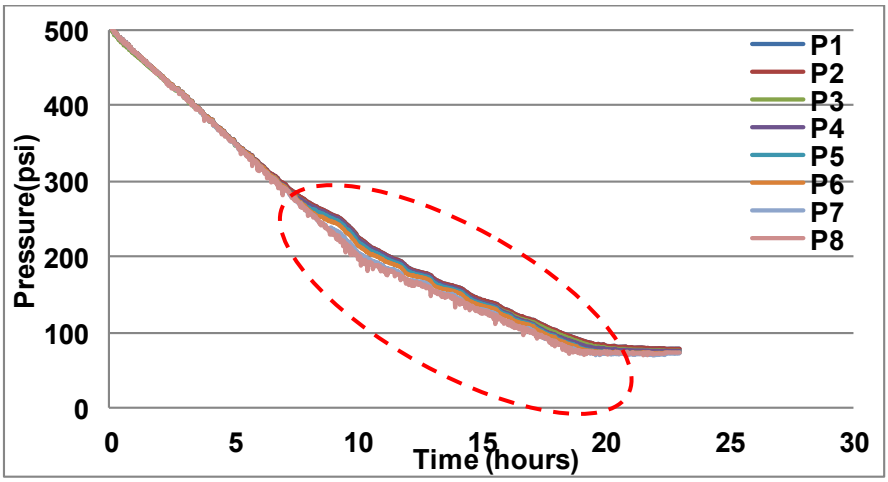

(a)

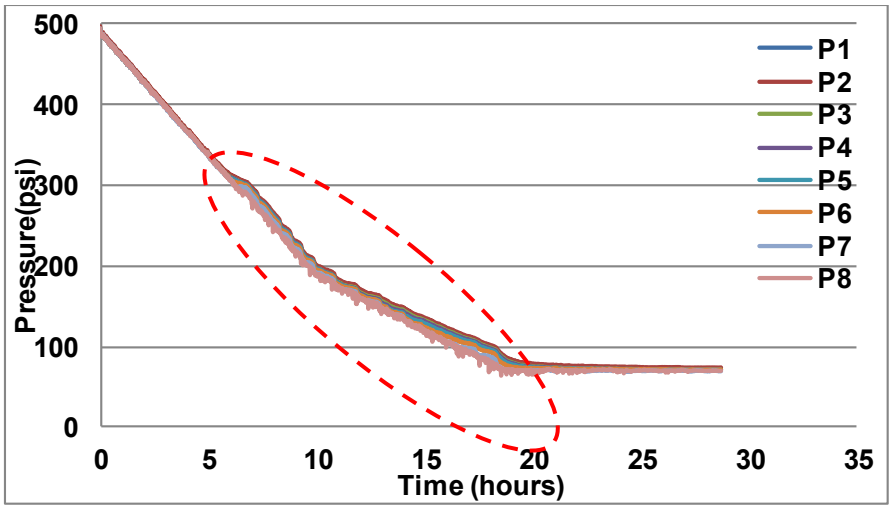

(b)

Figure 2.4—Pressure profile of CO_2 huff 'n' puff - (a) RUN 1 (b) RUN 2.

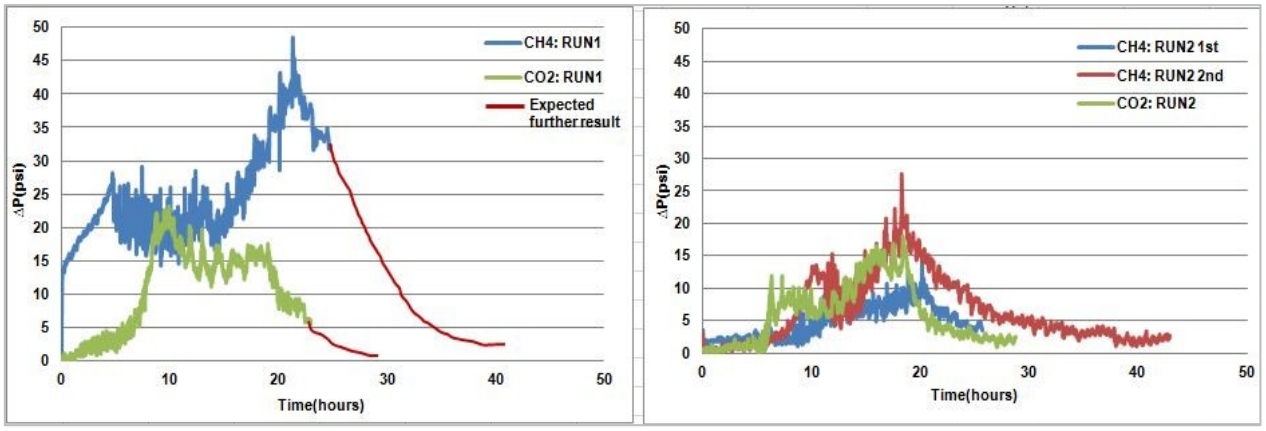

Figure 2.5—Pressure differential between P2 and P7 for RUN 1 (left) and RUN 2 (right).

	1st end	1st peak	2nd end	2nd peak
CH_4: RUN 1	13.40	7.42	22.09	21.32
CO_2: RUN 1	10.13	9.92	18.83	19.03
CH_4: RUN 2 1st	11.76	11.38	20.46	20.13
CH_4: RUN 2 2nd	10.13	15.97	18.83	18.28
CO_2: RUN 2	9.97	6.33	18.66	18.38

Table 2.4—Times when 1st/2nd end/peak appeared (hour).

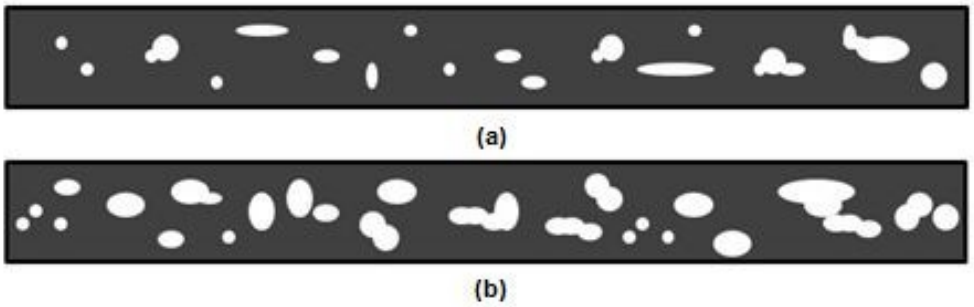

Figure 2.6—Drawing of foamy oil behaviour of (a) CH_4 and (b) CO_2.

Data	Value
Avg. porosity (%)	39.9
Avg. permeability (mD)	2,027.6
Initial water saturation (%)	8
Initial oil saturation (%)	92
Free gas saturation (%)	0

Table 2.5—Sand-pack properties for methane-propane mixture case.

Data	CH_4 62%-C_3H_8 38%	CH_4 50%-C_3H_8 50%
Produced Oil [ml]	60	51
Produced Gas [ml]	5,095	2,913
Cum. Producing GOR [vol/vol]	84.93	57.12
Oil Recovery Factor (%)	6.45	5.48

Table 2.6—Results of CH_4-C_3H_8 mixture cases.

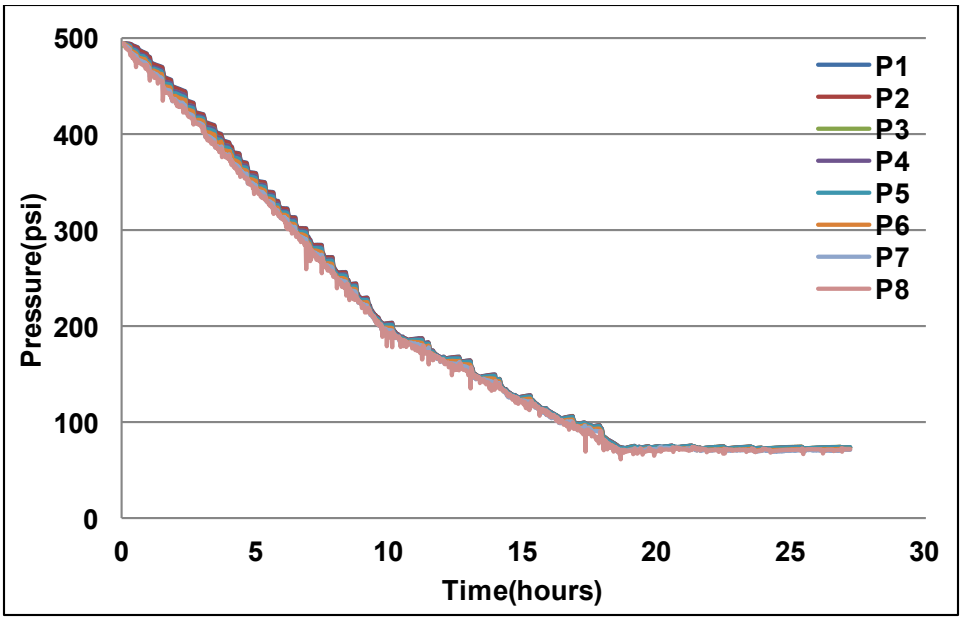

(a)

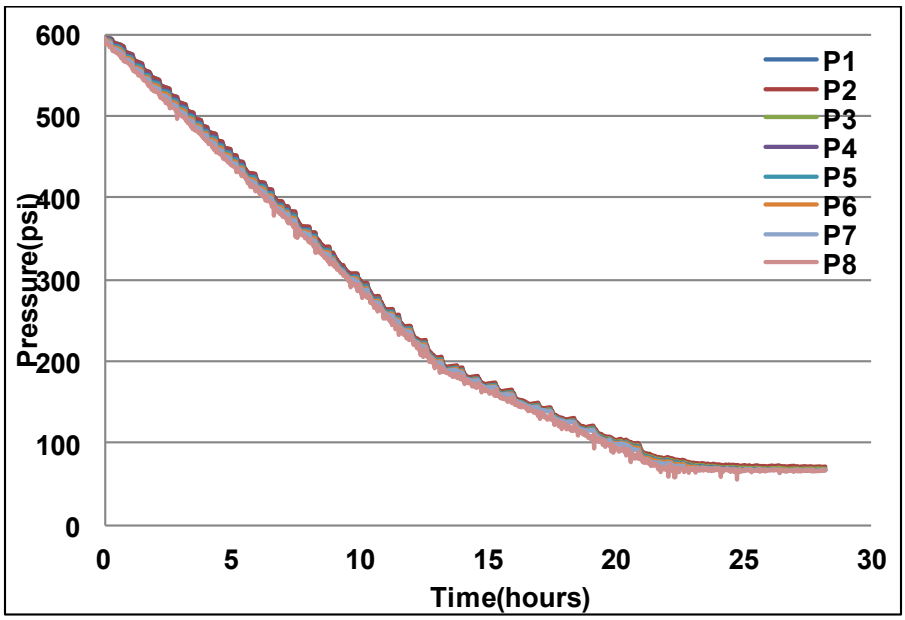

(b)

Figure 2.7—Pressure Profile of CH_4-C_3H_8 mixture Cases for (a) CH_4 62%-C_3H_8 38% and (b) CH_4 50%-C_3H_8 50%.

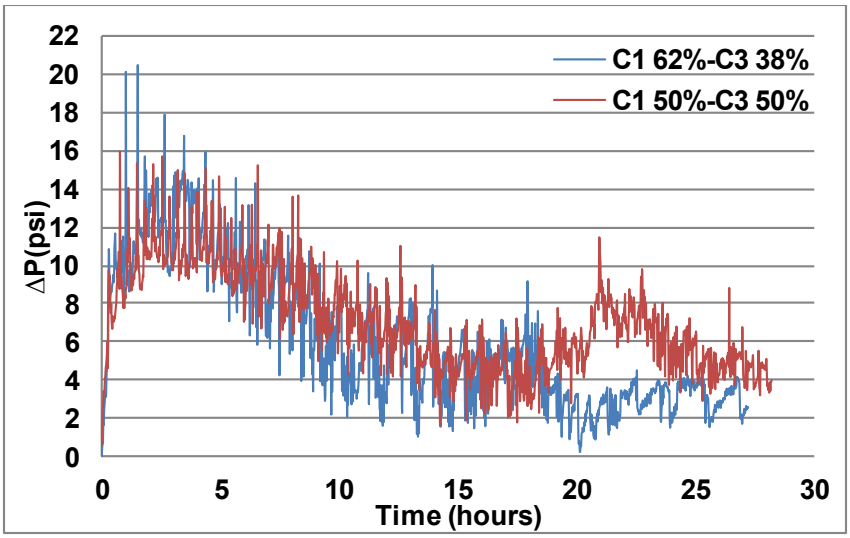

Figure 2.8—Comparison of ΔP between CH_4 62%-C_3H_8 38% and CH_4 50%-C_3H_8 50%.

	1st end	1st peak	2nd end	2nd peak
CH_4 62%-C_3H_8 38%	10.13	1.52	18.83	17.93
CH_4 50%-C_3H_8 50%.	13.40	0.77	22.09	20.93

Table 2.7—Time when 1st/2nd end/peak appeared (hour).

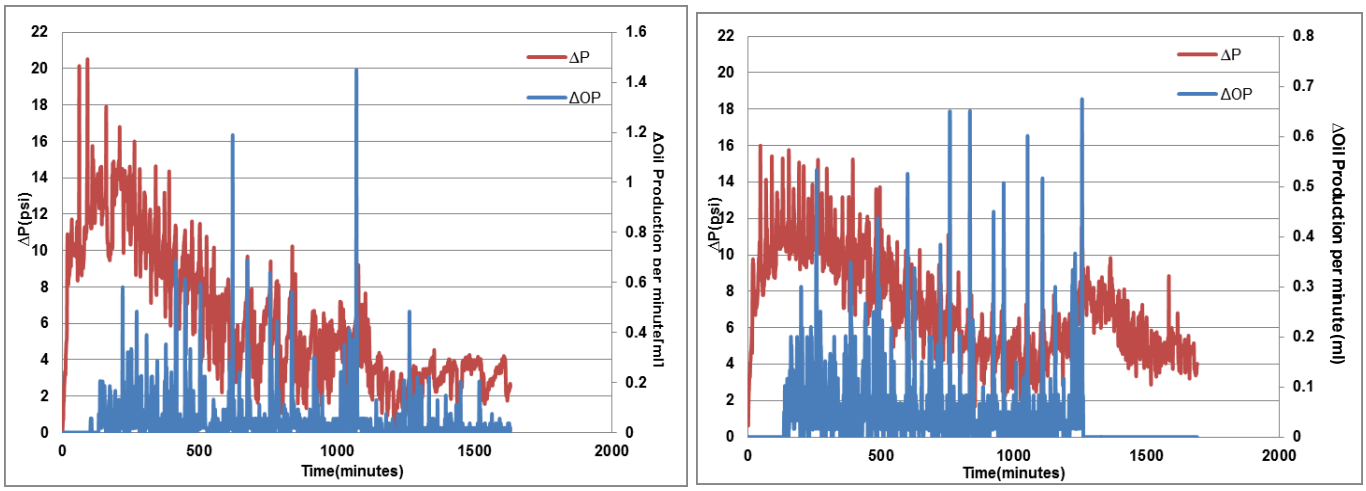

Figure 2.9—Similar shape of graphs - pressure differential and incremental oil production in 'CH_4 62%-C_3H_8 38%'(left) and CH_4 50%-C_3H_8 50% cases (right).

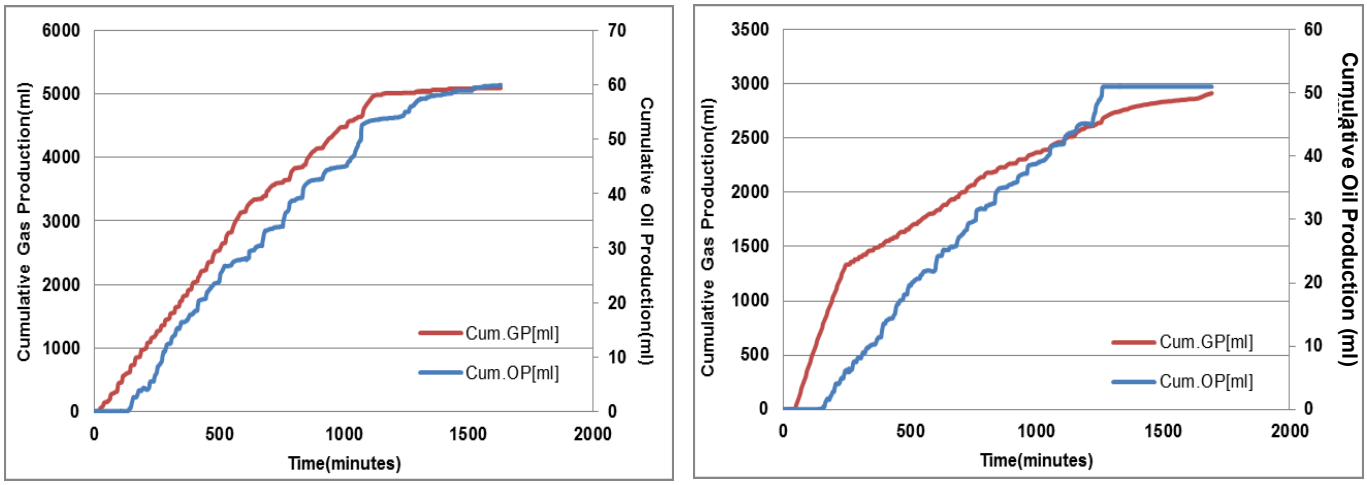

Figure 2.10—Cumulative oil and gas production of CH_4 62%-C_3H_8 38% (left) and CH_4 50%-C_3H_8 50% (right).

Data	CH_4 + CO_2 huff 'n' puff (1)		CH_4 + CO_2 huff 'n' puff (2)			CH_4- C_3H_8 Mixture		CO_2	
	CH_4 live oil	**Followed by CO_2**	**1st**	**2nd**	**Followed by CO_2**	**CH_4 62%-C_3H_8 38%**	**CH_4 50%-C_3H_8 50%**	**1st**	**2nd**
Produced Oil (ml)	120	114	98	131	114	60	51	192	172
Produced Gas (ml)	3,447	4,300	2,378	2,755	22,376	5,095	2,913	1360	2193
Cum. Producing GOR (vol/vol)	28.725	37.72	24.265	21.03	196.28	84.93	57.12	7.1	12.7
Oil Recovery Factor (%)	13.22	14.476	11.06	14.786	15.1	6.45	5.48	21.7	19.3
Total Oil Recovery Factor (%)	27.7		29.886						

Table 2.8—Summary of experimental results - CO_2 results from Rangriz-Shokri and Babadagli (2016).

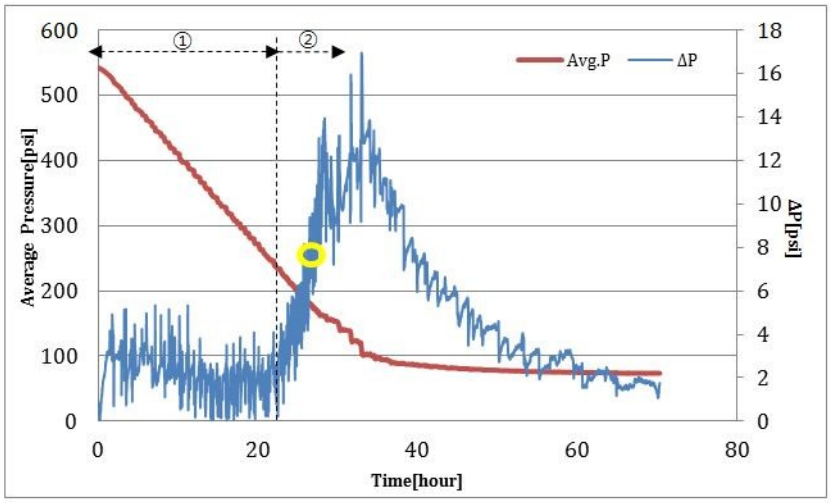

Figure 2.11—Pressure chart for -0.23 psi/min.

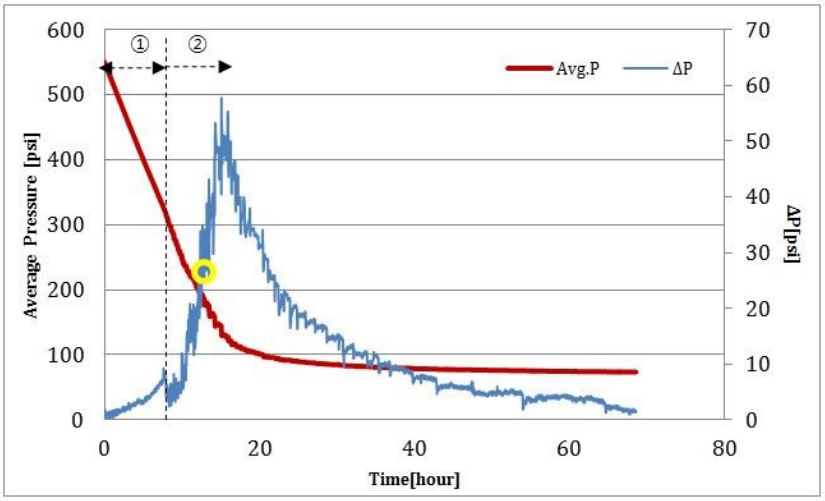

Figure 2.12—Pressure chart for -0.51 psi/min.

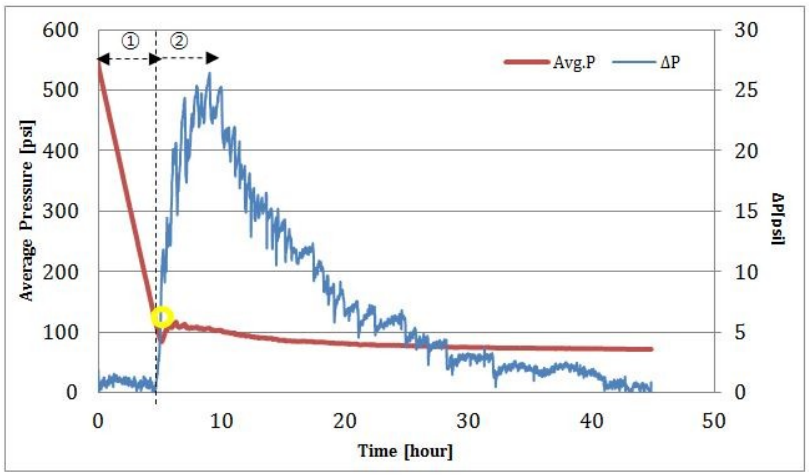

Figure 2.13—Pressure chart for -1.53 psi/min.

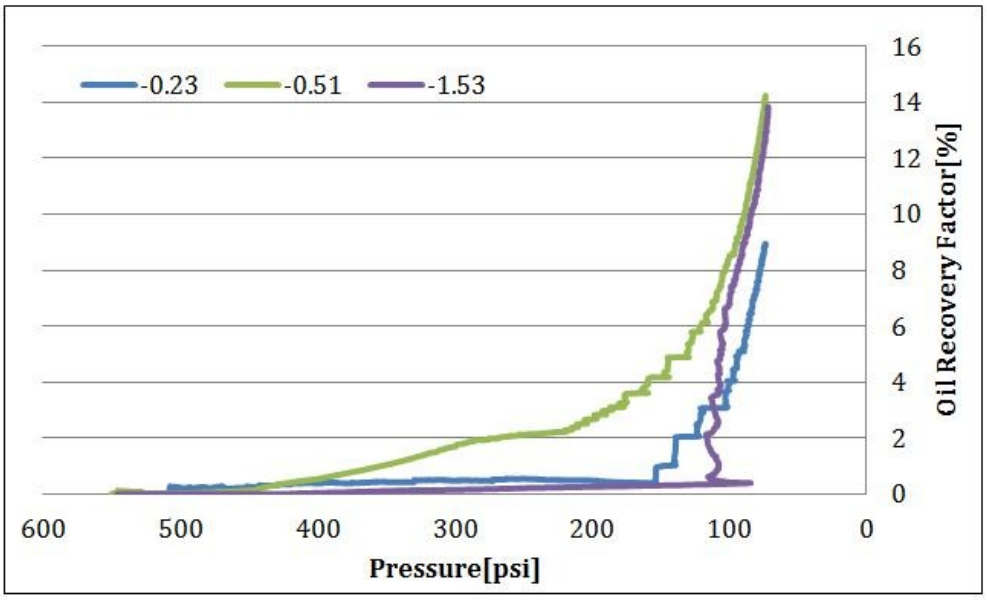

Figure 2.14—Oil recovery factor vs. pressure.

	-0.23 psi/min	-0.51 psi/min	-1.53 psi/min
Produced Oil [ml]	85	135	126
Produced Gas [ml]	4,673	2,005	1,500
Producing GOR [vol/vol]	54.97	14.85	11.9
Oil Recovery Factor [%]	8.95	14.21	13.84

Table 2.9—Results of CH_4 live oil core flooding with different depletion rates.

	Saturates	Asphaltenes	Resins	Aromatics
Initial oil	38.32	14.63	32.20	14.85
-0.23	31.36	13.91	36.93	17.80

Table 2.10—SARA results from initial oil and after the -0.23 psi/min experiment.

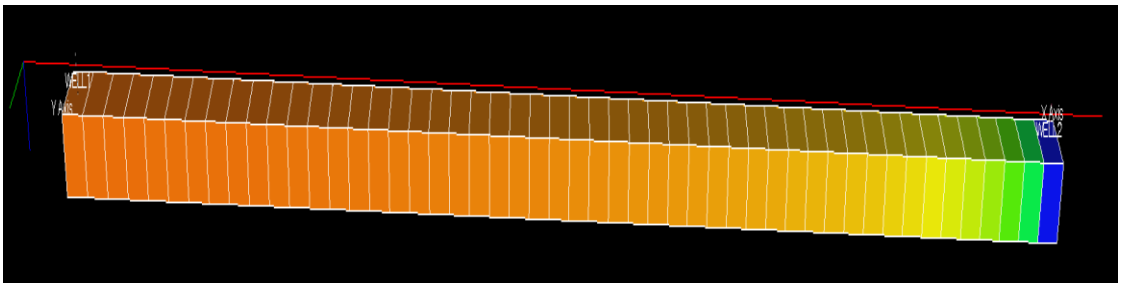

Figure 2.15—Simulated sand-pack model.

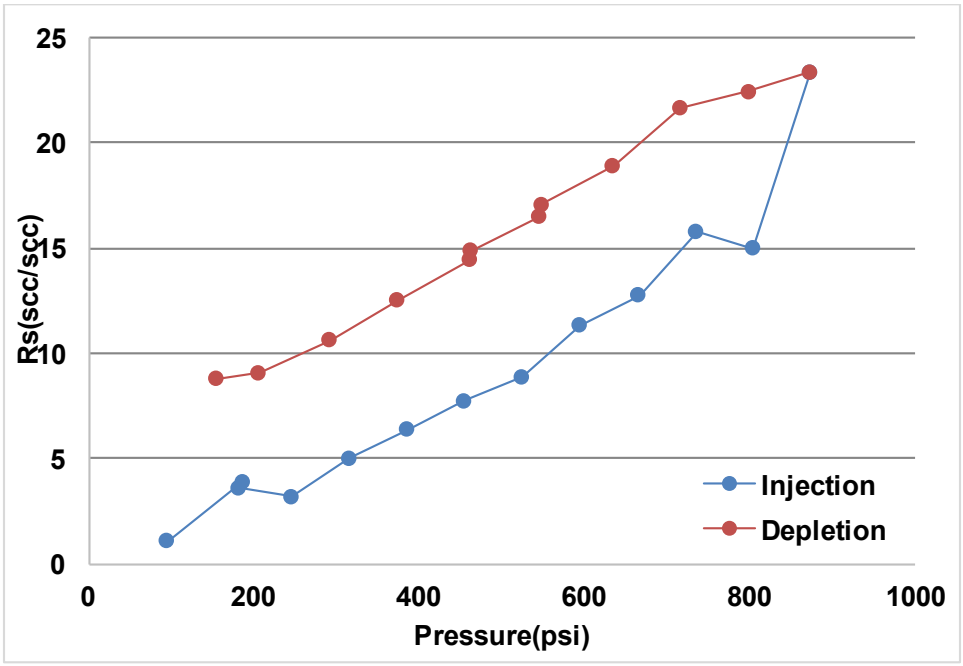

Figure 2.16—PVT experiment result: Solution GOR vs. pressure.

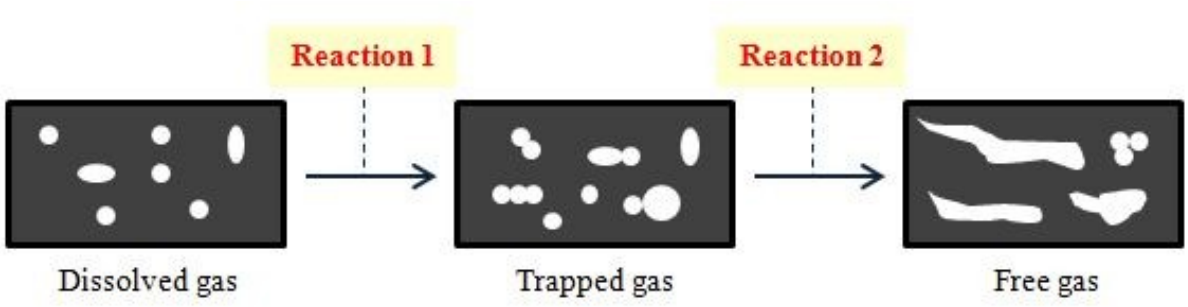

Figure 2.17—Schematic of reaction 1 and 2.

	Heavy Oil	Dissolved CH_4	Trapped CH_4	Free CH_4
Volatility type	Dead	Dead	Dead	Gas
Liquid-compressibility type	Oil	Oil	Gas	Oil
Molecular weight (kg/kg-mole)	486	16.043	16.043	16.043
Critical temperature (K)	1375.5	285.9	285.9	285.9
Critical pressure (kPa)	444.3	2302	2302	2302
K-values				
A, unitless	-1.686e-034	8.7565	8.7565	8.7565
B (barsa)	1.147e-032	560.8	560.8	560.8
C (1/bar)	-1.543e-035	0.231	0.231	0.231
D (K)	0.009997	570.4	570.4	570.4
E (K)	577.6	38.37	38.37	38.37

Table 2.11—Fluid characteristics in modeling 'Methane' case.

	Heavy Oil	Dissolved CH_4	Trapped CH_4	Free CH_4
Volatility type	Dead	Dead	Dead	Gas
Liquid-compressibility type	Oil	Oil	Gas	Oil
Molecular weight (kg/kg-mole)	486	16.043	16.043	16.043
Critical temperature (K)	917	190.6	190.6	190.6
Critical pressure (kPa)	1333	4604	4604	4604
K-values				
A, unitless	-1.844e-10	3.168	3.168	3.168
B (barsa)	1.339e-9	808.9	808.9	808.9
C (1/bar)	7.916e-12	0.004402	0.004402	0.004402
D (K)	0.01	319.9	319.9	319.9
E (K)	84	3.208	3.208	3.208

Table 2.12—Fluid characteristics in modeling 'Different depletion rates' case.

Sand-pack properties	Run 1			Run 2			Different depletion rates		
	Exp.	Simulation	Error (%)	Exp.	Simulation	Error (%)	Exp.	Simulation	Error (%)
Avg. porosity (%)	39.58	39.58	0	37.93	37.9	0	38.3	38.3	0
Avg. permeability (md)	12,657	11,500	9.1	990	1000	1	2105.88	2105	0
Bulk volume (ml)	2,533.54	2531.25	0	2,533.54	2531.25	0	2533.54	2531.25	0
Pore volume (ml)	1,002.85	1,001.87	0	961	959.34	0	970.6	969.5	0.1
Initial oil in place (ml)	907.5	911.7	0	886	873	0	950	950.11	0
Irreducible water saturation (%)	9.5	9	0.5	7.8	9	1.3	2.12	2	5.6
Initial oil saturation (%)	90.5	91	0.5	92.2	91	1.3	97.88	98	0.9
Free gas saturation (%)	0	0	0	0	0	0	0	0	0

Table 2.13—Comparison of experimental and numerical values – Sand-pack properties.

Final Results	Run 1			Run 2		
	Exp.	Simulation	Error (%)	Exp.	Simulation	Error (%)
Produced oil (ml)	120	123.96	3.2	98	93.6	4.5
Produced gas (ml)	3,447	3,599	4.4	2,378	2270	4.5
Produced water (ml)	0	0	0	0	0	0
Cum. Producing GOR (vol/vol)	28.725	29	4.4	24.265	24.25	0
Oil recovery factor (%)	13.22	13.6	2.8	11.06	10.72	3.1

Table 2.14—Comparison of experimental and numerical results (1).

Final Results	-0.23 psi/min			-0.51 psi/min			-1.53 psi/min		
	Exp.	Simulation	Error (%)	Exp.	Simulation	Error (%)	Exp.	Simulation	Error (%)
Produced oil (ml)	85	86	1.18	135	135.96	0.71	126	128.84	2.25
Produced gas (ml)	4,673	4,536	2.93	2,005	2,131.32	6.3	1,500	1526.4	1.76
Produced water (ml)	0	0	0	0	0	0	0	0	0
Cum. Producing GOR (vol/vol)	54.97	52.74	4.05	14.85	15.68	5.6	11.9	11.84	0.5
Oil recovery factor (%)	8.95	9.05	1.1	14.21	14.31	0.7	13.26	13.56	2.26

Table 2.15—Comparison of experimental and numerical results (2).

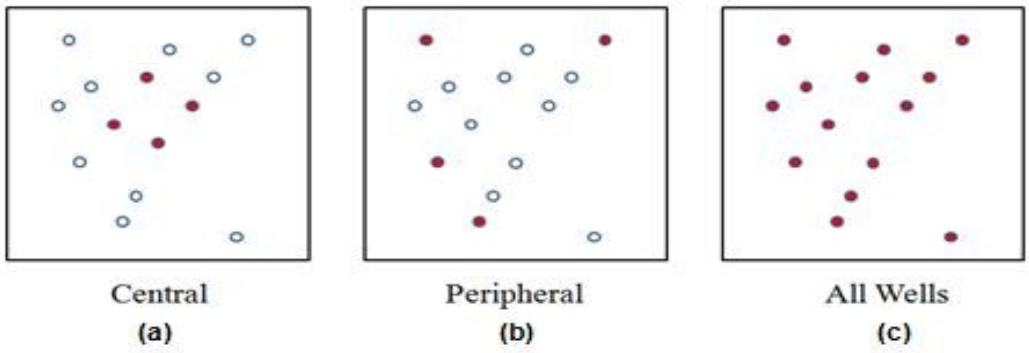

Figure 2.18—Well Patterns. Red: Injectors, white: producers in cases of (a) Central (b) Peripheral and (c) All-Wells.

	Cycle 1		Cycle 2		Cycle 3		Cycle 4		Cycle 5		Cycle 6	
Months	1	4	1	4	1	4	1	4	1	4	1	4
Central	11.49	11.17	14.67	14.05	17.75	16.87	20.63	19.66	22.64	22.33	24.31	24.37
Peripheral	11.79	11.17	15.24	14.05	18.58	16.87	20.88	19.66	22.73	22.22	24.27	24.34
All Wells	12.21	12.21	16.17	16.17	19.38	19.70	21.33	21.91	23.15	23.87	24.76	25.45

Table 2.16—Total oil recovery factor [%] after each cycle.

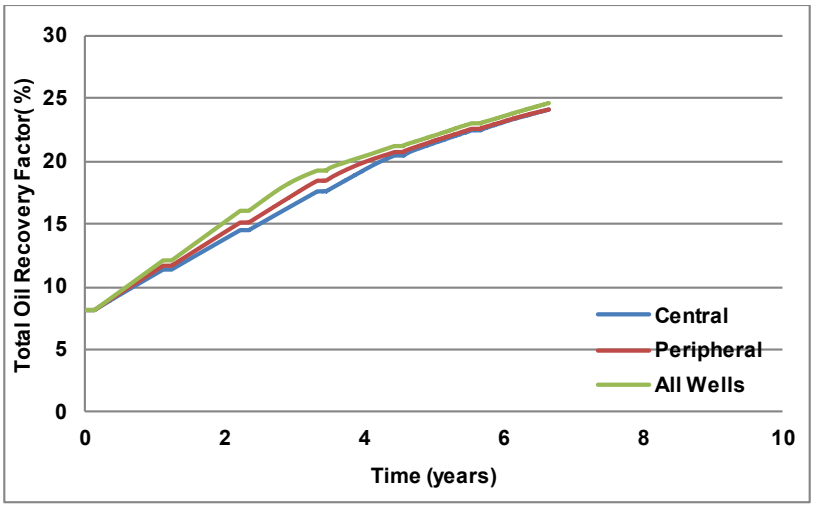

(a)

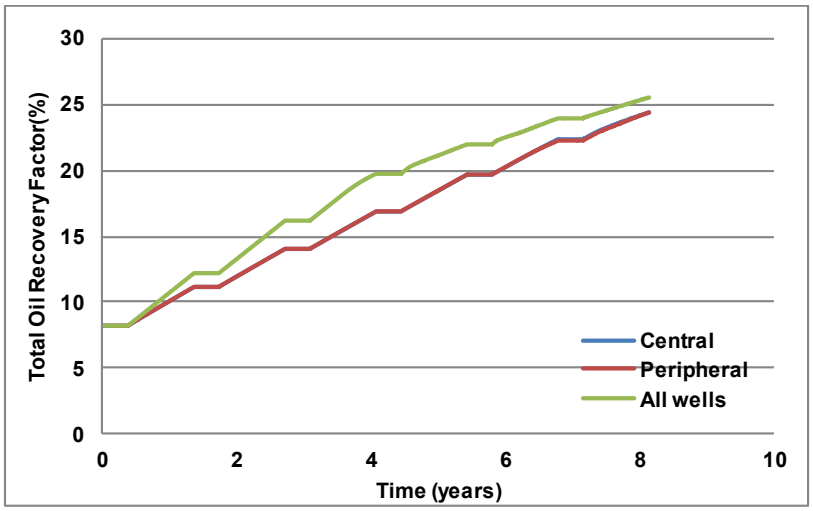

(b)

Figure 2.19—Total Oil Recovery Factor % in case of (a) 1-month Injection and (b) 4-month Injection.

	Central		Peripheral		All Wells	
	1 month	4 months	1 month	4 months	1 month	4 months
CH_4	17.75	16.87	18.58	16.87	19.38	19.70
CO_2	4	15.2	3.2	14	5.2	20.8

Table 2.17—Comparison of CH_4 and CO_2 field-scale simulation results - 3-cycle Injection.

Description	
Injection	
Control mode	2,000 sm3/day
BHP target	35 bar at 25°C
Production	
Duration	360 days
Control mode	Bottom-hole pressure (BHP)
Oil rate target	15 sm3/day
BHP lower limit	1 bar
Production economic limit	
Minimum oil production rate	1 sm3/day
Minimum gas or water rate	0

Table 2.18—Description of constraints/conditions.

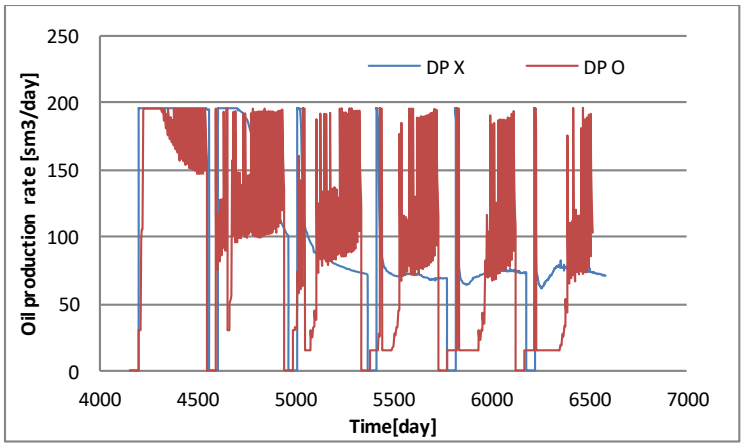

(a) Daily oil production rate vs. Time.

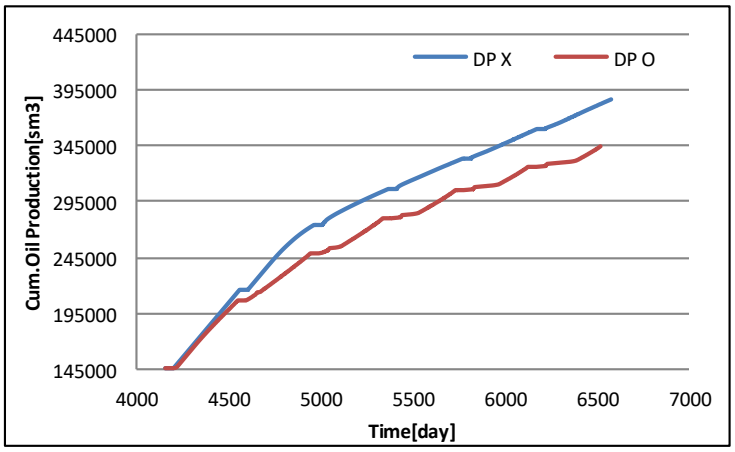

(b) Cumulative oil production vs. Time.

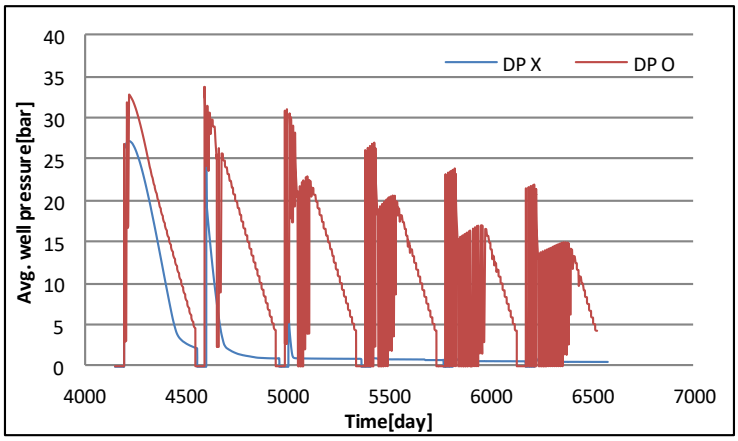

(c) Average well pressure vs. Time.

Figure 2.20—1-month injection/half-month soaking.

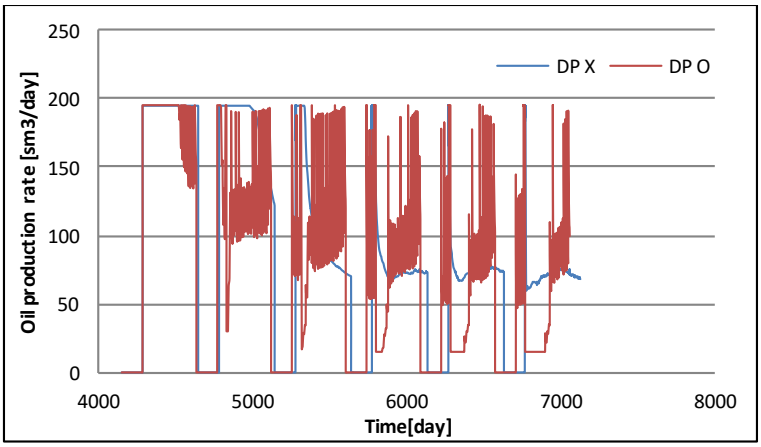

(a) Daily oil production rate vs. Time.

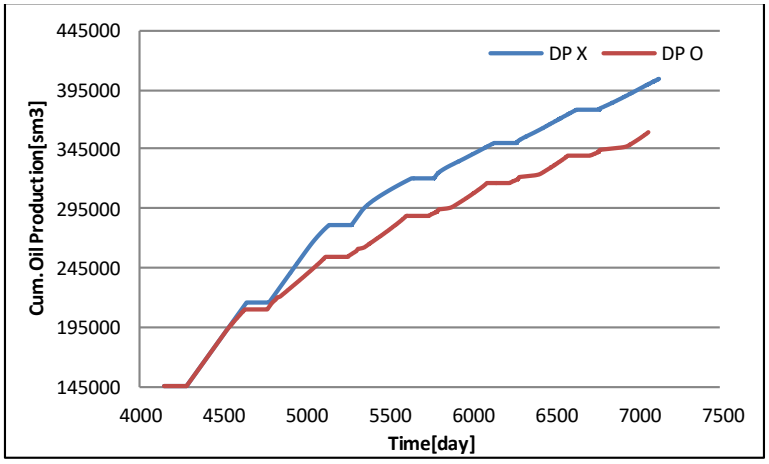

(b) Cumulative oil production vs. Time.

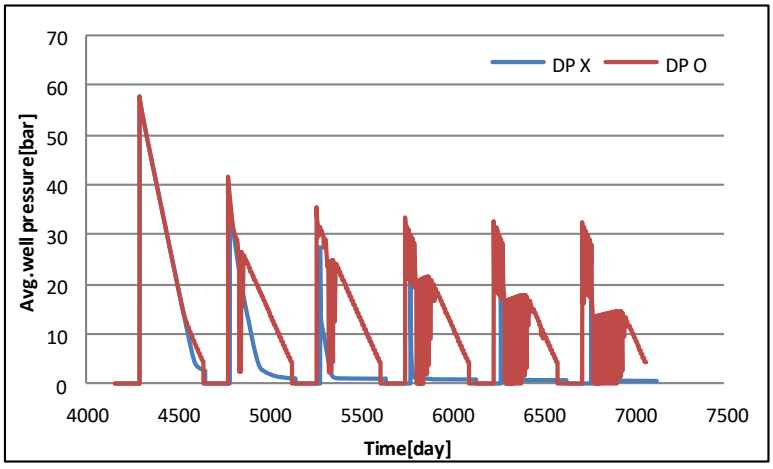

(c) Average well pressure vs. Time.

Figure 2.21—3-month injection/1.5-month soaking.

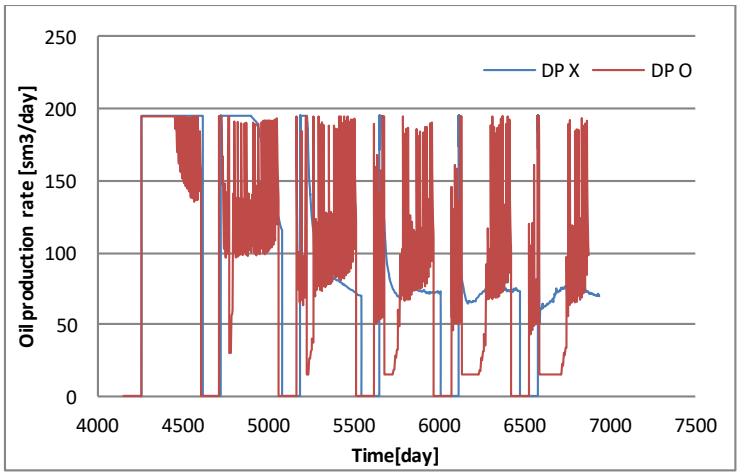

(a) Daily oil production rate vs. Time.

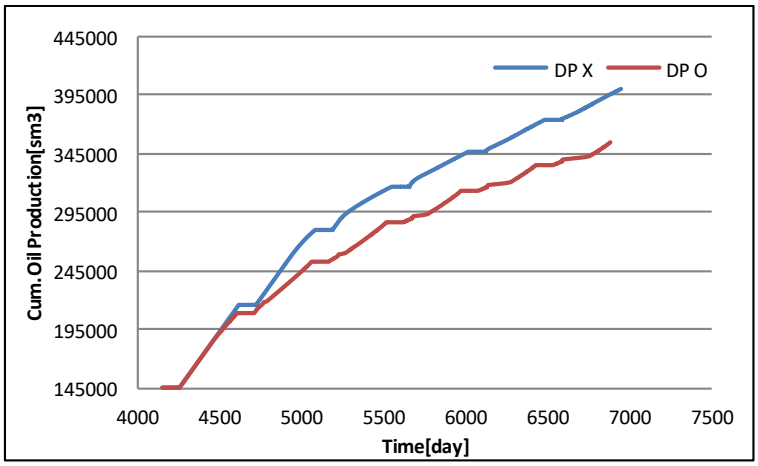

(b) Cumulative oil production vs. Time.

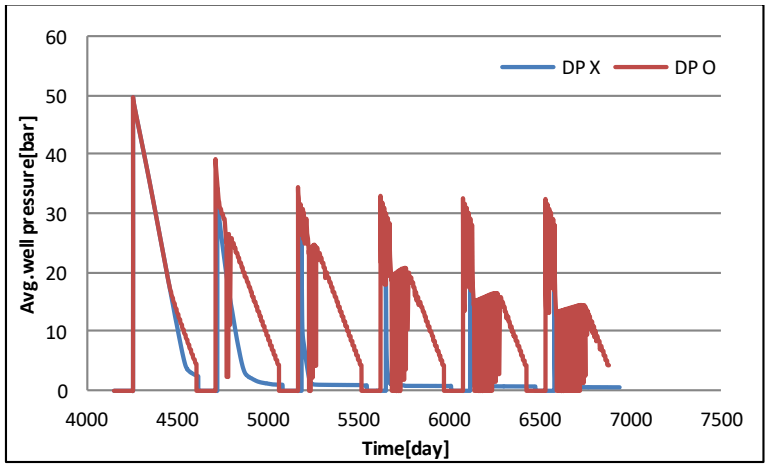

(c) Average well pressure vs. Time.

Figure 2.22—3-month injection/half-month soaking.

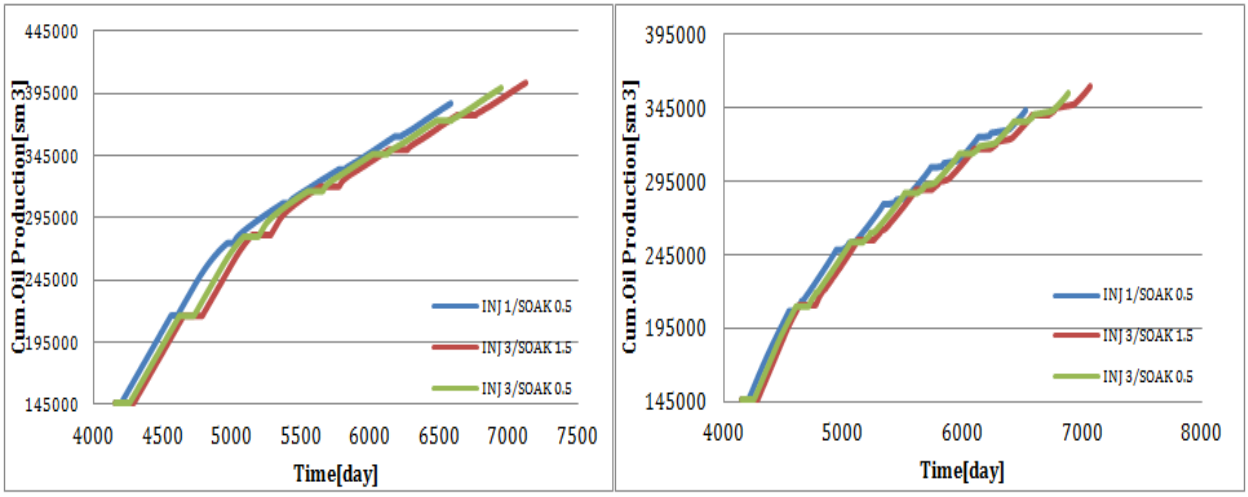

Figure 2.23—Cumulative oil production vs. Time for 'DP X' case (left) and 'DP O' case (right).

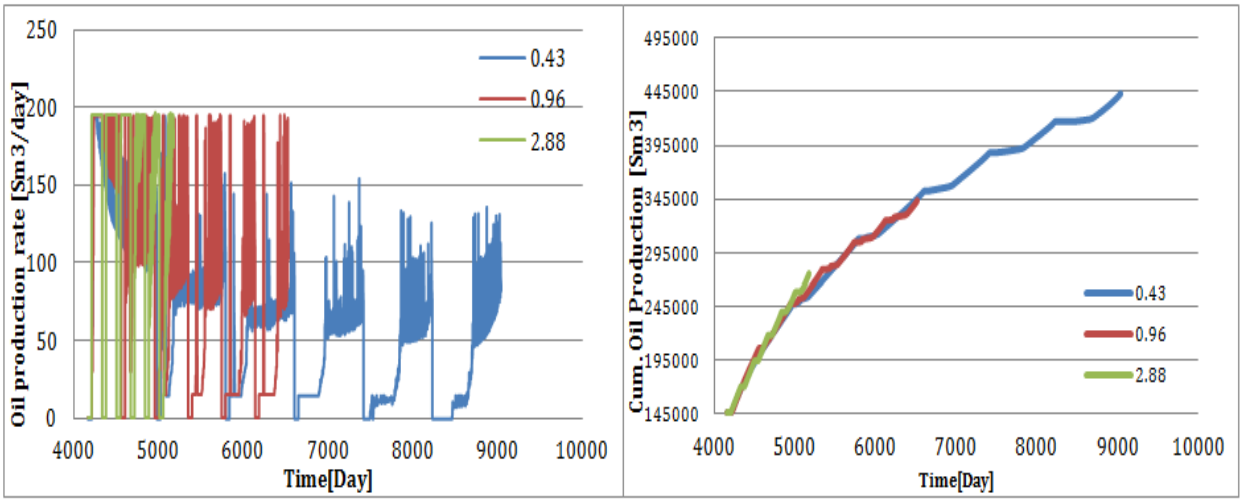

Figure 2.24—Scenario 1: 1-month Injection/half-month Soaking – left: Daily oil production rate, right: Cumulative oil production.

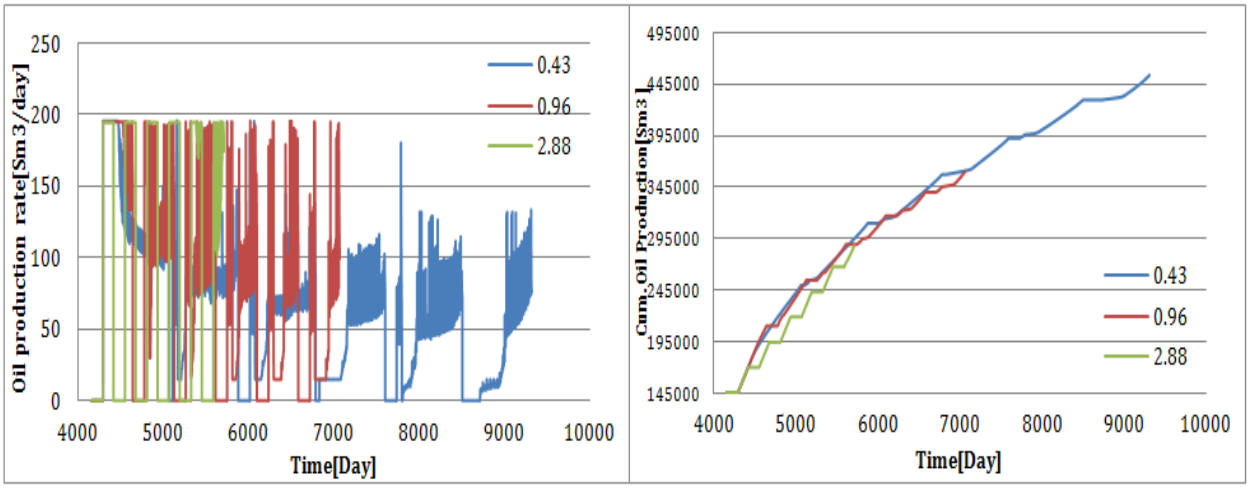

Figure 2.25—Scenario 2: 3-month injection/1.5-month soaking – left: Daily oil production rate, right: Cumulative oil production.

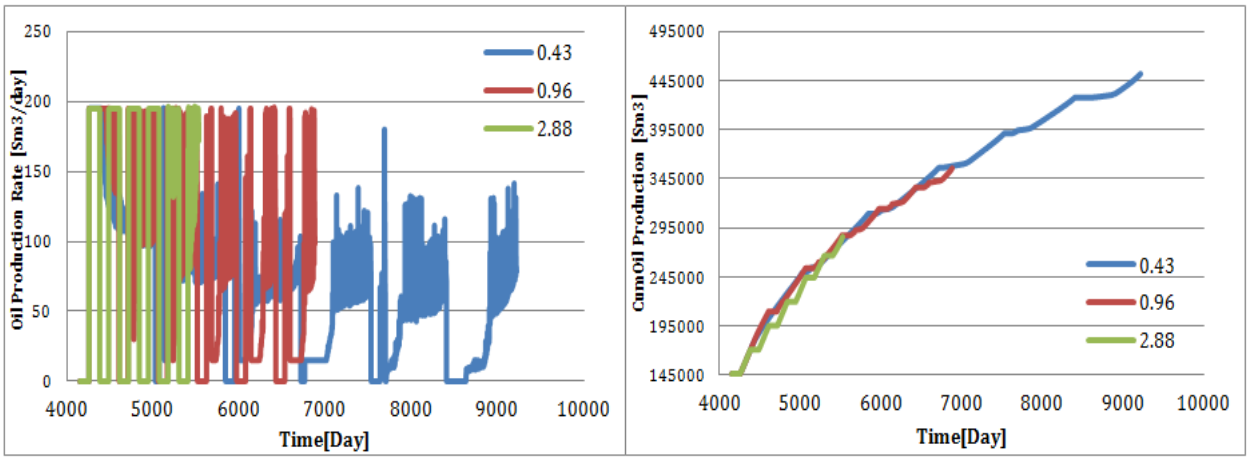

Figure 2.26—Scenario 3: 3-month injection/half-month soaking – left: Daily oil production rate, right: Cumulative oil production.

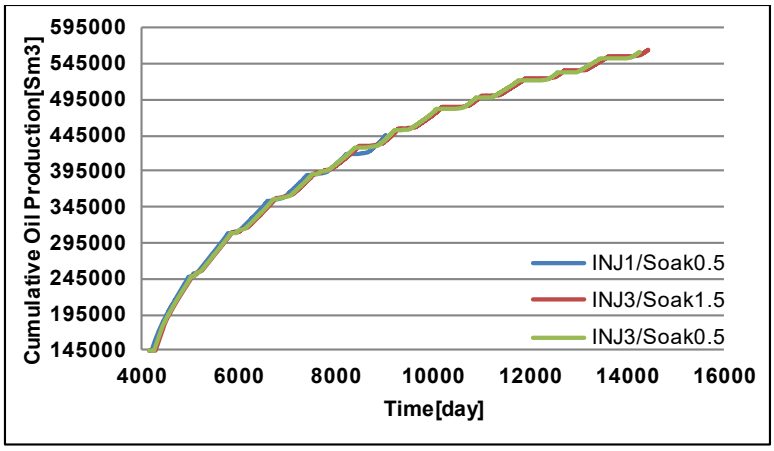

(a) Cumulative oil production for '-0.43 bar/10 day' case.

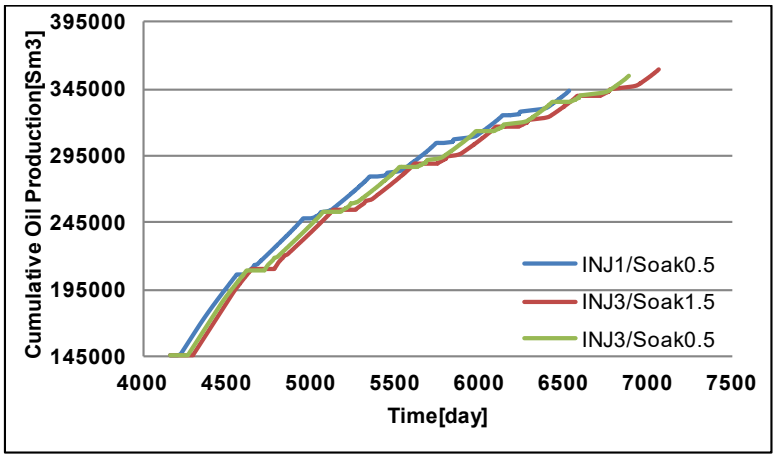

(b) Cumulative oil production for '-0.96 bar/10 day' case.

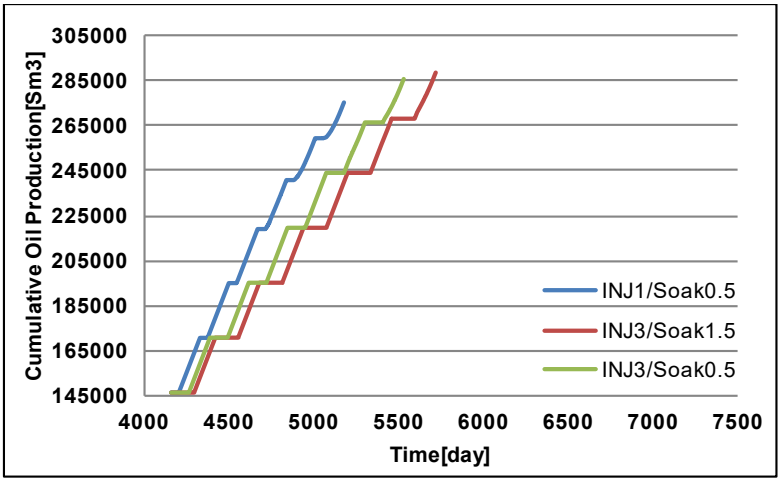

(c) Cumulative oil production for '-2.88 bar/10 day' case.

Figure 2.27—Results of three injection/soaking scenarios for each depletion-rate case.

Chapter 3 Cost-Effective Heavy Oil Recovery by Gas Injection: Improvement of the Efficiency of Foamy Flow and Pressurization

** Presented at the *SPE/IATMI Asia Pacific Oil & Gas Conference and Exhibition, Bali, Indonesia* in October 2017.

3.1 Preface

Primary recovery of heavy-oil is remarkably low due to high oil viscosity and low energy by solution gas ex-solution to drive the oil. Gas injection to improve foamy flow and also to dilute the oil in such reservoirs has been proposed as a secondary recovery method. However, because of the high costs of injected gases, efforts are needed to optimize the process by selection of proper gas type (or gas combinations) and suitable injection scheme. To achieve this goal, an experimental procedure was followed with rigorous analyses of the output. A 1.5 m long and 5 cm diameter sand-pack was first saturated with brine, which was replaced with dead oil. Then, gas solvents were injected to dead-oil containing core-holder until nearly reaching 500 psi, followed by a two-day soaking period. Pressures all along the sand-pack were recorded with eight pressure transducers. Different combinations of various gas solvents (methane, CO_2, and air) aiming to select the most competitive and economic formula were tested with a certain set of pressure depletion rates.

The physics of the foamy oil flow for different solvent mixtures and depletion conditions were analyzed using pressure profiles acquired, recorded oil/gas data with time, and gas chromatography and SARA analyses of the produced gas and oil. Three huff-n-puff cycles were applied. Compared with other light hydrocarbon solvents and carbon dioxide, air has its high advantage in terms of accessibility and lowered cost. Hence, attention was given to air that was mainly used to pressurize the system and increase oil viscosity due to oxidation process with an expectation of better foam quality when injected with other gases such as CO_2 and methane. Methane (CH_4) yielded the quickest response in terms of gas drive but, in the long run, CO_2 was observed to be more effective technically. Air was observed to be effective if mixed with CO_2 or methane from an economics point of view. To sum up the results, air Huff-n-Puff (HnP) followed by 2-cycles of CH_4 HnP yielded 36.21% recovery, while air HnP followed by 2-cycles of CO_2 HnP delivered 30.36% oil. When the gases are co-injected, air 50%-CO_2 50% and air 50%-CH_4 50% recovered 29.85% and 23.74% of total oil-in-place, respectively.

Key words: Cyclic solvent injection, post-CHOPS EOR, methane, CO_2, air, foamy oil corefloods

3.2 Introduction

Heavy-oil can be produced by its natural drive if the dissolved gases in the oil phase come out and create a discontinuous phase making oil foamy. This can be achieved by injecting light hydrocarbon gases or CO_2. As a follow-up method for Cold Heavy Oil Production with Sands (CHOPS), cyclic solvent injection (CSI) can be applied in this manner. The gas solvents can pressurize depleted reservoirs after CHOPS, and wormholes can work positively with solvents by increasing contact area between solvents and heavy oil in the matrix for effective diffusion. Under high pressure, solvents become dissolved into heavy oil and this heavy oil containing gas solvents starts to release gas gradually with given pressure drawdown. Because of high oil viscosity, compared with conventional solution-gas drive it takes a much longer time for dissolved gas-bubble to be completely separated from heavy oil to free-gas phase. This oil state is called "foamy oil". Foaminess gives efficient driving force for highly-viscous heavy oil to be produced. However, since the effective use of solvents is necessary due to the high solvent costs (especially propane and carbon dioxide), studies have focused on the effect of solvent type on the generation of good quality foamy oil (Sheng et al. 1997, 1999) and the impact of solvent type on the foaminess performance (Diedro et al. 2015).

Sheng et al. (1997) studied foamy oil stability and concluded that under the conditions with higher oil viscosity and higher dissolved gas amount, the foamy oil becomes more stable. When using faster pressure decline rates where fluid speed is most likely higher, they discovered the a lot of smaller bubbles were generated and scattered for a long time, which contributes to foamy oil stability. Alshmakhy and Maini (2012) defined foam stability as the reference point that shows the speed of foam decays when left in a static state, which is related to surface activity. This surface activity is influenced by viscosity, surfactant type, and concentration.

Looking into the process of gas-bubble formation to decay, Albartamani and Farouq Ali (1999) separated this process into four steps: supersaturation, bubble nucleation, bubble growth, and bubble coalescence/breakup. They illustrated that higher supersaturation led to more gas-bubbles, and, as bubble nucleation rate becomes slow with oil viscosity (Walton 1969), the degree of supersaturation also becomes higher for more viscous oil. Nevertheless, it should be noted that even if most of the gas solvents show consistency with these four steps when undergoing unconventional solution-gas drive, the degree of each step should be different according to

solvent type as every gas solvent manifests different chemical/physical behaviour with heavy oil (e.g. mass/heat transfer, surface tension, etc).

Previous studies were mostly on the performance of foamy oil or the factors that affect foam quality. Yet, studies on specific solvents individually and their chemical and physical behaviour with heavy oil are limited. This study reports an experimental study of foamy oil created by various gas solvents. The focus was on air used as an EOR agent due to its low cost. This idea stems from the fundamental knowledge that low-temperature oxidation increases oil viscosity (Mayorquin and Babadagli 2016a-b), and, under unconventional solution-gas drive, the more viscous oil is, the slower dissolved-gas is released, resulting in higher oil recovery. Sheng et al. (1997) also proved that higher oil viscosity plays a role in enabling higher resistance to the flow of gas bubbles in the liquid oil phase; hence the foamy oil system becomes more stable. This paper covers a comprehensive experimental analysis of gas injection for heavy-oil recovery. Operational conditions for the optimal use of different solvents in various combinations of methane, CO_2, and air, and for air to achieve an economically more feasible application.

3.3 Experimental Work

Sands were sorted with sieves and 250-500µm size sands were poured into a 1.5 m length and 5 cm diameter core-holder filled with water. During this process, the core-holder was vertically positioned and hammered until the sands have densely packed the core-holder. Porosity was measured by the difference of water in and out volumes. Absolute permeability was measured by injecting water into the system applying Darcy's law. Next, brine was flushed to replace water in the sand-pack. Note that brine was injected at a very slow rate and every port was open one-by-one to check if brine fully filled the system and removed existing free-gas. Subsequently, 1.2 PV of dead oil was injected until no more water came out. At the end of this process, the initial oil and water saturations were estimated.

Designated gas (solvent, air or mixture) was directly injected into the dead oil-filled sand-pack until the pressure reached 500 psi (injection stage). After 2-3 days of soaking (soaking stage), production was started with given depletion rates until all the pressure ports showed ~70 psi (production stage). Depletion rates used were -0.51 psi/min from ~500 to 190 psi (the 1st

depletion stage), and -0.23 psi/min from 190 to 70 psi (the 2nd depletion stage). These three stages—i.e., injection, soaking, production—were repeated whenever restarting a new cycle.

For the cases beginning with air huff-n-puff (air experiments showed the recovery of slightly lower than 10% original oil in-place), the next secondary recovery stage started. The experimental setup is displayed in **Figure 3.1**. All the pressure data were recorded with eight pressure transducers, of which the locations are shown in **Figure 3.2**. The properties of dead oil (obtained from a field in Eastern Alberta) were 0.95 of the specific gravity, and 27,400 cp of the viscosity measured at 25°C.

3.4 Results and Analysis

Four different experiments were carried out. Note that air was used to increase oil viscosity initially so that secondary recovery, such as CH_4 or CO_2 huff-n-puff, took advantage of this higher oil viscosity by making better foaming performance. Sand-pack properties are illustrated in **Table 3.1**. The experimental results for the four different injection schemes listed below are summarized in **Table 3.2**:

Exp.1: Air Huff-n-Puff, followed by CH_4 *Huff-n-Puff*

Exp.2: Air Huff-n-Puff, followed by CO_2 *Huff-n-Puff*

Exp.3: Air 50%-CO_2 *50% Huff-n-Puff*

Exp.4: Air 50%- CH_4 *50% Huff-n-Puff*

3.4.1 Pressure differential

Considering pressure differential, ΔP = P2-P7 (Figure 3.2), can be a useful indication of foaming capacity of oil (Soh et al. 2016), the first analysis of the experiments were done using this data. Air huff-n-puff experiments (**Figures 3.3 and 3.4**) showed smaller and less frequent fluctuations in ΔP compared with the experiments with CH_4 (**Figures 3.5 and 3.6**) and CO_2 (**Figures 3.7 and 3.8**) huff-n-puff, and showed lower oil recovery. When comparing the ΔP profiles of the 1st and 2nd cycles of methane and CO_2, great reduction in ΔP amplitude was observed in the 1st depletion stage (about/above 500 to 190 psi) of the 2nd cycle (compare Figure 3.5 with 3.6 for methane, and Figure 3.7 with 3.8 for CO_2). This ΔP "shape" difference between the 1st and 2nd cycle was similarly noticed in the case of CH_4 live oil depletion between lower and higher depletion rate by

Soh et al. (2017). This implies that the higher the depletion rate given, the bigger the reduction of ΔP in the 1st depletion stage observed. The difference—shown in the 1st and 2nd cycle and shown in the higher and lower rate—stems from the degree (or quality) of foaminess. As the cycle is repeated, the impact of air left in the sand-pack from the very first air huff-n-puff is reduced and the contribution of foaminess of CH_4 or CO_2 to oil production becomes greater. Likewise, as depletion rate is faster, a larger number of small-size bubbles tend to be formed, which can stay in oil phase for a longer time. Therefore, oil recovery becomes higher compared with when depletion rate is low (Sheng et al. 1997).

Exp. 3 (Air 50%- CO_2 50% co-injection) presented very unique patterns (**Figures 3.9-11**). The 1st cycle of Exp. 3 did not recover much oil (5.78%). From this low oil recovery and similar ΔP profile to air huff-n-puff (Figures 3.3 and 3.4), one may conclude that air, out of the mixture of air and CO_2 gas, dominated the whole process in the 1st cycle. Another supporting data for this observation was GC analysis of the produced gas, which consisted of mostly nitrogen and oxygen (**Table 3.3**). In the 2nd cycle, the governing gas became CO_2 rather than air as high oil recovery (14.72%) was obtained and a similar ΔP graph-shape to the one usually obtained for highly foamy oil. These observations also imply that different diffusion rates are of significant importance when using gas mixtures; CO_2 showed slower diffusion rate than air did but the recovery (or foaming capability) was much higher. Heavier molecular weight of CO_2 (44.04 g/mol) than air (28.97 g/mol) might be one of the reasons for this. The ΔP profile in the 3rd cycle (Figure 3.11) displayed bigger fluctuations than any other foamy oil. Inconsistency in the composition of the flowing gas can be suspected to cause this high fluctuation, as air and CO_2 gas left in the sand-pack from the 1st and 2nd cycle and the mixture-gas newly-injected conflicted with each other during overall production.

Exp. 4 (Air 50%-CH_4 50%) showed very different way of pressure depletion from other experiments, and accordingly, pressure differential change with time was also detected to be peculiar (**Figures 3.12 to 3.14)**. Starting from ~110 psi (green-circles on Figures 3.12 to 3.14), regardless of the depletion rate, pressure depletion was disturbed and static pressure was maintained only for 10-20 hours. Then, pressure reacted to the given depletion rate, and a decline in ΔP reappeared which led to additional oil recovery. This period – static pressure for 10-20 hours and sudden depletion – is repeated until the end of production.

In Exp. 3, main composition of released gas from live oil was different in each cycle, possibly due to the difference of each gas' (air, CO_2) molecular weight. In contrast, in every cycle of Exp. 4, each gas – air and CH_4 – from the mixture-form of injected gas tended to flow together. Since air and CH_4 gas bubbles are more likely to flow together, but their sizes are different, more numbers of bubbles are easily trapped in the pores. ~110 psi is assumed to be the pressure where the gas bubbles fills up (to the maximum capacity that pores can contain). Then, the pressure of overall depleting environment becomes static. While the pressure being static (marked as 'static pressure' in Figures 3.12 to 3.14), the gas bubbles still change their position and there is a possibility to connect to each other, generating a small pressure drop and oil recovery.

3.4.2 Comparison of methane (CH_4) live oil production in different scenarios

One of the most common and current practices is to inject methane for enhanced heavy-oil recovery due to availability and lower cost compared to other solvents. The foaming and recovery capability of methane was investigated in our earlier study (Soh et al. 2017) and current work following four different production schemes:

Case 1: CH_4 live oil production with different depletion rate
Case 2: CH_4 live oil production with typical depletion rate
Case 3: CH_4 live oil production after air huff-n-puff
Case 4: Air 50%-CH_4 50% live oil production

Four results of these cases are summarized in **Table 3.4**. It was observed that higher foam quality and fast pressure depletion rate are needed for high oil recovery (Soh et al. 2017). However, after certain depletion rate, it was observed that foam quality became the dominating factor (-0.51 psi/min depletion rated yielded almost similar recoveries as the -1.53 psi/min case, refer to Case 1 in Table 3.4). Better foam quality was proven by having bigger amplitude of ΔP (Compare ΔP in Figure 3.15 with Figures 3.16 and 3.17) and a longer time to reach $\Delta P = 0$ (compare pressure charts in **Figures 3.16 and 3.17**).

When oil was soaked with air prior to methane injection (Exp. 1), oil production obviously increased. With the impact of air, which allows a longer time in non-equilibrium status of live oil, the gas phase of methane can stay in the oil phase more stably and generate better foam quality,

eventually yielding more oil recovery. The CH_4 cycles in Case 3 gave higher oil recovery than higher depletion rate (-0.51 and -1.53 psi/min) in Case 1 and the same typical depletion rate in Case 2. Hence, the role of air huff-n-puff period to induce more oil production in advance to CH_4 huff-n-puff proved beneficial. However, when CH_4 and air was injected simultaneously (Case 4), the result is not as much positive as Case 3. Since "normal" (or expected) pressure depletion did not proceed and disturbed behaviour was observed starting from certain pressure (~110 psi), Case 4 did not produce as much oil as the other cases. However, this disadvantage could be helpful in terms of maintaining pressure for longer periods in the depleted system.

3.4.3 The importance of the amount of air injected

From the experimental results of CH_4 and CO_2 live oil depletion (Soh et al. 2016; Rangriz-Shokri and Babadagli 2016), it was expected that Exp. 2 would show higher oil recovery than Exp. 1, but the results were the opposite; i.e., Exp. 1 produced about 6% more oil than Exp. 2. This can be attributed to the difference in the air volumes injected. In fact, air volumes injected of air huff-n-puff for CO_2 case was about 3 times more than for the CH_4 case. This outcome can also be supported by the shape of the Exp. 2-Cycle 1 shown in **Figure 3.19**, which does not follow the trend of typical foamy oil recovery behaviour (Compare the Exp. 1 – Cycle 1 in **Figure 3.18**).

Due to the low diffusion rate of air, a big portion of air from the previous injection stage had an impact on the cycles of the secondary recovery. Hence, it is crucial to inject a proper amount of air at the first stage, which was found to be less than 1/3 PV in this case based on the experimental results in order to take advantage of the air for better foaminess of the secondary recovery. Note that the optimal amount of air to be injected is yet to be determined; 1/3 PV suggested here is only an empirical value.

3.4.4 Production mechanisms of air huff-n-puff and the effect of air phase on the subsequent cycles

After air was injected to dead oil and "soaked", the dead oil became polymerized due to the oxidization effect causing an increase in oil viscosity. It also did not show a high degree of foaming. Therefore, at the air huff-n-puff stage, the contribution of driving force to oil

production was mostly from gradual pressure drawdown with only a small amount of foamy contribution. It was observed that a small amount of oil was obtained through the pressure depletion and the production barely occurred towards the end of depletion period (**Figures 3.18 and 3.19 –** Air [Exp. 1], Air [Exp. 2]). On the other hand, experiments conducted with methane or CO_2 (Exps. 1, 2 – Cycle 1, 2) after air huff-n-puff showed different reactions to pressure depletion compared to the ones shown in the initial air cases. The period of the oil production can be divided into 3 parts, depending on the pressure decline when using -0.51 psi/min and -0.23 psi/min decline rates and after the pressure reached its threshold value of 70 psi. As can be inferred from **Figures 3.18, 3.19, and 3.20**, all the cases except the air case showed that almost nothing was produced until pseudo-bubble point pressure (P_{bs}, which is around 450 to 500 psi for both Exps. 1 and 2).

According to Tang and Firoozabadi (2001), above the pseudo-bubble point pressure, oil production occurs only from expanded oil volume. Because of high surface tension and high viscosity of oil, oil did not seem to expand sufficiently to contribute to oil production in this period. Higher pressure depletion rate causes more and smaller bubbles to be formed, which can be dispersed for a longer time in the oil and lead to higher oil recovery than lower depletion rate (Sheng et al. 1997). In other words, under low pressure depletion rate, small bubbles coalesce to generate larger bubbles and eventually form into continuous-phase gas clusters (Sheng et al. 1997). For -0.51 psi/min depletion rate starting from pseudo-bubble point pressure, small-size bubbles, which have enough size to drive oil to be produced, were developed and oil began to be delivered actively.

Comparing the oil recovery graphs (air huff-n-puff) and Cycle 1 cases (of Exps. 1 and 2) in Figures 3.18 and 3.19 it can be observed that the 1st cycle follows a similar shape pattern with air huff-n-puff (HnP), but yielded much higher oil recovery. The reason for this similar shape but showing higher oil recovery can be explained by the phenomena that a certain amount of air left in the core system is produced together with CH_4 or CO_2 gas-bubbles staying in the foamy-and-oxidized-oil. In addition, as noted earlier, higher oil viscosity obtained through oxidation gives better stability of dispersed gas bubbles, which yields a much stronger driving force for oil to be delivered. Hence, when air and CO_2/CH_4 huff-n-puff is applied in a sequence, as CO_2/CH_4 cycle

is repeated, foamy behaviour becomes more distinctive and more oil production occurs with the cycle.

On the other hand, when mixture-form of gas solvent [air+CO2 (Exp. 3) or air+CH4 (Exp. 4)] was applied, the influence of air and CO_2/CH_4 was observed at the same time. As mentioned earlier in the "Pressure differential" section, the governing gas composition in each cycle was different due to the difference in each gas' diffusion rate. This difference was more distinctive in Exp. 3 than in Exp. 4. As can be speculated from Figures 3.9 to 3.11 and Figure 3.20 for Exp. 3, air dominated most of the flowing gas in cycle 1, while the dominating gas was CO_2 in cycle 2, and both air and CO_2 in cycle 3. As air and CH_4 gas bubbles were more likely flowing together in Exp. 4 (see Figures 3.12 to 3.14 and **Figure 3.21**), not sufficient force was obtained to deliver as much oil as when they flow separately.

3.4.5 Gas chromatography and SARA analyses

Since extra-heavy oil was used in this study (API ≈ 17.45; viscosity = 27,400 cp at 25°C) and experiments were conducted under isothermal conditions without any diluent, no remarkable change in oil components were observed in the SARA analysis (**Table 3.5**). Gas Chromatography (GC) results of oil after each cycle of experiments are shown in **Figures 3.22** to **3.25**. Oil compositions were arbitrarily divided into 6 groups by carbon numbers: 5 to 20, 21 to 40, 41 to 60, 61 to 80, 81 to 100, and over 100. One may observe that mass percent change in the first three and the last three groups displayed opposite outcomes. This can be attributed to an increase in oil viscosity that caused an augmentation of high carbon number-compositions (61-80, 81-100, 100+) and a decrease in low carbon number components (5-20, 21-40, 41-60); see the values of oil viscosity in **Table 3.6** and Figures 3.22-25. Only a small change in oil composition was detected in Exp. 2 compared with the others.

3.4.6 Producing gas-to-oil ratio (GOR)

According to Alshmakhy and Maini (2012), GOR appears with a high number due to the tubing length between the outlet and the oil collector, initially. After some time, this error is reduced and initial GOR can be accurately known. Whilst oil producing rate stays high, GOR is more or

less kept as a constant during heavy-oil recovery by depletion. When the system goes down to a certain pressure, the continuous phase of gas starts to flow and GOR increases linearly with time. Note that during this time, there are still dispersed-phase gas bubbles flowing as well as continuous ones. Based on these observations, the initial GOR of air huff-n-puff could be estimated to be ~6 (**Figures 3.26 and 3.27**), and air provided oil with very little "foaminess", thereby giving only a small amount of oil recovery. Nonetheless, CH_4 and CO_2 cycles in Exp. 1 and 2 (Figures 3.28 to 3.31) did not show any accordance with Alshmakhy and Maini's (2012) observations; GOR is increasing while pressure depletion is ongoing and starts to decrease or to be constant after reaching 70 psi. This can be attributed to the fact that not all of the injected gas solvents (e.g. CH_4, CO_2) were dissolved in the dead oil, and therefore there could be free gas in the beginning. As the pressure reached pseudo-bubble point, both free gas and dispersed gas bubbles started to flow together. Needless to say, oil production was accompanied more actively with dispersed gas flow and, as a result, the rate of GOR increase became slower. Therefore, if all the injected gas solvents were dissolved by longer soaking or possible methods to accelerate the diffusion of the solvent into the oil, there should have been more oil recovery with larger driving force by a larger amount of dispersed gas bubbles.

Also, in two cycles of Exps.1 and 2, oil production went on even after pressure was stabilized at 70 psi while GOR was decreasing or constant (**Figures 3.28-31**). This was much more critical for the 2nd cycle of Exp. 1 and 2(Figure 3.29, 3.31), showing that most of oil recovery was attained after this final pressure. This can also be observed in Figures 3.18 and 3.19 through steep incline of recovery after 100 psi (when P8 reaches 70 psi) for all cases but air. The GOR behaviour in Exps. 3 and 4 is different from Exps. 1 and 2. In case of Exps. 3 and 4 (Figures 3.32 to 3.36), GOR started to decrease from the point when oil is actively recovered. From ~110 psi (point where the pressure stabilized first time), oil recovery was stabilized (constant). However, since the gas did not produce further after this point, GOR decreased in step-like manner starting from ~110 psi.

3.4.7 Different foamy oil behaviour

The reason for different pressure fluctuation and oil recovery is mainly based on different foamy oil behaviour. To look into this, pictures were taken every two hour and are shown in **Figures**

3.37-39, of which the first one represents when the first oil-bubble dropped at the bottom of cylinder.

As concluded in earlier sections through the analysis of pressure differential and producing GOR, oil was delivered with considerably little foams caused by air, which were highly unstable and prone to collapse easily (Figure 3.37). Yellow circles in this figure show where the bubbles appeared. Three to four bubbles were observed initially but within about 12-hour, bubble collapse was observed (only one bubble was left at this time). Due to this very low foam quality, the rate of oil production was not affected by the depletion rate (Figures 3.26 and 3.27). Therefore, it can be stated that the producing mechanisms of oil at the air huff-n-puff stage was the expansion of oil with trivial contribution of foaminess, which resulted in low oil recovery.

Unlike the air huff-n-puff case, obvious foaminess was observed in the subsequent phases (CH_4 and CO_2 huff-n-puff). Note that the first photo in Figure 3.38 of the methane case was taken after 4 minutes when the first oil drop appeared in order to capture the gas bubbles. The size of oil drop containing CH_4 gas bubble inside was about 0.5-1 cm (**Figure 3.40**) when the bubble was about to be burst. However, this size cannot correspond with the one in the core-holder or reservoir because the gas-bubble size is influenced by surrounding pore geometry or structure (Kovscek et al. 2007). It was observed that, in Exp. 1 – Cycle 2, foamy oil was vigorously gained at the beginning (for the first 10 hours), but after the produced gas bubbles were collapsed quickly while the production stopped (see the yellow circles in Figure 3.38; starting from t = 10, the number of bubbles was obviously reduced).

Active foamy oil recovery, at the initial stage of Exp. 1 – Cycle 2 (within the first hours) with no oil production (Figure 3.29) until final pressure, was attributed to high gas mobility. Due to excessively high volume of injected gas (1,404 ml), it can be suspected that there could be a large amount of gas that was not fully dissolved staying in free-gas phase in the beginning. As noted, free-gas flow was not helpful in delivering high oil recovery, unlike dispersed-gas flow. Hence, after the pressure is reached its threshold value of 70 psi, this free-gas flow was restrained and dispersed gas contributed more to delivering oil (Figure 3.29), while GOR started to decrease from this point and oil started to be recovered effectively. Different foaminess was observed between Exp. 1 – Cycle 2 and Exp. 2 – Cycle 1. Oil production initiated with bigger-

sized bubbles for the former case (Figure 3.38), while the latter case started with smaller-sized bubbles and the bubble coalesce was more clearly seen as time went by (Figure 3.39).

The air 50%-CO_2 50% foamy oil showed a quite different behaviour from the CH_4 and CO_2 cases applied after air injection (Exp. 1 and Exp. 2). **Figure 3.41** shows the foaming behaviour in the beginning of the production in Exp. 3 – Cycle 2. The gas bubble size was about 1.25 to 2.5 cm (Figure 3.41). The difference between foamy behaviours observed in Figure 3.40 and Figure 3.41 is that the 'Air+CO_2' case showed more continuous-phase oil production. Ignoring the impact of high oil viscosity due to polymerization (produced oil had very high viscosity as seen in Table 3.6), the reasons for the continuous-phase oil production can be explained by the low diffusion rate of CO_2. CO_2 injected in the 1st cycle did not contribute significantly to oil recovery because of its low diffusion rate. Remained CO_2 gas from the 1st cycle gives an auxiliary driving force to the foamy-oil drive by newly-injected CO_2 from the 2nd cycle. Hence, more continuous oil phase was observed in Exp. 3 – Cycle 2 (Figure 3.41) than in Exp. 2 – Cycle 1 (Figure 3.40). Much smaller-sized gas bubbles (Figure 3.42) were observed in the case of air and CH_4 co-injection compared to Exp. 1 (Figure 3.38; air followed by CH_4 huff-n-puff).

3.5 Economic Analysis

In this study, two distinct injection schemes were followed: (1) Alternate injection of air and solvent (Exps. 1 and 2) and (2) co-injection of air and solvent (Exps. 3 and 4). The recovery results are well-summarized in **Figure 3.43**. Methane yielded better recovery than CO_2 (compare the total recoveries of Exps. 1 and 2) in a short run. Note, however, that co-injection (Exp. 3) was as successful as the alternate injection scheme (Exp. 2). What is critical in this evaluation is to consider the minimized amount of solvent used and the time required for the whole process to be ended. From these points of view, one may conclude that the mixture form (co-injection) of air and CO_2 (Exp. 3) is economically better as it consumes less solvent (~347.33 ml) per oil produced than the one in the alternate injection case presented as Exp. 2 (~2,934 ml).

However, in cases of methane (Exp. 1 and Exp. 4), the result is different. Even if the amount of methane used in Exp. 1 (2,134 ml) is much more than in Exp. 4 (~782 ml), considering CH_4 is

not as expensive as CO_2 and Exp. 1 gives ~12.5% of higher oil recovery, it can be concluded that alternate injection scheme is more feasible than co-injection one.

3.6 Conclusions

1. For heavy oil recovery, air can be used initially in a huff-n-puff manner to increase oil viscosity and eventually give better foam stability for the subsequent secondary solvent (CH_4 or CO_2) huff-n-puff applications.
2. CH_4 huff-n-puff preceded by air huff-n-puff showed a higher oil recovery than CH_4 live oil production with high depletion rate.
3. When using mixture-form of gas solvent, different diffusion rates of each gas should be considered. In this paper, CO_2 showed the slowest diffusion rate followed by air and CH_4, even though it created effective foam at later stages. Therefore, for faster response to solution-gas drive, methane is better, while CO_2 can be more effective in the long run.
4. Good foam quality in heavy oil can be established when gas bubbles are well-dispersed and stable enough to have long time in non-equilibrium status until reaching free-gas phase. Two keys factors that indicate high quality of foam are high amplitude of pressure differential (ΔP) and adequate time for ΔP to reach almost zero.
5. It is important to inject the proper amount of air in the beginning phase. Based on the experience gained through the experiments in this study, around 1/3 PV is suggested as proper empirical value to take advantage of its positive role (viscosity increase for better foaminess with methane or CO_2). Otherwise, the air left in the core system would hinder the foaming capability of the solvents used in the subsequent phase.
6. There were no specific observations in GC and SARA analyses of the produced oil. Generally, the augmentation of high carbon numbers (81+) and decrease in low carbon numbers (below 81) were related to the oil viscosity increase.
7. It is crucial to inject the appropriate volume of gas solvent so that the injected oil is fully dissolved into the dead oil.
8. Economically, simultaneous injection of air and CO_2 is more efficient than alternate injection of them. However, considering the lower price of CH_4 and the big difference of oil recovery between these two schemes, alternate injection of air and CH_4 is more

feasible than the co-injection of them.

3.7 References

Albartamani, N. S., Farouq Ali, S. M. F., and Lepski, B. 1999. Investigation of Foamy Oil Phenomena in Heavy Oil Reservoirs. International Thermal Operations/Heavy Oil Symposium, Bakersfield, California, 17-19 March. doi:10.2118/54084-MS.

Alshmakhy, A. and Maini, B. B. 2012. Effects of Gravity, Foaminess, and Pressure Drawdown on Primary-Depletion Recovery Factor in Heavy-Oil Systems. *JCPT* 51 (06): doi:10.2118/163067-PA.

Diedro, F., Bryan, J., Kryuchkov, S. et al. 2015. Evaluation of Diffusion of Light Hydrocarbon Solvents in Bitumen.SPE Canada Heavy Oil Technical Conference, Calgary, Alberta, Canada, 9-11 June.. doi:10.2118/174424-MS.

Kovscek, A. R., Tang, G. Q. and Radke, C. J. 2007. Verification of Roof Snap Off as a Foam-Generation Mechanism in Porous Media at Steady State. *Colloids and Surfaces A: Physicochemical and Engineering Aspects* 302: 251-260.

Mayorquin, J. and Babadagli, T. 2016a. Low Temperature Air Injection with Solvents in Heavy-Oil Containing Naturally Fractured Reservoirs: Effects of Matrix/Fracture Properties and Temperature on Recovery. *Fuel* 179: 376–390.

Mayorquin, J. and Babadagli, T. 2016b. Optimal Design of Low Temperature Air Injection with Propane for Efficient Recovery of Heavy Oil in Deep Naturally Fractured Reservoirs: Experimental and Numerical Approach. *Energy and Fuels* 30 (4): 2662–2673.

Rangriz-Shokri, A. and Babadagli, T. 2016. Experimental and Numerical Core-to-Field Scale Modeling of Non-Equilibrium CO_2 Bahaviour in Post-CHOPS Applications. Submitted to *SPE Reservoir Evaluation and Engineering* 2016 (under review).

Sheng, J. J., Maini, B. B., Hayes, R. E. et al. 1997. Experimental Study of Foamy Oil Stability. *JCPT* 36 (04). doi:10.2118/97-04-02.

Sheng, J.J., Maini, B.B., Hayes, R.E. et al. 1999. Critical Review of Foamy Oil Flow. *Transport in Porous Media* 35: 157. doi:10.1023/A:1006575510872.

Soh, Y. J., Rangriz-Shokri, A., and Babadagli, T. 2016. A New Modeling Approach to Optimize Methane-Propane Injection in a Field After CHOPS. SPE Annual Technical Conference and Exhibition, Dubai, UAE, 26-28 September.doi:10.2118/181322-MS.

Soh, Y. J., Rangriz-Shokri, A., and Babadagli, T. 2017. Cost Effective Heavy-Oil Recovery after Primary Production: Optimization of Methane Use in Cyclic Solvent Injection through Experimental and Numerical Studies. Submitted to *Fuel* (under review).

Tang, G. and Firoozabadi, A. 2001. Effect of GOR, Temperature, and Initial Water Saturation on Solution-Gas Drive in Heavy-Oil Reservoirs. SPE Annual Technical Conference and Exhibition, New Orleans, Louisiana, 30 September-3 October.doi:10.2118/71499-MS.

Walton, A.G. 1969. Nucleation in Liquids and Solutions, in *Nucleation, Zettlemoyer*, A.C., Ed., Marcel Dekker, New York.

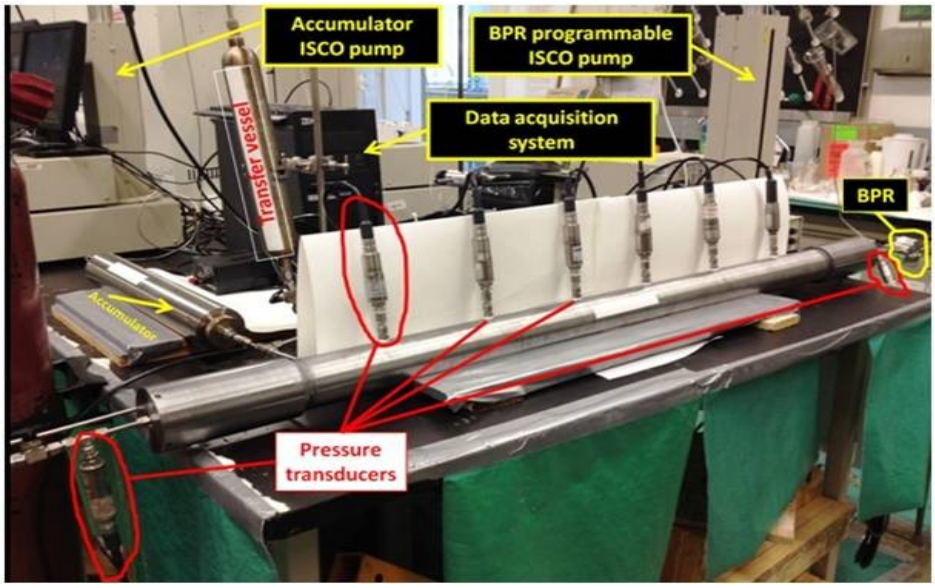

Figure 3.1—Experimental set-up (Rangriz-Shokri and Babadagli 2016).

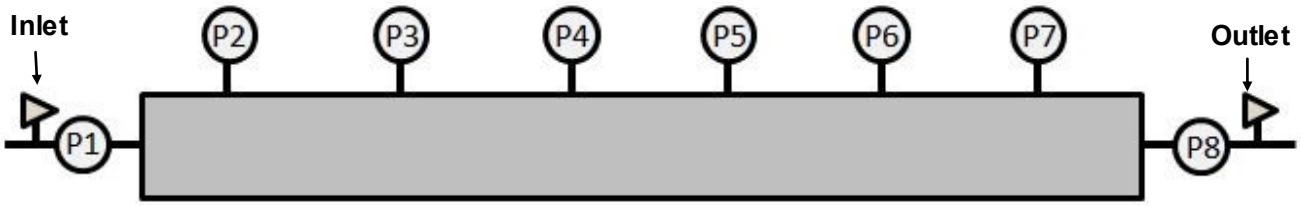

Figure 3.2—Schematic of pressure ports.

	Exp. 1	Exp. 2	Exp. 3	Exp. 4
Average porosity (%)	34.46	36.74		38.13
Average absolute permeability (mD)	1,409.93	9,072		2,510
Initial water saturation (%)	9.5	7		8
Initial oil saturation (%)	90.5	93		92
Initial gas saturation (%)	0	0		0

Table 3.1—Sand-pack properties.

	Exp. 1			Exp. 2			Exp. 3			Exp. 4		
	Air HnP	CH_4 HnP		Air HnP	CO_2 HnP		Air 50%-CO_2 50%			Air 50%-CH_4 50%		
		Cycle 1	Cycle 2		Cycle 1	Cycle 2	Cycle 1	Cycle 2	Cycle 3	Cycle 1	Cycle 2	Cycle 3
Produced Oil (ml)	35	110	111	30	90	120	50	120	65	75	60	60
Injected Gas (ml)	269.1	460.95	1,404	844	911.96	2,022	128.52	220.58	345.55	356.96	197.47	227.43
Produced Gas (ml)	3,100	2,190	10,637	400	1,500	16,175	420	1,950	6,796	800	3,250	6570
Producing GOR (ml/ml)	88.57	19.91	95.82	13.33	16.67	134.8	8.4	16.25	104.55	10.67	54.17	109.5
Oil Recovery Factor (%)	4.43	14.57	17.21	3.47	10.78	16.11	5.78	14.72	9.35	8.43	7.36	7.95
Total Oil Recovery Factor (%)	19			14.25			20.50			15.79		
	36.21			30.36			29.85			23.74		

Table 3.2−Experimental results.

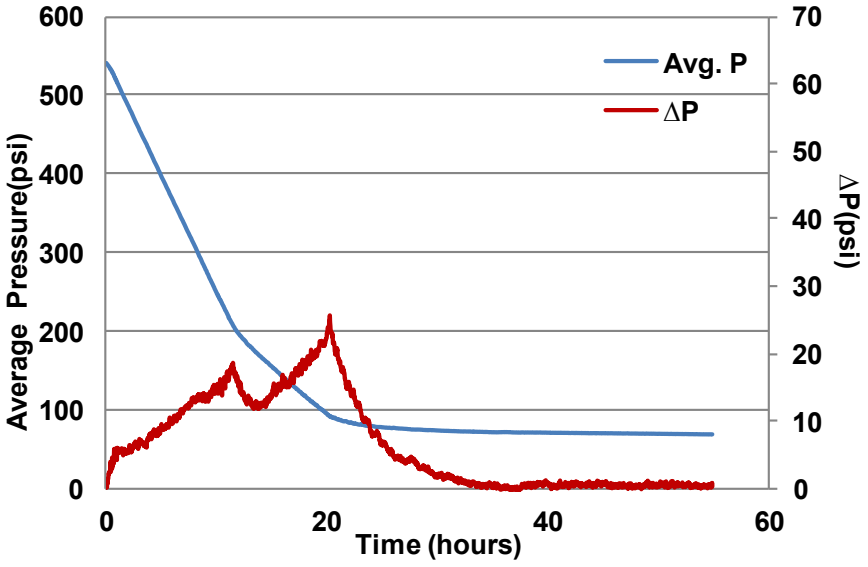

Figure 3.3—Pressure/ΔP profile for air huff-n-puff from Exp. 1.

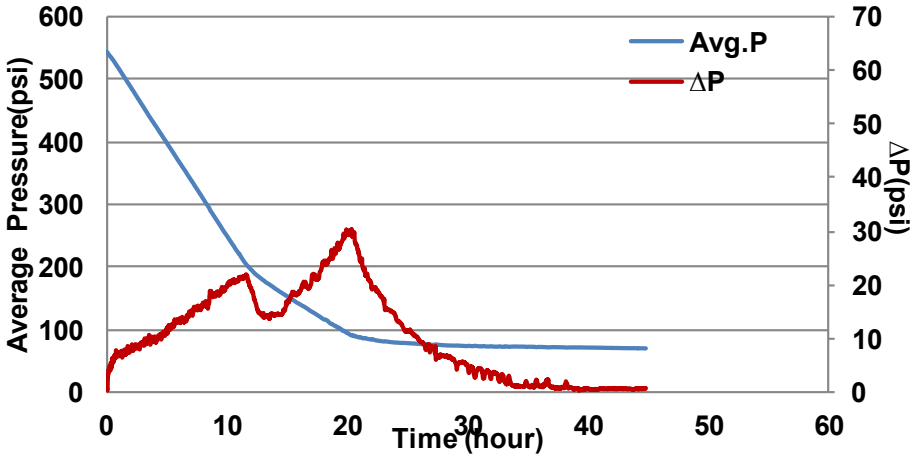

Figure 3.4—Pressure/ΔP profile for air huff-n-puff from Exp. 2.

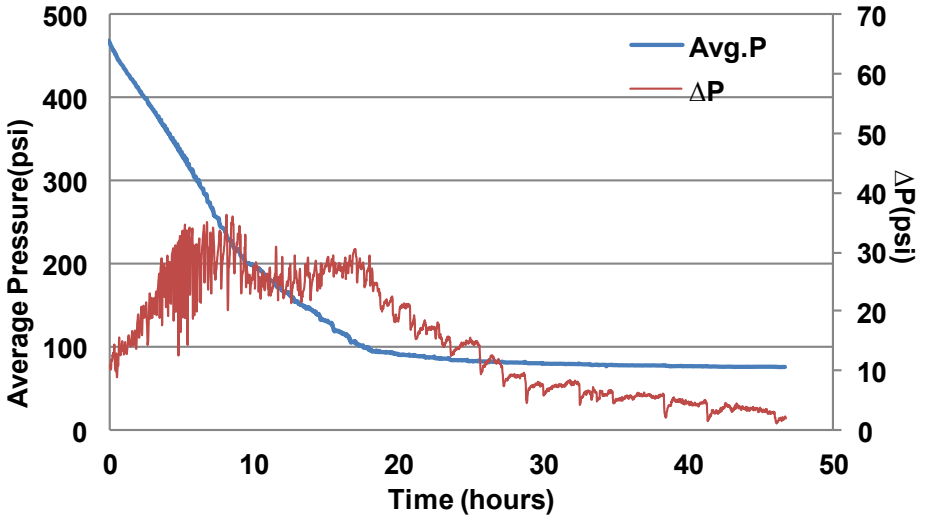

Figure 3.5—Pressure/ΔP profile for CH_4 huff-n-puff - Cycle 1 (Exp. 1).

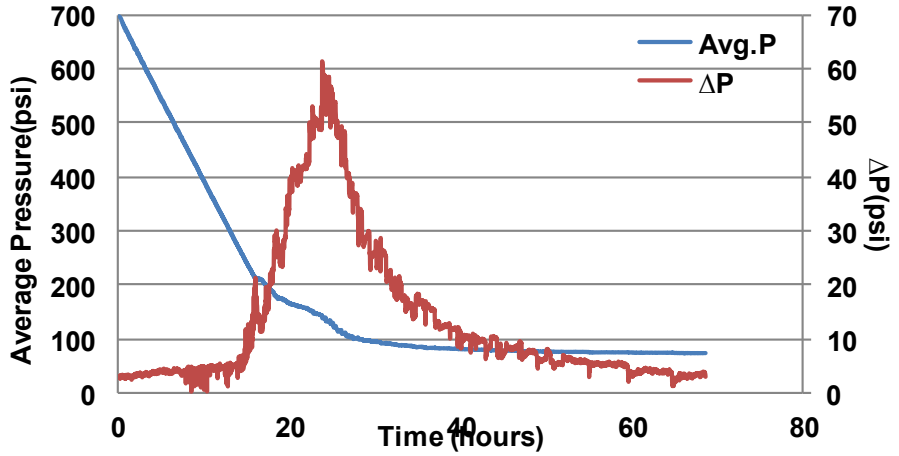

Figure 3.6—Pressure/ΔP profile for CH_4 huff-n-puff - Cycle 2 (Exp. 1).

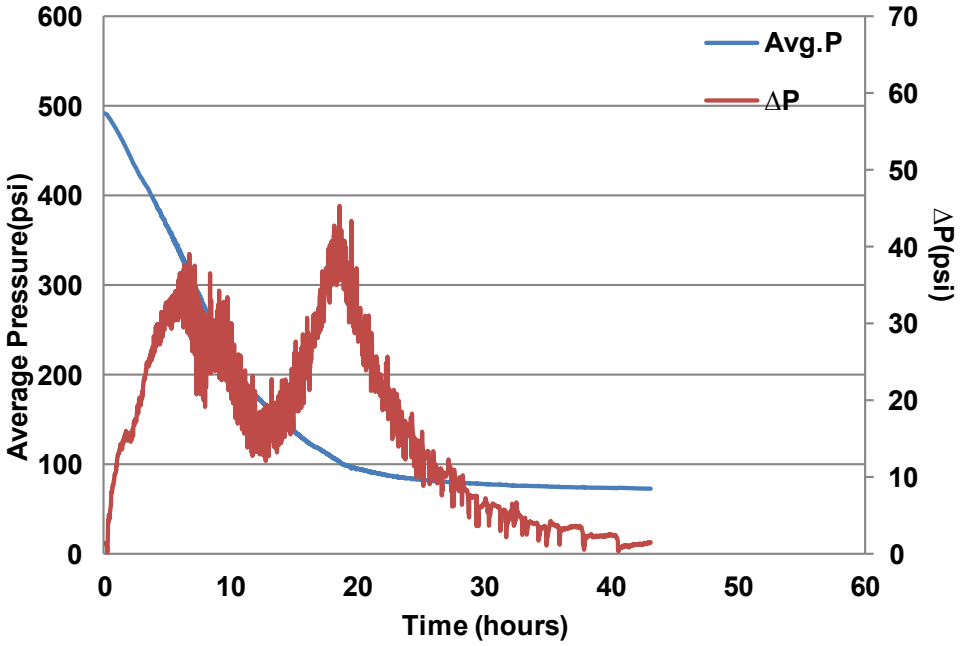

Figure 3.7—Pressure/ΔP profile for CO_2 huff-n-puff - Cycle 1 (Exp. 2).

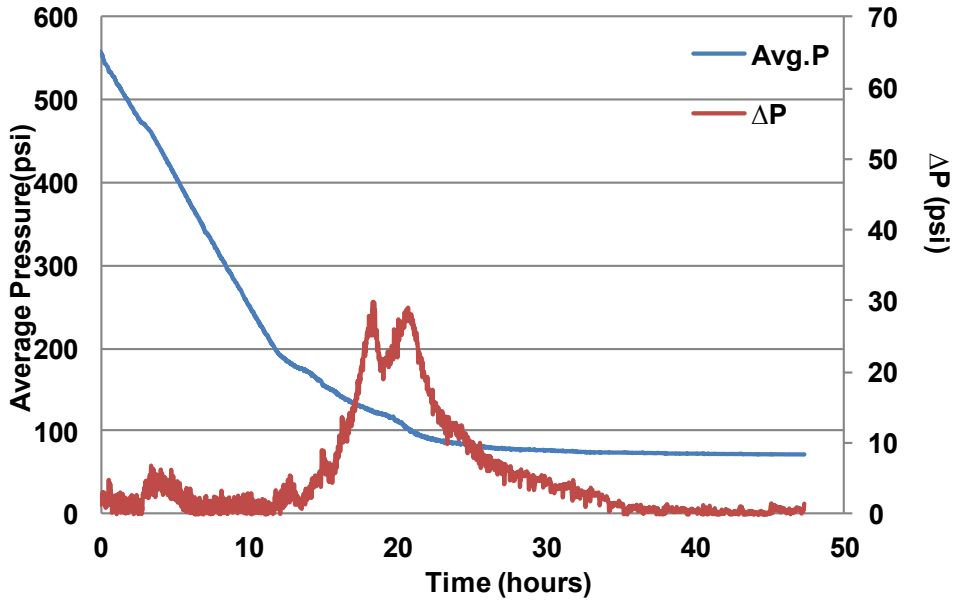

Figure 3.8—Pressure/ΔP profile for CO_2 huff-n-puff - Cycle 2 (Exp. 2).

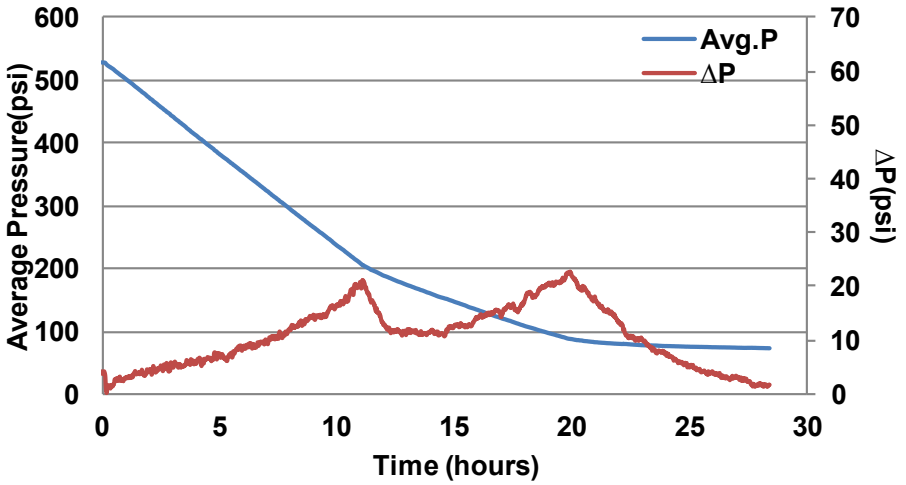

Figure 3.9—Pressure/ΔP profile for Air 50%-CO_2 50% - Cycle 1.

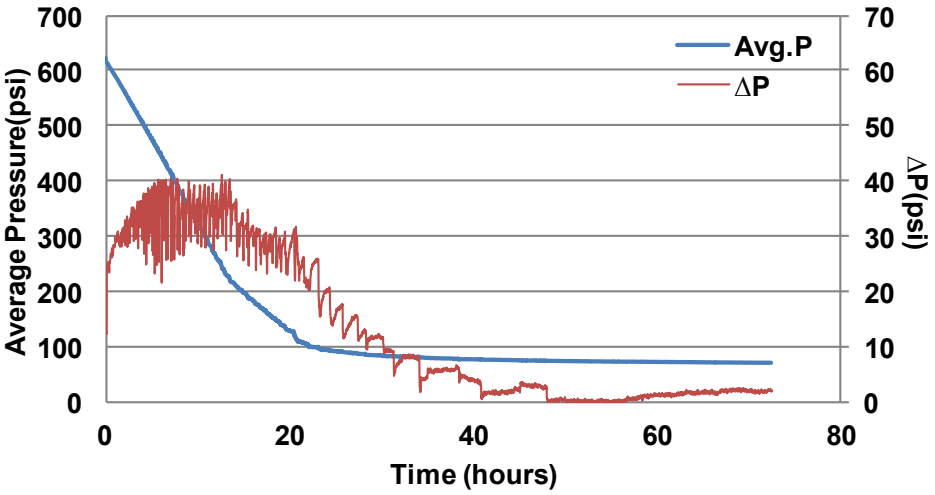

Figure 3.10—Pressure/ΔP profile for Air 50%-CO_2 50% - Cycle 2.

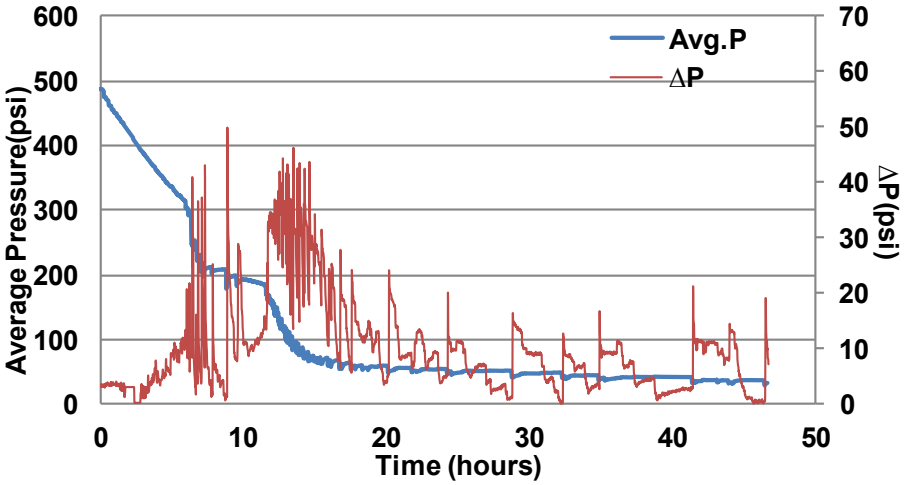

Figure 3.11—Pressure/ΔP profile for Air 50%-CO_2 50% - Cycle 3.

	Air (Exp.1)	CH_4 HnP– Cycle 1	CH_4 HnP – Cycle 2	Air (Exp.2)	CO_2 HnP– Cycle 1	CO_2 HnP – Cycle 2	Exp. 3 –Cycle 1	Exp. 3 –Cycle 2	Exp. 3 –Cycle 3	Exp. 4-Cycle 1	Exp. 4-Cycle 2	Exp. 4-Cycle 3
Methane	0.068	19.87	0.001	0.58	0.4923	0.0082		0.005	3.157	2.22		0.007
C2H4/C2H2	0.012	1.826	10.38	0.297	0.0472	0.022		1.6	0.468	2.7	7.974	0.181
Ethane		0.54	0.36	0.0197	0.0096	0.001			0.032	0.2	6	0.0004
Propylene										0.0022	0.0028	
C4H8			0.0011					0.0004		0.00041	0.0006	
Propane	0.0005	0.0037	0.0014		0.0042	0.0007				0.0011	0.0009	
Oxygen	8.99	5.14	8.2	21.43	13.88	11.4244	3.9	9.654	9.512	6.813	5.966	9.958
Nitrogen	36.756	30.4	27.95	46.457	56.375	43.6	18.485	39.846	26.384	37.054	25.103	38.6224
CO							2	4.8				

Table 3.3—GC results of the produced gas.

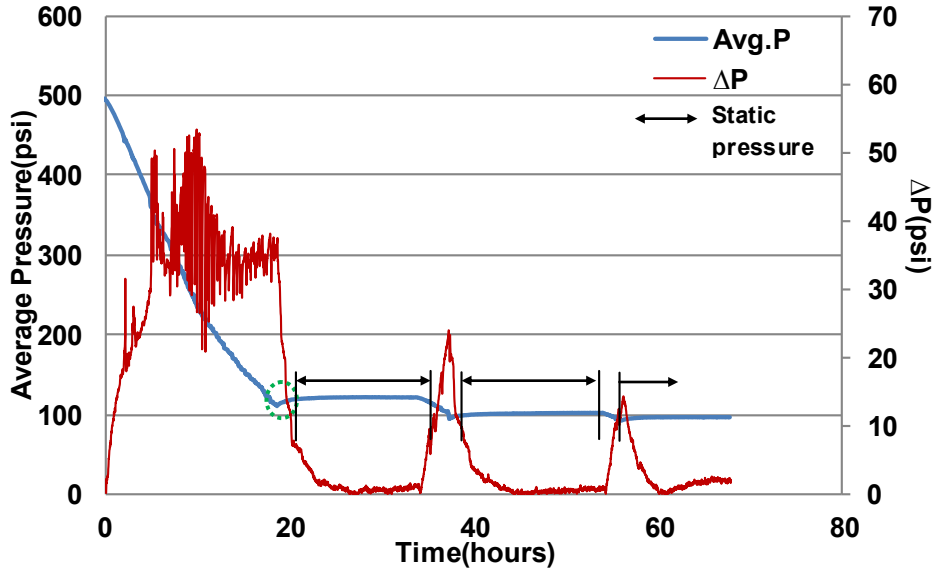

Figure 3.12−—Pressure/ΔP profile for Air 50%-CH_4 50% - Cycle 1.

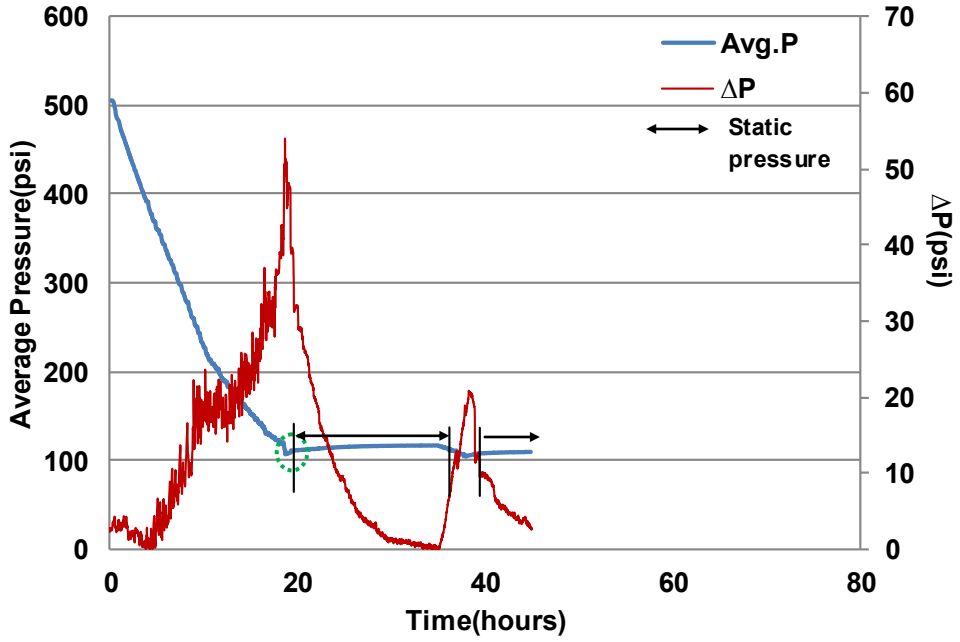

Figure 3.13—Pressure/ΔP profile for Air 50%-CH4 50% - Cycle 2.

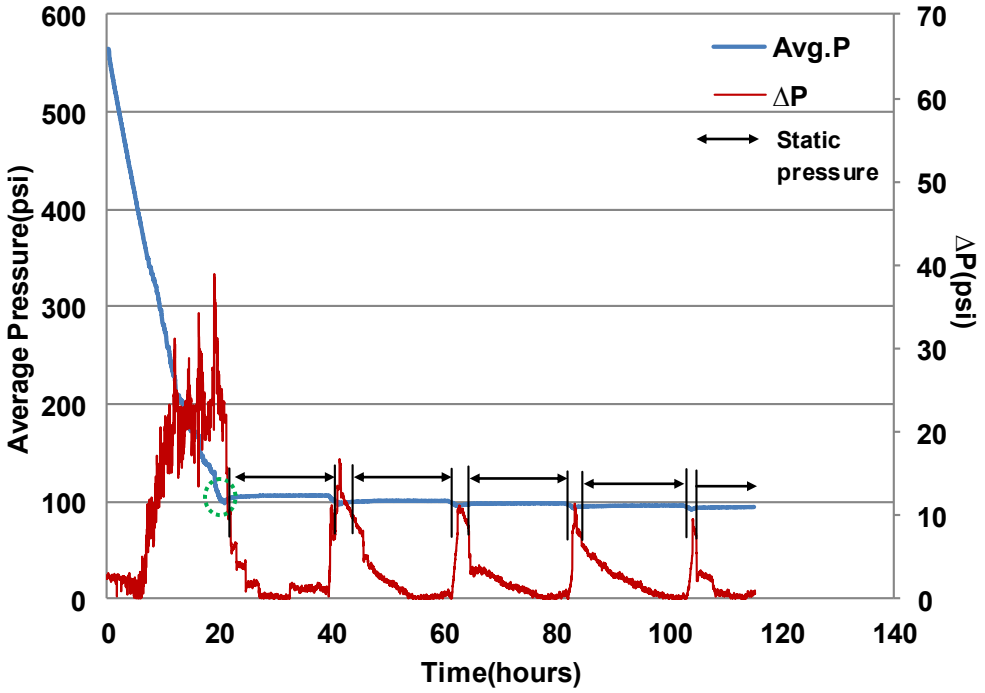

Figure 3.14—Pressure/ΔP profile for Air 50%-CH4 50% - Cycle 3.

	Case 1			Case 2		Case 3			Case 4		
	-0.23 psi/min	-0.51 psi/min	-1.53 psi/min	-0.51 + -0.23 psi/min		Air HnP	CH_4 HnP		Air 50%-CH4 50%		
				(1)	(2)		Cycle 1	Cycle 2	Cycle 1	Cycle 2	Cycle 3
Produced Oil (ml)	85	135	126	120	98	35	110	111	75	60	60
Produced Gas (ml)	4,673	2,005	1,500	3,447	2,378	3,100	2,190	10,636	800	3,250	6570.13
Producing GOR (ml/ml)	54.97	14.85	11.9	28.73	24.26	88.57	19.91	95.82	10.67	54.17	109.5
Oil Recovery Factor (%)	8.95	14.21	13.84	13.22	11.06	4.43	14.57	17.21	8.43	7.36	7.95
Total Oil Recovery Factor (%)						19			15.79		
						36.21			23.74		

Table 3.4—Comparison of CH4 live oil production in different scenarios: Cases 1, 2 from Soh et al. (2017).

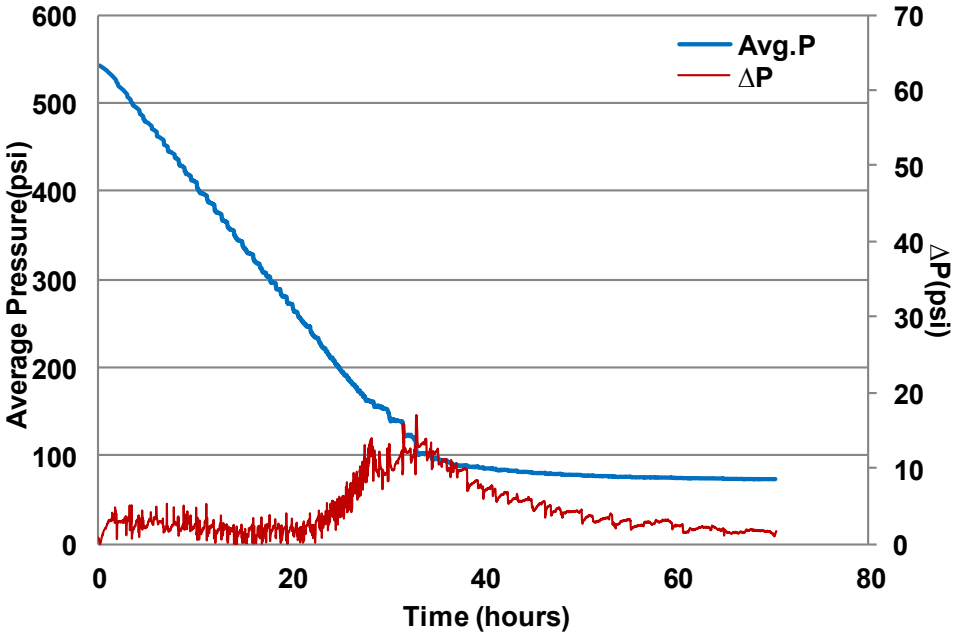

Figure 3.15—Pressure/ΔP profile for '-0.23 psi/min' in Case I (Soh et al. 2017).

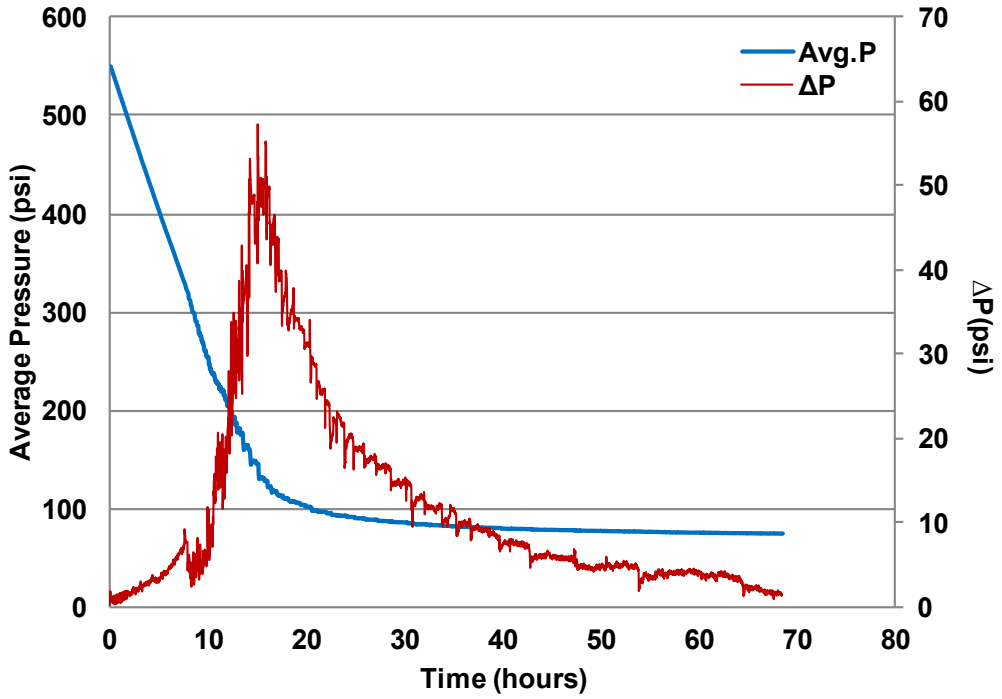

Figure 3.16—Pressure/ΔP profile for '-0.51 psi/min' in Case I (Soh et al. 2017).

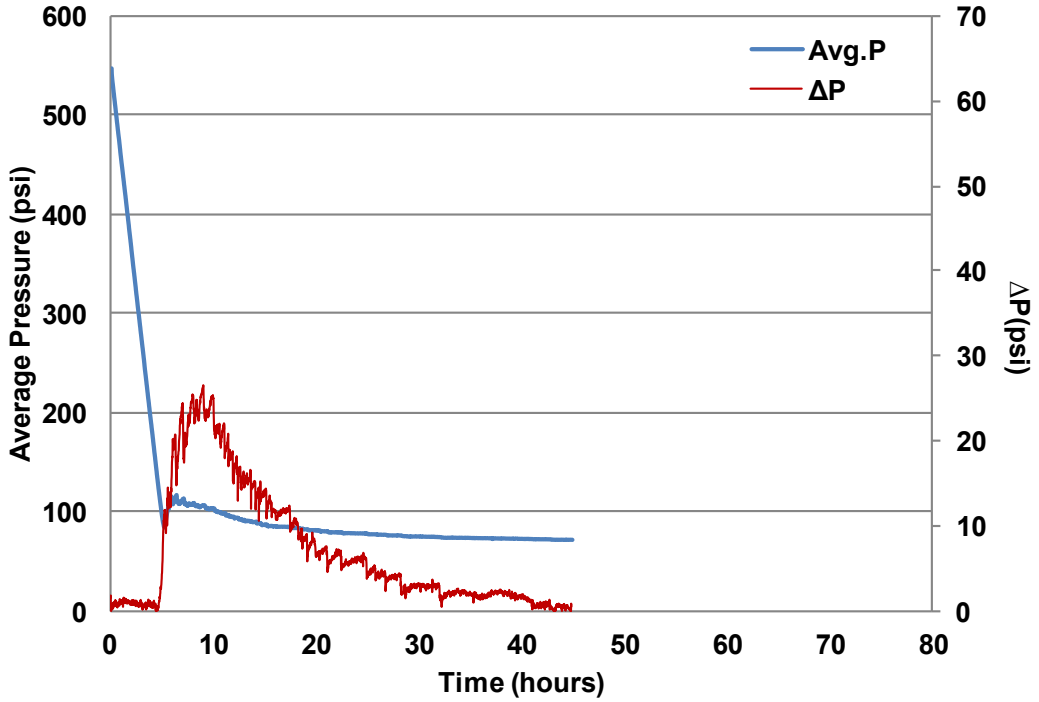

Figure 3.17—Pressure/ΔP profile for '-1.53 psi/min' in Case I (Soh et al. 2017).

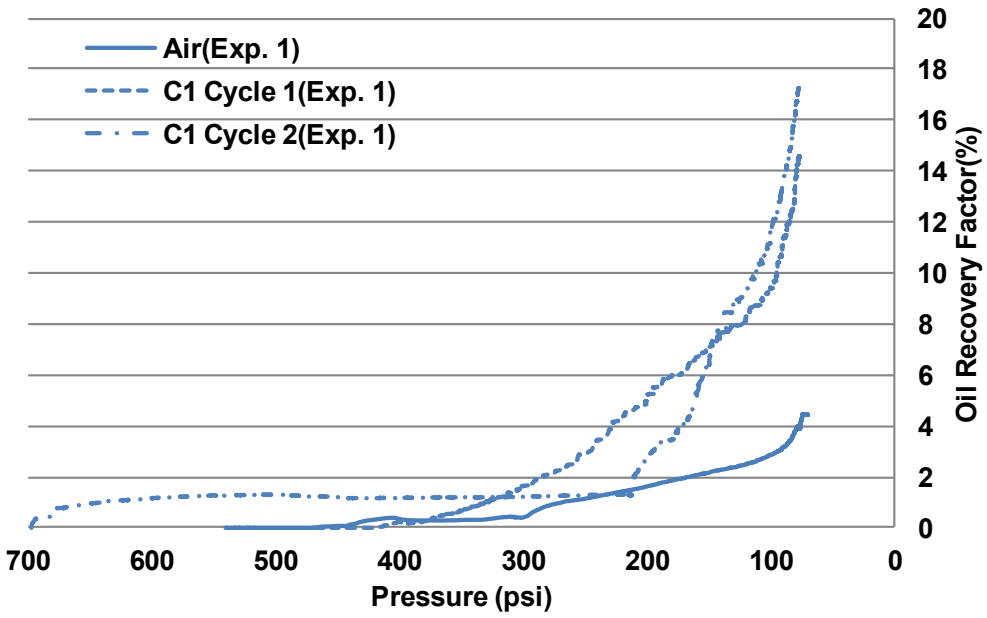

Figure 3.18—Oil recovery factor vs. Pressure – Exp. 1.

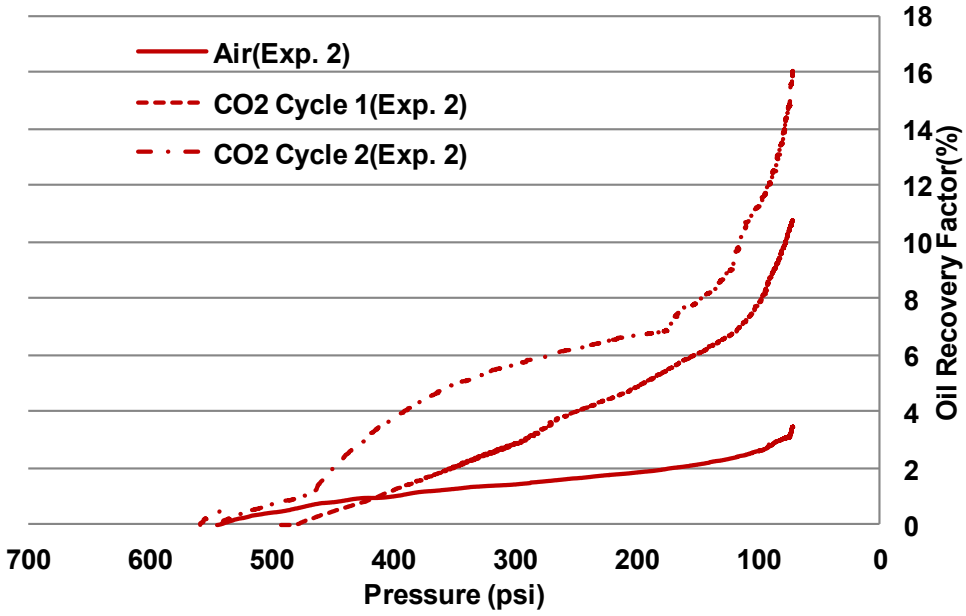

Figure 3.19—Oil recovery factor vs. Pressure - Exp. 2.

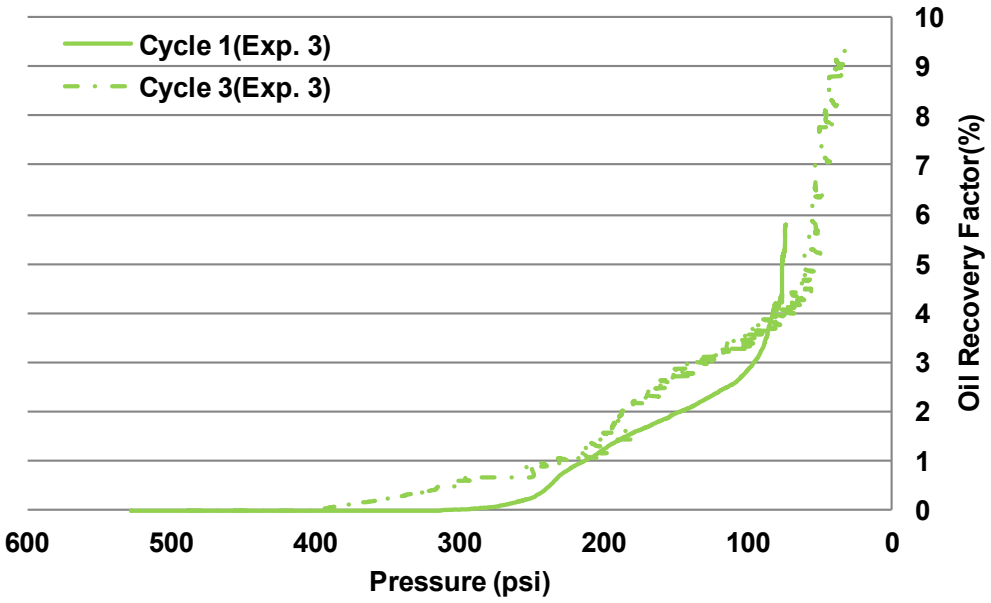

Figure 3.20—Oil recovery factor vs. Pressure - Exp. 3.

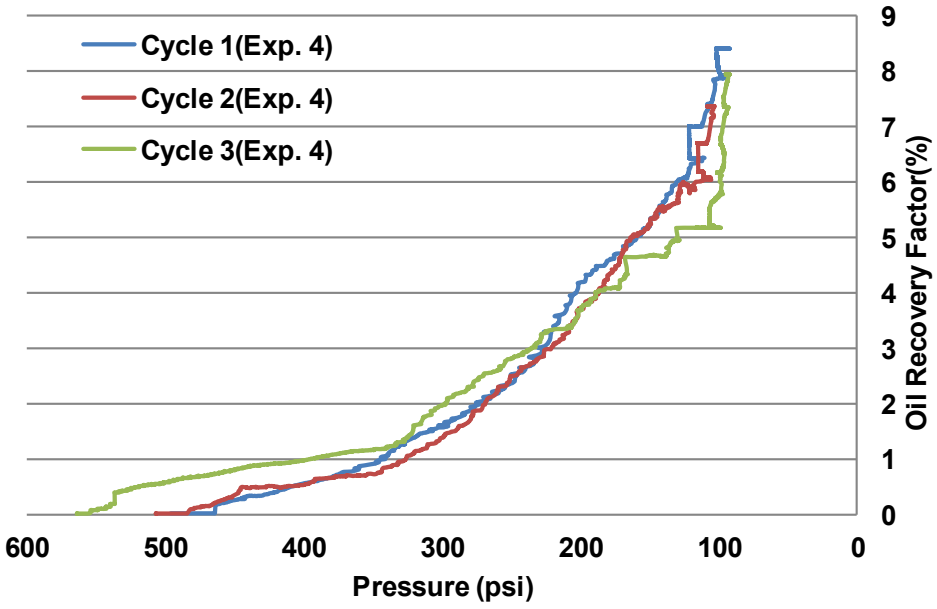

Figure 3.21—Oil recovery factor vs. Pressure - Exp. 4.

	Saturates	Asphaltenes	Resins	Aromatics
Initial oil	38.16	15.03	31.99	14.82
Air (Exp. 1)	40.49	14.8	29.58	15.13
CH_4 HnP – Cycle 1	40.11	14.16	26.39	19.34
CH_4 HnP – Cycle 2	37.16	16.21	26.69	19.94
Air (Exp. 2)	37.54	14.12	27.95	19.68
CO_2 HnP – Cycle 1	37.69	14.88	26.20	19.98
CO_2 HnP – Cycle 2	38.9	14.08	26.21	19.4
Exp. 3 – Cycle 1	39.36	17.05	23.64	18.79
Exp. 3 – Cycle 2	40.28	18.2	22.95	17.23
Exp. 3 – Cycle 3	39.28	17.66	21.58	20.23
Exp. 4 – Cycle 1	38.32	16.99	23.18	19.51
Exp. 4 – Cycle 2	36.68	16.75	20.68	24.85
Exp. 4 – Cycle 3	35.49	15.55	19.24	28.12

Table 3.5—SARA results of the produced oil.

Measured at 25°C	Viscosity(cp)
Initial oil	27,400
Air (Exp. 1)	28,510
CH_4 HnP – Cycle 1	21,140
CH_4 HnP – Cycle 2	23,340
Air (Exp. 2)	32,380
CO_2 HnP – Cycle 1	32,510
CO_2 HnP – Cycle 2	29,070
Exp. 3 – Cycle 1	26,690
Exp. 3 – Cycle 2	29.660
Exp. 3 – Cycle 3	24,560
Exp. 4 – Cycle 1	25,830
Exp. 4 – Cycle 2	40,830
Exp. 4 – Cycle 3	40,090

Table 3.6—Viscosity of produced oil.

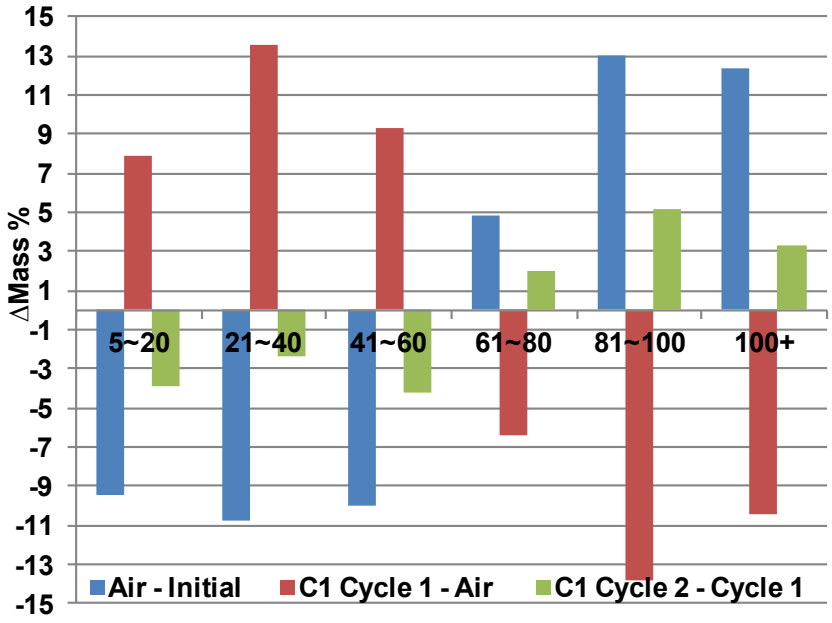

Figure 3.22—Oil GC Result (x-axis - Carbon no.): Blue - Total mass % change from initial oil to air HnP, Red - from air HnP to Exp. 1 - Cycle 1, Green - from Exp. 1 – Cycle 1 to 2.

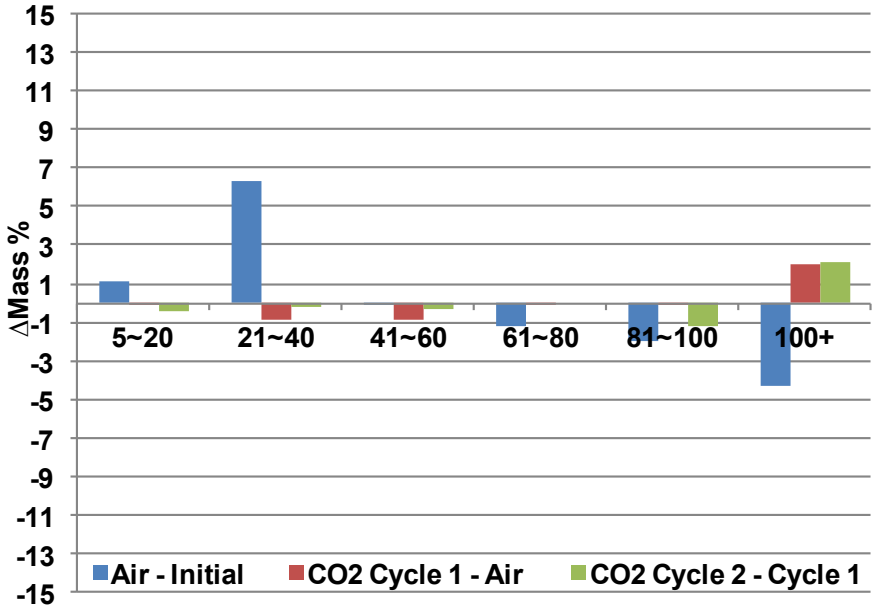

Figure 3.23—Oil GC Result (x-axis - Carbon no.): Blue - Total mass % change from initial oil to air HnP, Red - from air HnP to Exp. 2 - Cycle 1, Green - from Exp. 2 – Cycle 1 to 2.

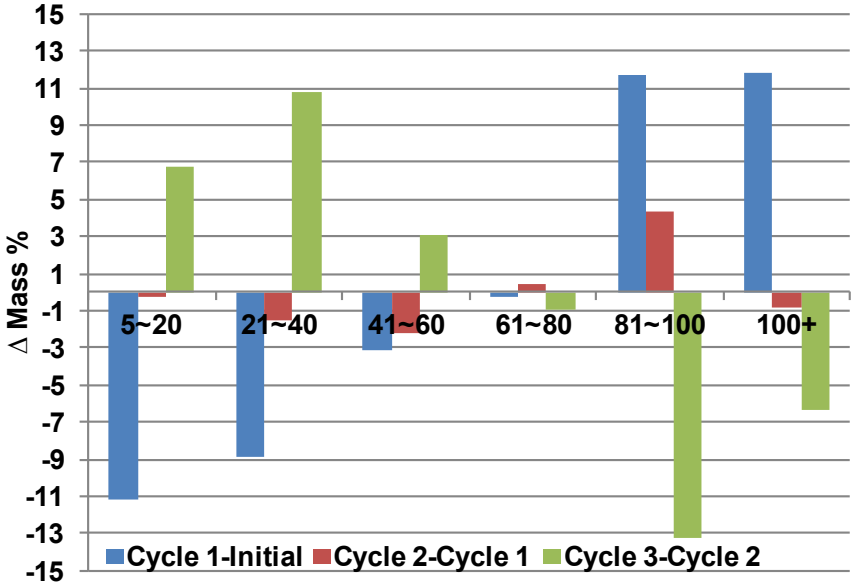

Figure 3.24—Oil GC Result (x-axis - Carbon no.): Blue - Total mass % change from initial oil to air 50%-CO2 50% Cycle 1, Red - from air 50%-CO2 50% Cycle 1 to Cycle 2, Green - from Cycle 2 to Cycle 3.

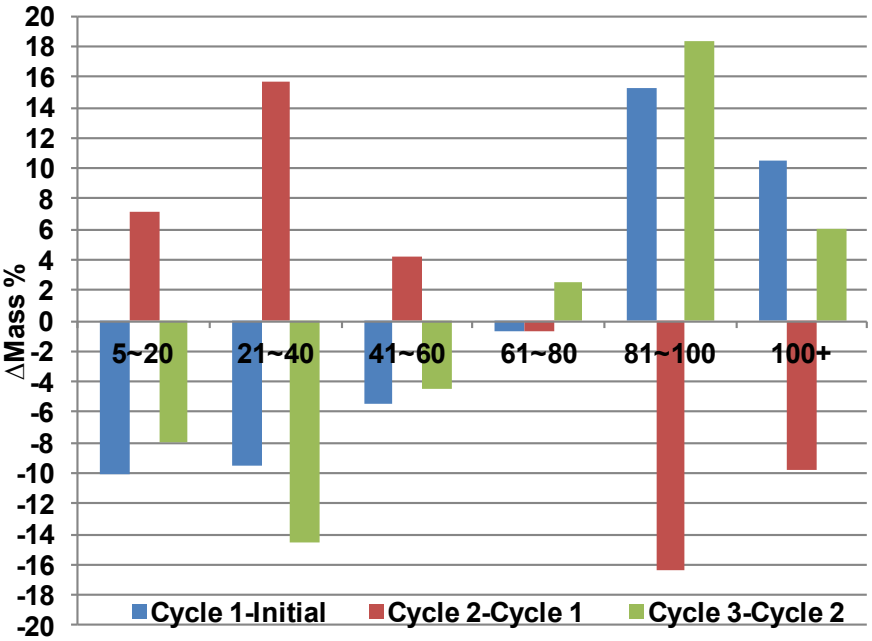

Figure 3.25—Oil GC Result (x-axis - Carbon no.): Blue - Total mass % change from initial oil to air 50%-CH4 50% Cycle 1, Red - from air 50%-CH4 50% Cycle 1 to Cycle 2, Green from Cycle 2 to Cycle 3.

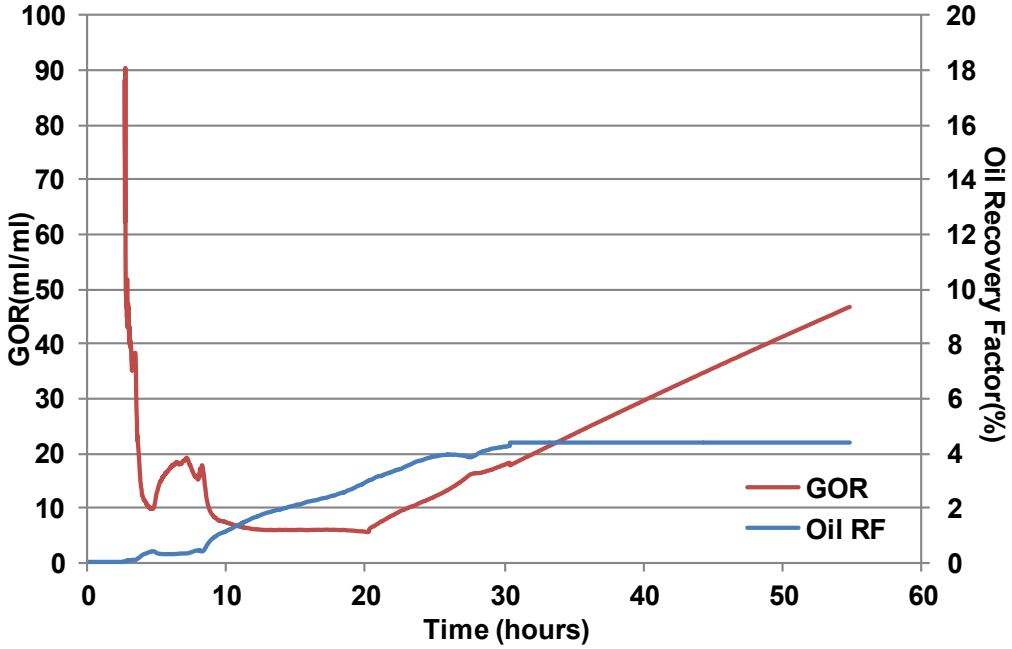

Figure 3.26—GOR and Oil Recovery Factor for air huff-n-puff from Exp. 1.

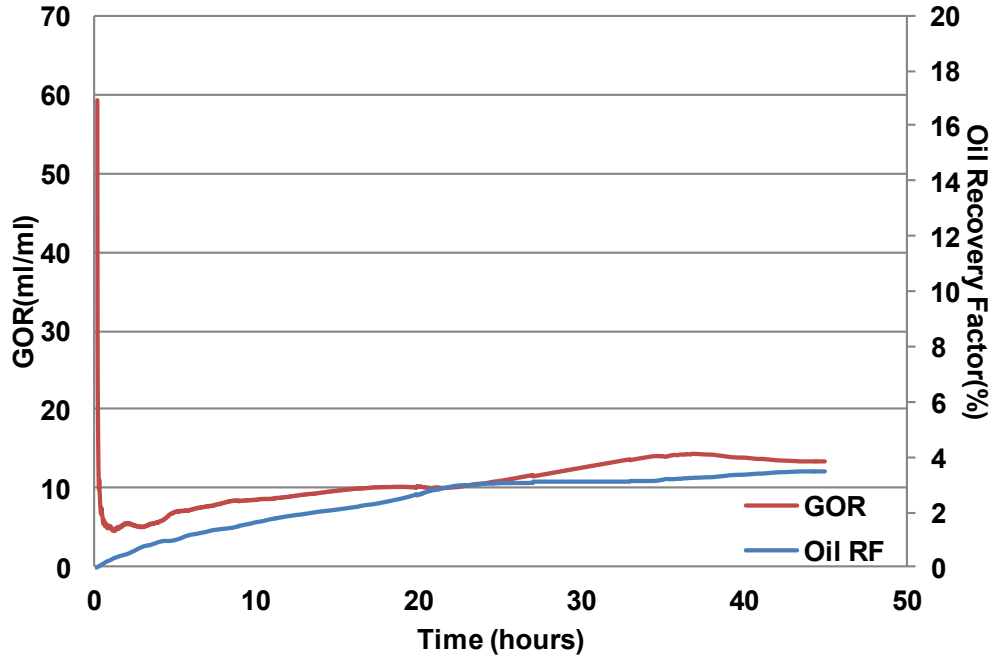

Figure 3.27—GOR and Oil Recovery Factor for air huff-n-puff from Exp. 2.

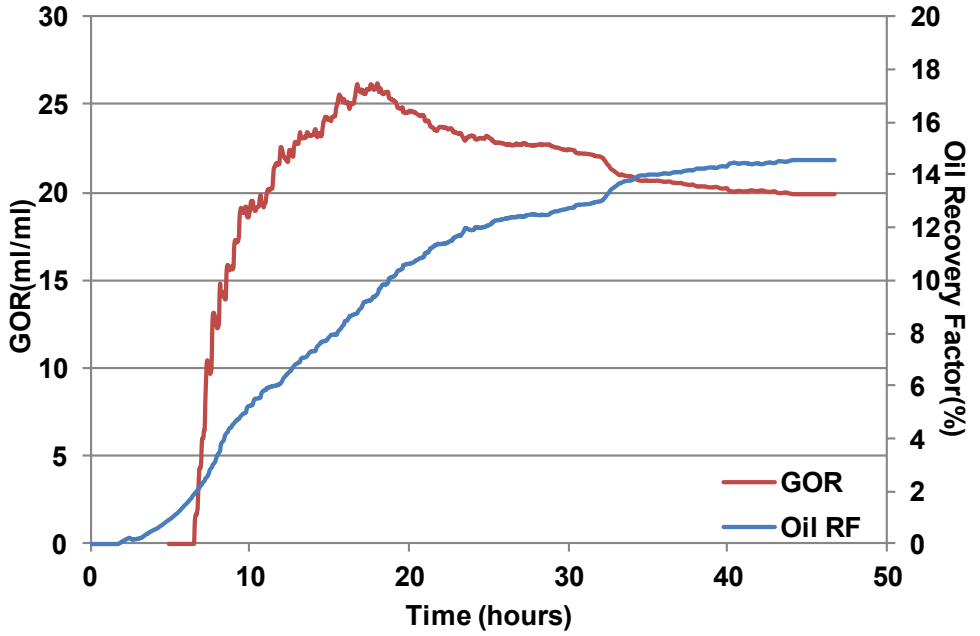

Figure 3.28—GOR and oil recovery factor for CH4 huff-n-puff - Cycle 1 (Exp. 1).

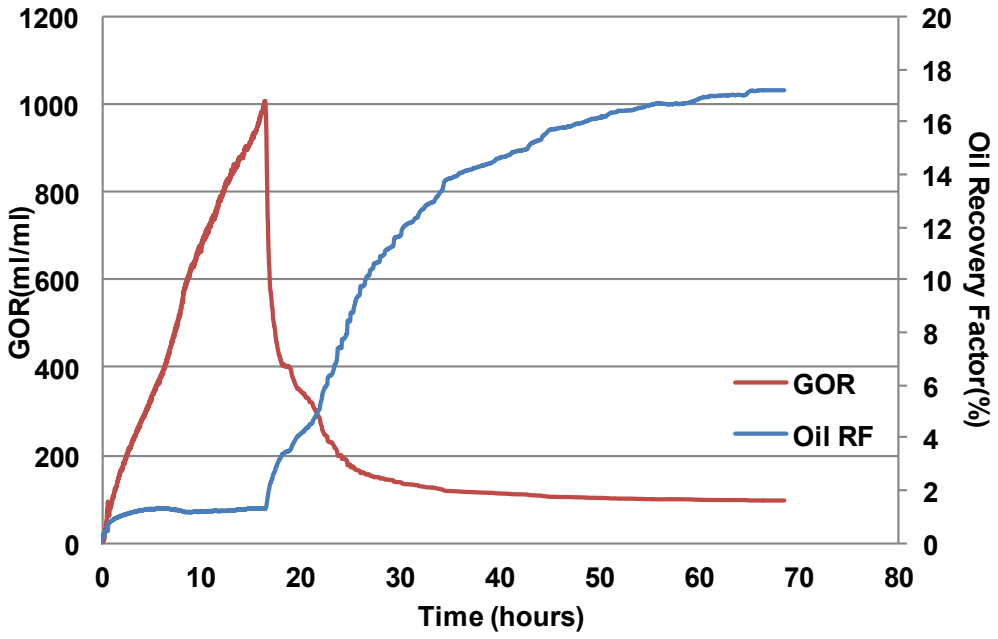

Figure 3.29—GOR and oil recovery factor for CH4 huff-n-puff - Cycle 2 (Exp. 1).

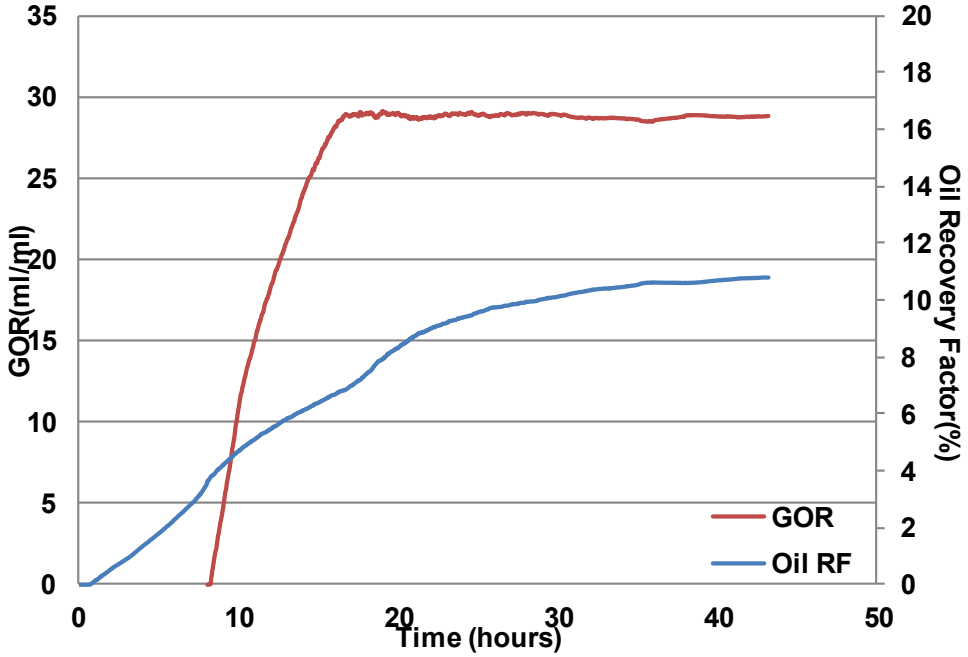

Figure 3.30—GOR and oil recovery factor for CO2 huff-n-puff - Cycle 1 (Exp. 2).

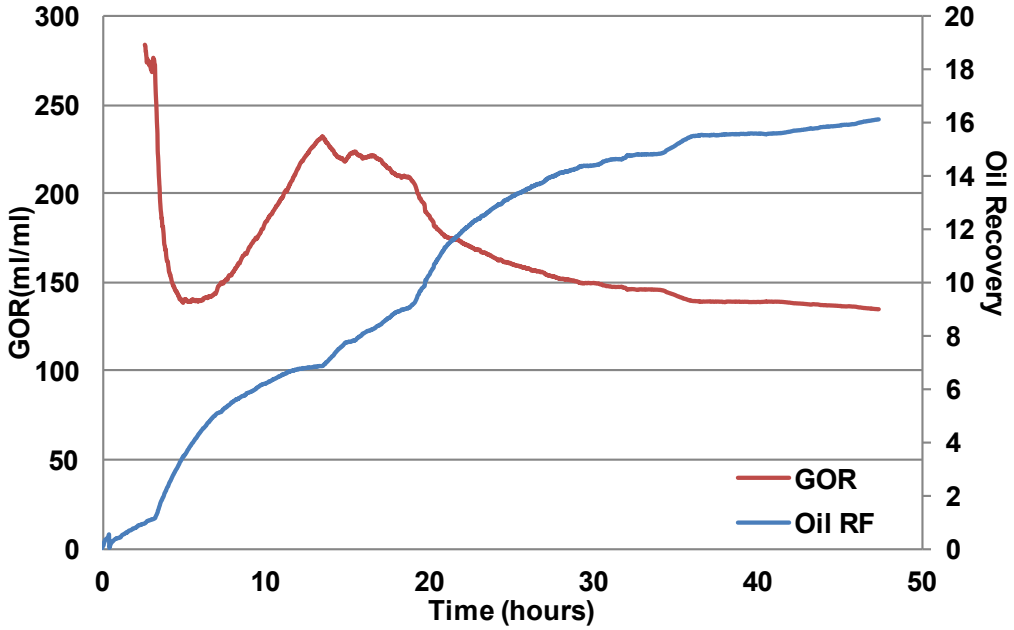

Figure 3.31—GOR and oil recovery factor for CO2 huff-n-puff - Cycle 2 (Exp. 2).

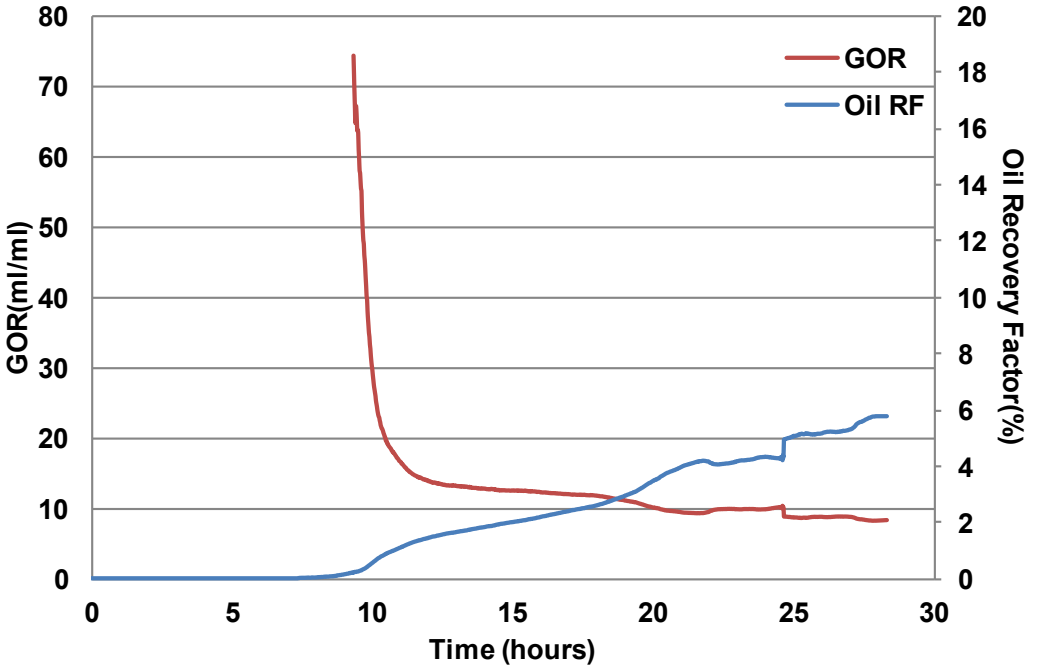

Figure 3.32—GOR and oil recovery factor for air 50%-CO2 50% - Cycle 1 (Exp. 3).

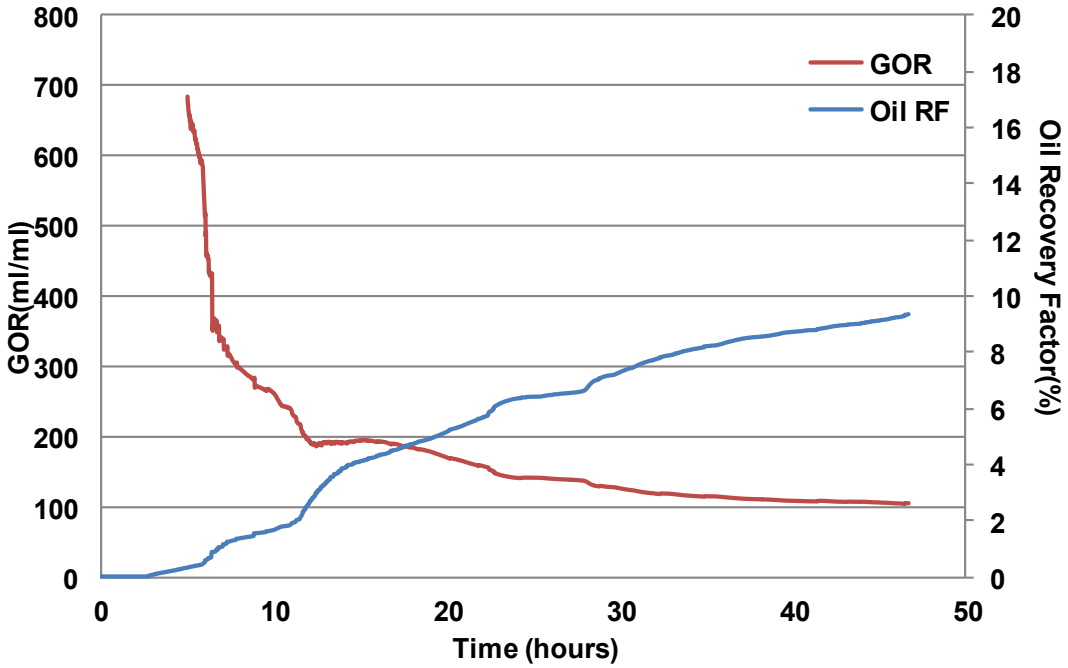

Figure 3.33—GOR and oil recovery factor for air 50%-CO2 50% - Cycle 3 (Exp. 3).

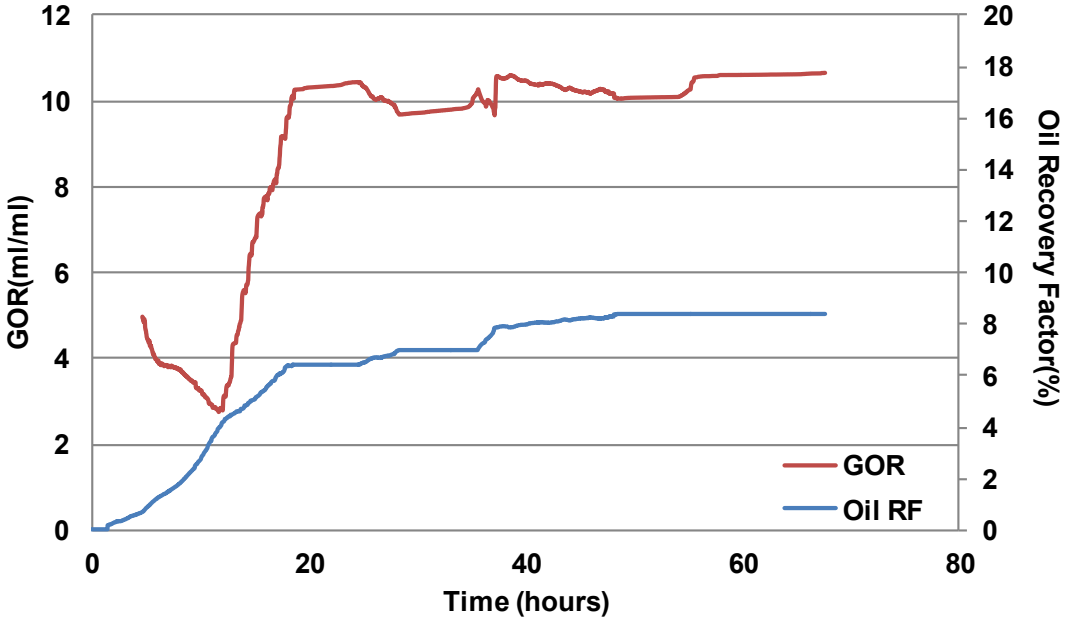

Figure 3.34—GOR and oil recovery factor for air 50%-CH4 50% - Cycle 1 (Exp. 4).

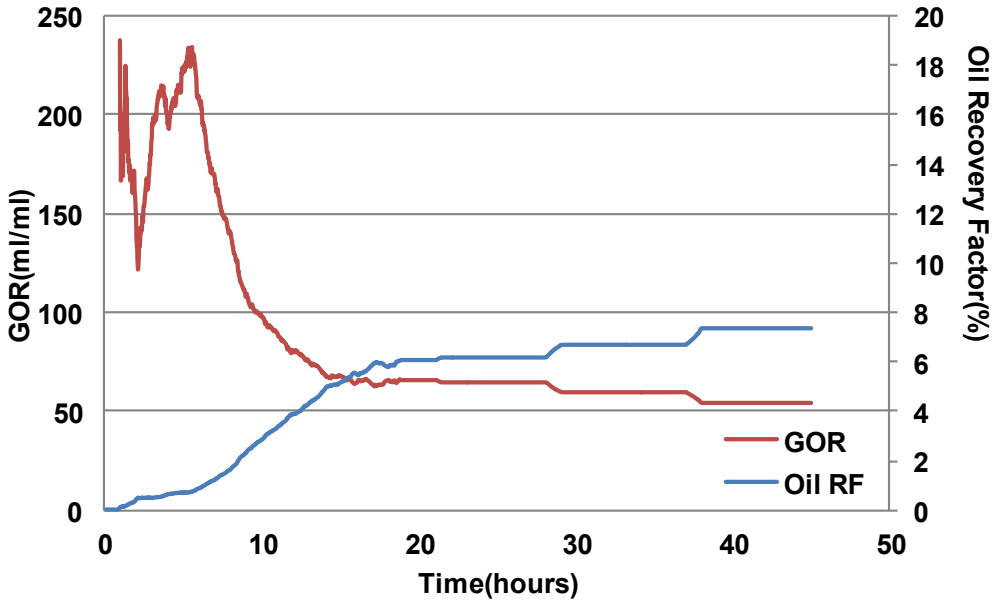

Figure 3.35—GOR and oil recovery factor for air 50%-CH4 50% - Cycle 2 (Exp. 4).

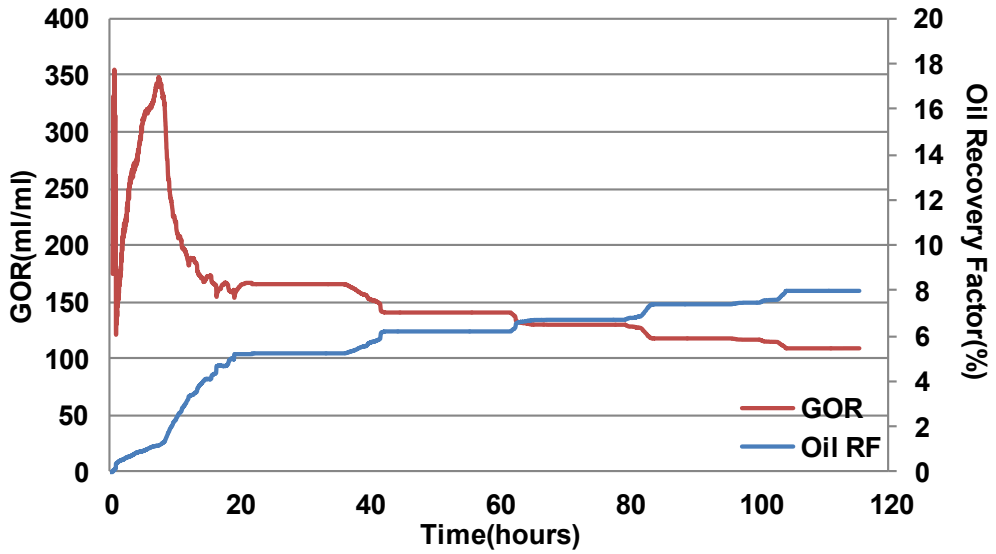

Figure 3.36—GOR and oil recovery factor for air 50%-CH4 50% - Cycle 3 (Exp. 4).

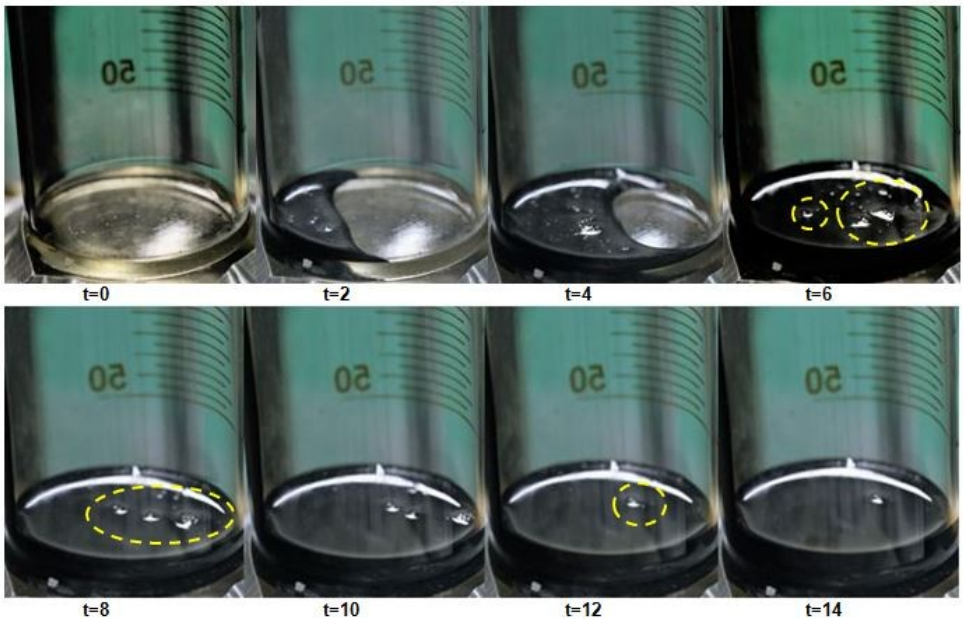

Figure 3.37—Oil production in 'Air Huff-n-Puff' (t = hour): Yellow circles on where bubbles appeared.

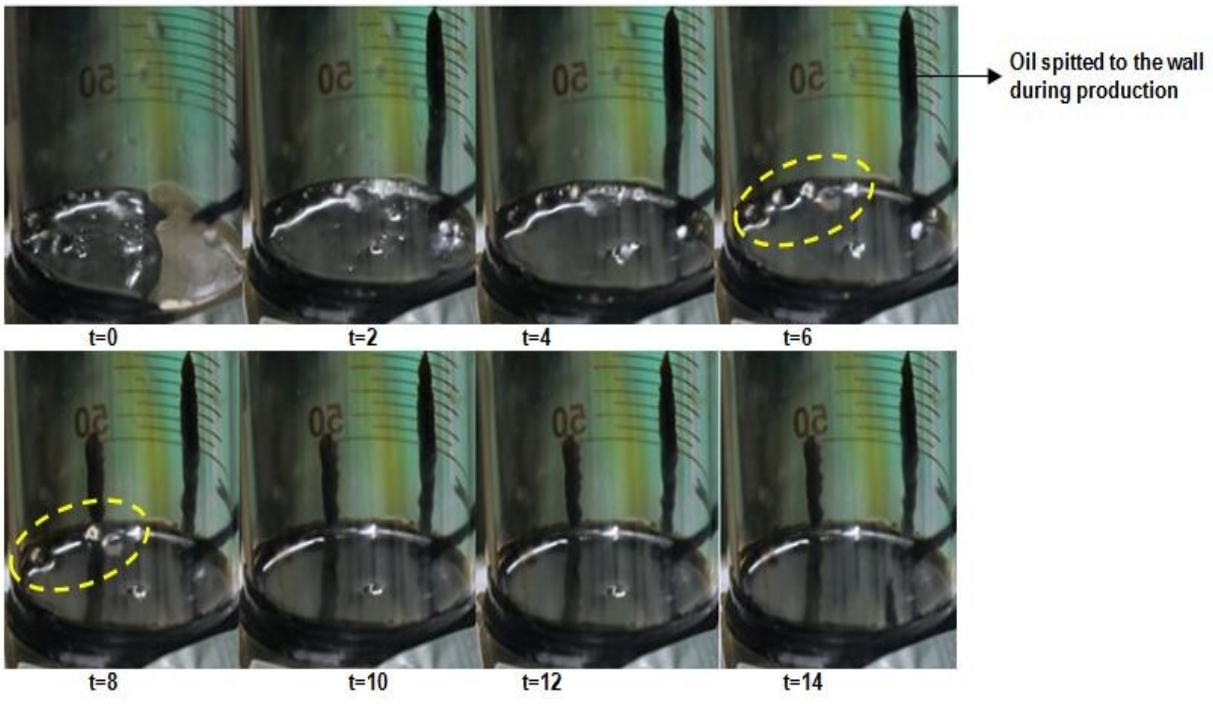

Figure 3.38—Oil production in Exp. 1 – Cycle 2 (t = hour): Yellow circles on where bubbles appeared.

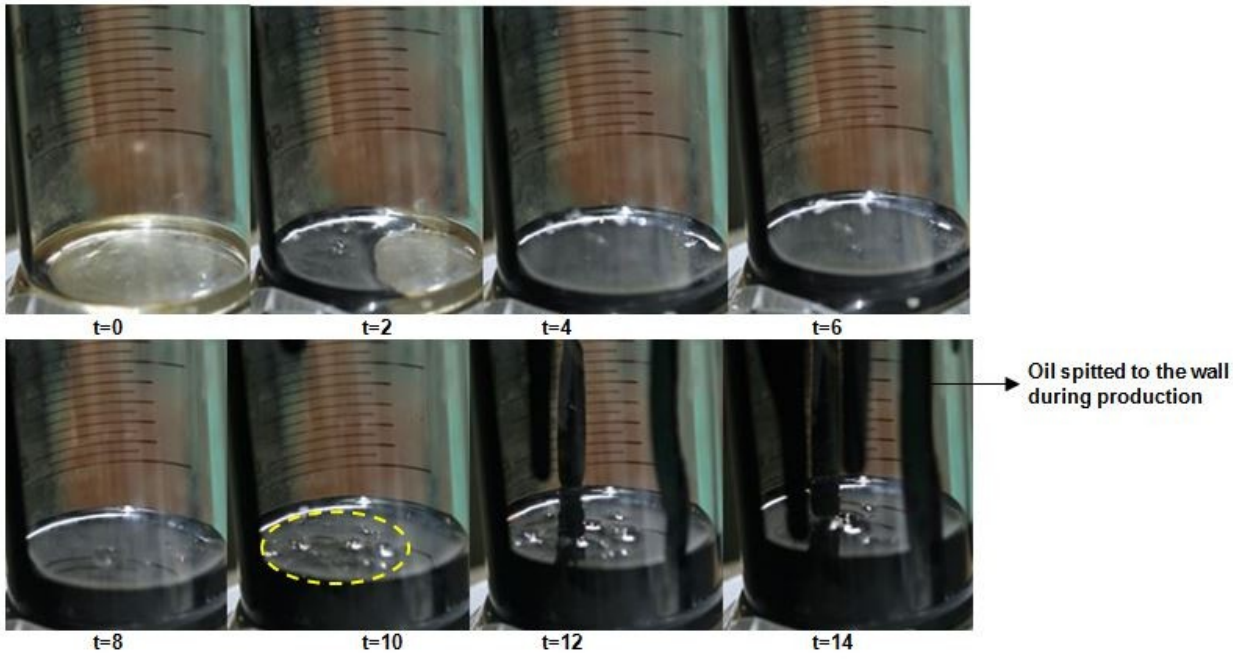

Figure 3.39—Oil production in Exp. 2 – Cycle 1 (t = hour): Yellow circles on where bubbles appeared.

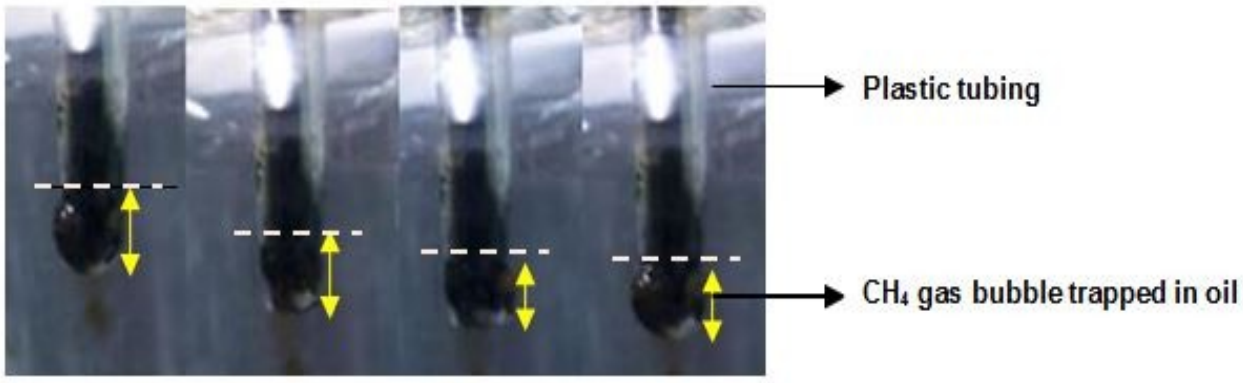

Figure 3.40—CH_4 gas bubble size (0.5-1 cm, the height of yellow arrow) during Exp. 1 – Cycle 2.

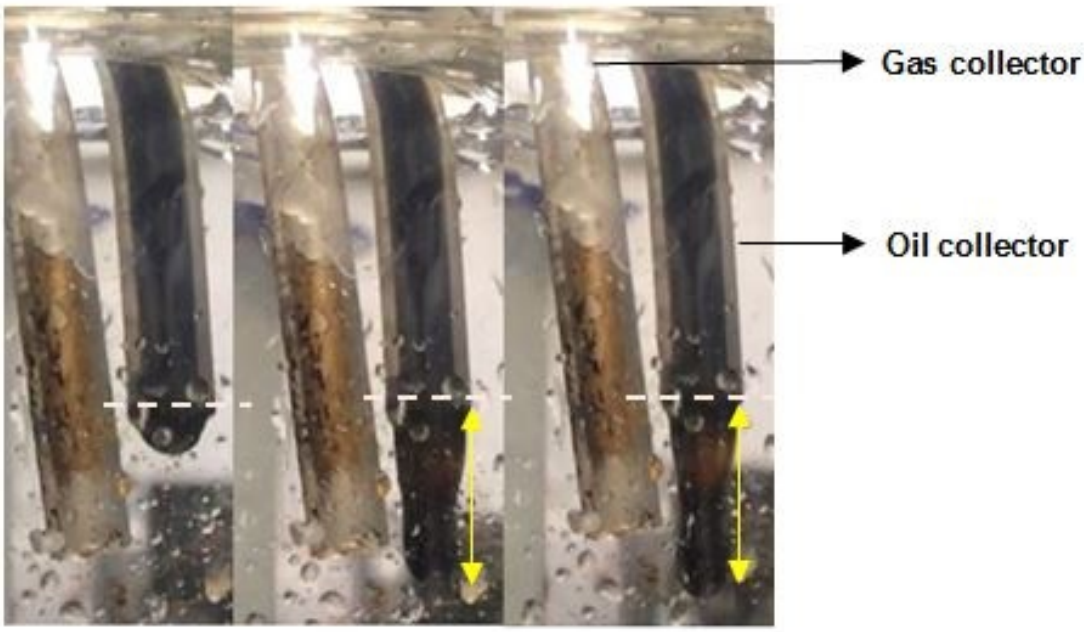

Figure 3.41—Air 50%+CO2 50% gas bubble size (1.25-2.5 cm, the height of yellow arrow) during Exp. 3 – Cycle 2.

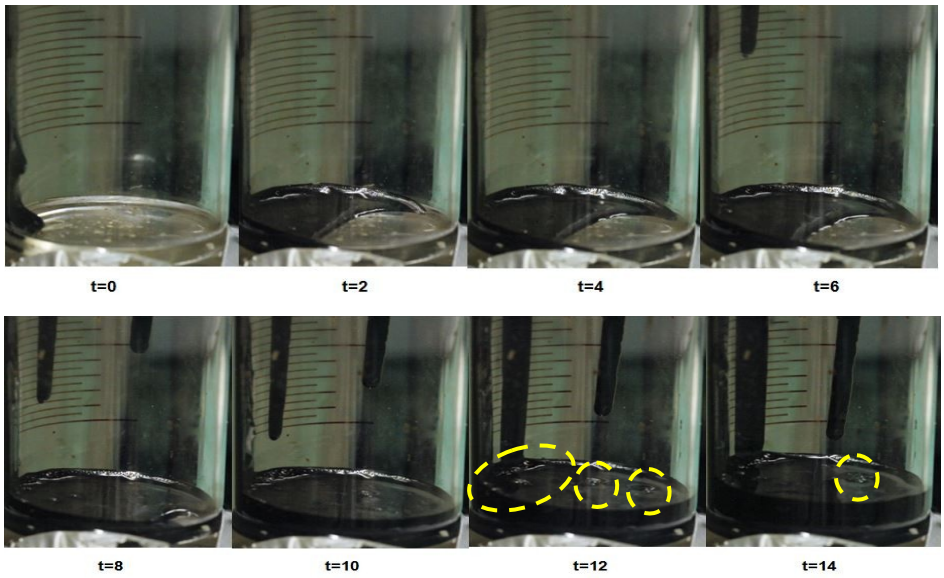

Figure 3.42—Oil production in Exp. 4 – Cycle 2 (t = hour): Yellow arrows pointed where bubbles appeared.

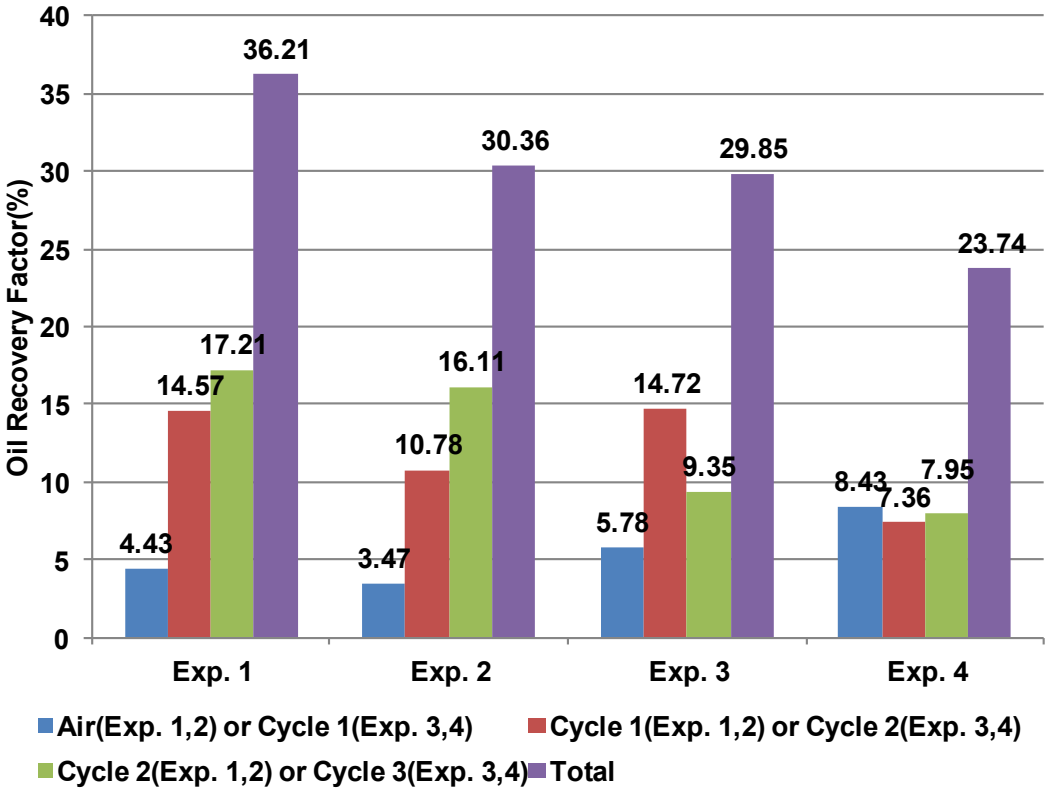

Figure 3.43−Oil recovery summary for each experiment.

Chapter 4 Conclusions and Contributions

4.1 Conclusions and Contributions

To understand the dynamics of foamy oil properly, having equal foam quality across the sand-pack is important. To do that, live oil was made separately, transferred to sand-pack and live oil depletion experiments started (Chapter 2). Conclusions for experimental study in Chapter 2 are follows:

- ✓ The pressure differential can be a good marker of foamy oil behaviour associated with oil and gas production.
- ✓ Depending on the solvent type, the pressure differential versus time behaviour is different. Comparing the cases using the same solvent, the higher pressure differential led to higher oil/gas recovery. However, comparing with other solvent cases, this sometimes might not be valid because of the different foamy oil behaviour. In the case of CO_2, better foaminess and accordingly more nucleation of gas bubbles were observed, even with lower pressure differentials.
- ✓ The gas solvents with good foaming property (methane or carbon dioxide) and with good mixing property (propane) are better to be used separately, because the mixed form of them creates less foaminess.
- ✓ Generally, giving a higher depletion rate induce producing greater amount of oil. However, after a certain high value of depletion rate is achieved, foam quality showed the greatest importance.

These experiments were simulated with core-scale sand-pack model made by ECLIPSE, Schlumberger. Further, with the K-values and reaction coefficients obtained from core-scale simulation, field-scale modeling was carried out in different well-pattern, injection/soaking time. Conclusions for numerical study in Chapter 2 are follows:

- ✓ Tuning K-values and having proper reaction coefficients are useful approaches to include the foamy oil behaviour in core- and field-scale simulations.
- ✓ Since methane-propane mixture reduces the foaminess of methane and non-equilibrium status turns into equilibrium condition, equilibrium methane-behaviour is suitable to be applied to numerical simulation of methane-propane mixture live oil production.
- ✓ As a result of field-scale simulation, all-wells pattern showed a slightly higher recovery than central and peripheral well patterns did. Also, setting the proper period of injection and soaking time is crucial to deliver more oil efficiently.

To be closer to realistic recovery method, experimental procedure is slightly changed to be close to a cyclic-solvent-injection manner. In addition, to seek a more economical way of producing oil, air was newly tested in Chapter 3. Conclusions in Chapter 3 are follows:

- ✓ For heavy oil recovery, air can be used initially in a huff-n-puff manner to increase oil viscosity and eventually give better foam stability for the subsequent secondary solvent (CH_4 or CO_2) huff-n-puff applications.
- ✓ CH_4 huff-n-puff preceded by air huff-n-puff showed higher oil recovery than CH_4 live oil production with higher depletion rate.
- ✓ When using mixture-form of gas solvent, different diffusion rates of each gas should be considered. Here, CO_2 showed the slowest diffusion rate followed by air and CH_4, even though it created effective foam at later stages. Therefore, for faster response to solution-gas drive, methane is better, while CO_2 can be more effective in the long run.
- ✓ Good foam quality in heavy oil can be established when gas bubbles are well-dispersed and stable enough to a have long time in non-equilibrium status until reaching free-gas phase. Two keys factors that indicate high quality of foam are high amplitude of pressure differential (ΔP) and adequate time for ΔP to reach almost zero.
- ✓ It is important to inject the proper amount of air in the beginning phase; otherwise, air gas bubbles, which are left in a great volume in the sand-pack, would hinder the foaming capability of the solvents used in the subsequent cycles.
- ✓ It is crucial to inject the appropriate volume of gas solvent so that the injected oil is fully dissolved into the dead oil. Otherwise, continuous-phase gas, which is not dissolved into heavy oil, would not be helpful to drive oil to be produced, unlike dispersed-phase flow.
- ✓ There were no specific observations in GC and SARA analyses of the produced oil. Generally, the augmentation of high carbon numbers (81+) and decrease in low carbon numbers (below 81) were related to the oil viscosity increase.
- ✓ Economically, co-injection of air and CO_2 is more efficient than alternate injection of them. However, considering the lower price of CH_4 and the significant difference in oil recovery between these two schemes, alternate injection of air and CH_4 is more feasible than the co-injection of them.

References

Albartamani, N. S., Farouq Ali, S. M. F., and Lepski, B. 1999. Investigation of Foamy Oil Phenomena in Heavy Oil Reservoirs. International Thermal Operations/Heavy Oil Symposium, Bakersfield, California, 17-19 March. doi:10.2118/54084-MS.

Alshmakhy, A. and Maini, B. B. 2012. Effects of Gravity, Foaminess, and Pressure Drawdown on Primary-Depletion Recovery Factor in Heavy-Oil Systems. *JCPT* 51 (06). doi:10.2118/163067-PA.

Bera, A. and Babadagli, T. 2016. Relative Permeability of Foamy Oil for Different Types of Dissolved Gases. *SPE Res Eval & Eng*. 19 (4). SPE-180913-PA. http://dx.doi.org/10.2118/180913-PA.

Bjorndalen, N., Jossy, E., and Alvarez, J. 2012. Foamy Oil Behaviour in Solvent Based Production Processes. SPE Heavy Oil Conference Canada, Calgary, Alberta, 12-14 June. SPE-157905-MS. http://dx.doi.org/10.2118/157905-MS.

Chang, J. and Ivory, J. 2013. Field-Scale Simulation of Cyclic Solvent Injection (CSI). *J Can Pet Technol*. 52 (4). SPE-157804-PA. http://dx.doi.org/10.2118/157804-PA.

Chang, J., Ivory, J., and London, M. 2015. History Matches and Interpretation of CHOPS Performance for CSI Field Pilot. SPE Canada Heavy Oil Technical Conference, Calgary, Alberta, 9-11 June. SPE-17466-MS. http://dx.doi.org/10.2118/174466-MS.

Diedro, F., Bryan, J., Kryuchkov, S. et al. 2015. Evaluation of Diffusion of Light Hydrocarbon Solvents in Bitumen. SPE Canada Heavy Oil Technical Conference, Calgary, Alberta, 9-11 June. SPE-174424-MS. http://dx.doi.org/10.2118/174424-MS.

Diedro, F., Bryan, J., Kryuchkov, S. et al. 2015. Evaluation of Diffusion of Light Hydrocarbon Solvents in Bitumen.SPE Canada Heavy Oil Technical Conference, Calgary, Alberta, Canada, 9-11 June.. doi:10.2118/174424-MS.

Du, Z., Zeng, F., and Chan, C. 2014. Effects of Pressure Decline Rate on the Post-CHOPS Cyclic Solvent Injection Process. SPE Heavy Oil Conference Canada, 10-12 June. SPE-170176-MS. http://dx.doi.org/10.2118/170176-MS.

Dusseault, M.B. (2002). Chapter 2. Alberta Government. "*World Conventional and Heavy Oil, CHOPS: Cold heavy oil production with sand in the Canadian heavy oil industry"*. p. 46-47. Retrieved from https://open.alberta.ca/publications/2815953. Accessed on July 20th 2017

ECLIPSE Technical Description. 2014, Schlumberger.

Firoozabadi, A. and Aronson, A. 1999. Visualization and Measurement of Gas Evolution and Flow of Heavy and Light Oil in Porous Media. *SPE Reservoir Evaluation & Engineering* 2 (6). doi:10.2118/59255-PA.

Handy, L. L. 1958. A laboratory study of Oil Recovery by Solution Gas Drive. *Trans. AIME* 213: 310-315.

Ivory, J., Chang, J., Coates, R. et al. 2010. Investigation of Cyclic Solvent Injection Process for Heavy Oil Recovery. *J Can Pet Technol*. 49 (09). http://dx.doi.org/10.2118/140662-PA.

Kovscek, A. R., Tang, G. Q. and Radke, C. J. 2007. Verification of Roof Snap Off as a Foam-Generation Mechanism in Porous Media at Steady State. *Colloids and Surfaces A: Physicochemical and Engineering Aspects* 302: 251-260.

Maini, B. B. 2001. Foamy-Oil Flow. *JPT* 53 (10). doi:10.2118/68885-JPT.

Maini, B. B., Sheng, J. J. and Bora, R. 1996. Role of foamy oil flow in heavy oil production. International Energy Agency (IEA) Workshop/Symp. on EOR, Sydney, Australia, Sept. 29-2 Oct.

Mayorquin, J. and Babadagli, T. 2016a. Low Temperature Air Injection with Solvents in Heavy-Oil Containing Naturally Fractured Reservoirs: Effects of Matrix/Fracture Properties and Temperature on Recovery. *Fuel* 179: 376–390.

Mayorquin, J. and Babadagli, T. 2016b. Optimal Design of Low Temperature Air Injection with Propane for Efficient Recovery of Heavy Oil in Deep Naturally Fractured Reservoirs: Experimental and Numerical Approach. *Energy and Fuels* 30 (4): 2662–2673.

Peng, D. Y. and Robinson, D.B. 1976. A New Two-Constant Equation of State. *Industrial and Engineering Chemistry: Fundamentals* 15: 59–64. doi:10.1021/i160057a011.

Rangriz-Shokri, A. and Babadagli, T. 2012. An Approach to Model CHOPS (Cold Heavy Oil Production with Sand) and Post-CHOPS Applications. SPE Annual Technical Conference and Exhibition, San Antonio, Texas, 8-10 October. SPE-159437-MS. http://dx.doi.org/10.2118/159437-MS.

Rangriz-Shokri, A. and Babadagli, T. 2016. Experimental and Numerical Core-to-Field Scale Modeling of Non-Equilibrium CO_2 Behaviour in Post-CHOPS Applications. Submitted to *SPE Reservoir Evaluation and Engineering* 2016 (under review).

Rangriz-Shokri, A. and Babadagli, T. 2016. Experimental and Numerical Core-to-Field Scale Modeling of Non-Equilibrium CO_2 Bahaviour in Post-CHOPS Applications. Submitted to *SPE Reservoir Evaluation and Engineering* 2016 (under review).

Sheng, J. J., Maini, B. B., Hayes, R. E. et al. 1997. Experimental Study of Foamy Oil Stability. *JCPT* 36 (04). doi:10.2118/97-04-02.

Sheng, J.J., Maini, B.B., Hayes, R.E. et al. 1999. Critical Review of Foamy Oil Flow. *Transport in Porous Media* 35 (2):157-187. doi:10.1023/A:1006575510872.

Sheng, J.J., Maini, B.B., Hayes, R.E. et al. 1999. Critical Review of Foamy Oil Flow. *Transport in Porous Media* 35: 157. doi:10.1023/A:1006575510872.

Soh, Y. J., Rangriz-Shokri, A., and Babadagli, T. 2016. A New Modeling Approach to Optimize Methane-Propane Injection in a Field After CHOPS. SPE Annual Technical Conference and Exhibition, Dubai, UAE, 26-28 September.doi:10.2118/181322-MS.

Soh, Y. J., Rangriz-Shokri, A., and Babadagli, T. 2017. Cost Effective Heavy-Oil Recovery after Primary Production: Optimization of Methane Use in Cyclic Solvent Injection through Experimental and Numerical Studies. Submitted to *Fuel* (under review).

Tang, G. and Firoozabadi, A. 2001. Effect of GOR, Temperature, and Initial Water Saturation on Solution-Gas Drive in Heavy-Oil Reservoirs. SPE Annual Technical Conference and Exhibition, New Orleans, Louisiana, 30 September-3 October. :10.2118/71499-MS.

Tang, G. and Firoozabadi, A. 2001. Effect of GOR, Temperature, and Initial Water Saturation on Solution-Gas Drive in Heavy-Oil Reservoirs. SPE Annual Technical Conference and Exhibition, New Orleans, Louisiana, 30 September-3 October.doi:10.2118/71499-MS.

Walton, A.G. 1969. Nucleation in Liquids and Solutions, in *Nucleation, Zettlemoyer*, A.C., Ed., Marcel Dekker, New York.

Wang, H., Zeng, F., and Zhou, X. 2015. Study of the Non-Equilibrium PVT Properties of Methane- and Propane-Heavy Oil Systems. SPE Canada Heavy Oil Technical Conference, Calgary, Alberta, 9-11 June. SPE-1794498-MS. http://dx.doi.org/10.2118/174498-MS.